

MAGNETIZATION AND A.C. HALL EFFECTS IN  
TWO SUPERCONDUCTORS

By

Gordon L. Nelson, Jr.

Bachelor of Science

Oklahoma State University

Stillwater, Oklahoma

1966

Submitted to the faculty of the Graduate College  
of the Oklahoma State University  
in partial fulfillment of the requirements  
for the degree of  
MASTER OF SCIENCE  
August, 1969

NOV 5 1969

MAGNETIZATION AND A.C. HALL EFFECTS IN  
TWO SUPERCONDUCTORS

Thesis Approved:

*James Lange*  
\_\_\_\_\_  
Thesis Adviser

*W. Kolm*  
\_\_\_\_\_

*N. V. V. J. Swamy*  
\_\_\_\_\_

*N. D. Surdam*  
\_\_\_\_\_

Dean of the Graduate College

730045

## TABLE OF CONTENTS

Chapter	Page
I. INTRODUCTION . . . . .	1
II. THEORY . . . . .	2
Theory of Normal-State Magnetization in Solids. . . . .	2
Superconductivity . . . . .	5
Ginsburg-Landau Equations . . . . .	12
III. EXPERIMENTAL APPARATUS AND PROCEDURE . . . . .	14
IV. PREDICTIONS CONCERNING THE BEHAVIOR OF THE SYSTEM-- A MODEL. . . . .	25
Contributions to the Induced Field. . . . .	25
V. EXPERIMENTAL RESULTS . . . . .	30
Nitrogen (77°K) and Room Temperature Data . . . . .	30
Results in the Superconducting Region . . . . .	30
VI. SUMMARY AND CONCLUSIONS. . . . .	41
SELECTED BIBLIOGRAPHY . . . . .	81
APPENDIX A, ANALYSIS OF THE A.C. HALL EFFECT. . . . .	83
APPENDIX B, QUASISTATIC APPROXIMATION . . . . .	89
APPENDIX C, UNITS AND DIMENSIONS. . . . .	91

LIST OF TABLES

Table	Page
I. Summary of Data for $\bar{H}$ Increasing. . . . .	38
II. Summary of Data for $\bar{H}$ Decreasing. . . . .	39
III. Interpretation of Data. . . . .	40
IV. Temperature and Field Dependence of Amplitude . . . . .	87
V. Units and Dimensions. . . . .	92

## LIST OF FIGURES

Figure	Page
1. Induced Dipole Effects. . . . .	4
2. Magnetization Curve for Type I Material . . . . .	6
3. Graph of $H_c$ vs $T_c$ . . . . .	7
4. Graph of $M$ vs $H$ (Transverse Field). . . . .	8
5. Graph of $M$ vs $H$ (Type II) . . . . .	9
6. Flux Patterns in Superconducting and Normal States. . . . .	10
7. Graph of $M$ vs $H$ (Field Reversal). . . . .	12
8. Method of Suspension and Coil Position. . . . .	17
9. Electronic Exciting Network . . . . .	18
10. Horizontal Coils and Specimen . . . . .	19
11. Vertical Coils and Specimen . . . . .	20
12. End Effects . . . . .	21
13. Lorentz Effects . . . . .	22
14. Superconducting Effects . . . . .	23
15. Normal State (A.C. Hall Effects). . . . .	24
16. Superposition of Voltage Contributions. . . . .	29
17. Coils H, Amplitude for Pb . . . . .	42
18. Coils V, Amplitude for Pb . . . . .	43
19. Coils H and V, Phase for Pb . . . . .	44
20. Coils H, Amplitude for Nb I . . . . .	45
21. Coils V, Amplitude for Nb I . . . . .	46
22. Coils H and V, Phase for Nb I . . . . .	47

Figure	Page
23. Coils V, Amplitude for Nb II. . . . .	48
24. Coils H, Amplitude for Pb I, H Increasing . . . . .	49
25. Coils V, Amplitude for Pb I, H Increasing . . . . .	50
26. Coils H and V, Amplitude for Pb I, H Increasing . . . . .	51
27. Coils H and V, Phase for Pb I, H Increasing . . . . .	52
28. Coils H and V, Amplitude for Pb I, H Decreasing . . . . .	53
29. Coils H and V, Phase for Pb I, H Decreasing . . . . .	54
30. Coils H and V, Amplitude for Pb I, H Decreasing . . . . .	55
31. Coils H and V, Phase for Pb I, H Decreasing . . . . .	56
32. Coils H, Amplitude for Pb II, H Increasing. . . . .	57
33. Coils V, Amplitude for Pb II, H Increasing. . . . .	58
34. Coils H and V, Amplitude for Pb II, H Increasing. . . . .	59
35. Coils H and V, Phase for Pb II, H Increasing. . . . .	60
36. Coils H and V, Amplitude for Pb II, H Decreasing. . . . .	61
37. Coils H and V, Phase for Pb II, H Decreasing. . . . .	62
38. Coils H and V, Amplitude for Pb II, H Decreasing. . . . .	63
39. Coils H and V, Phase for Pb II, H Decreasing. . . . .	64
40. Coils H and V, Amplitude for Nb II, H Increasing. . . . .	65
41. Coils H and V, Phase for Nb II, H Increasing. . . . .	66
42. Coils H and V, Amplitude for Nb II, H Decreasing. . . . .	67
43. Coils H and V, Phase for Nb II, H Decreasing. . . . .	68
44. Coils H and V, Amplitude for Nb III, H Increasing . . . . .	69
45. Coils H and V, Phase for Nb III, H Increasing . . . . .	70
46. Coils H and V, Amplitude for Nb III, H Decreasing . . . . .	71
47. Coils H and V, Phase for Nb III, H Decreasing . . . . .	72
48. Coils H and V, Amplitude for Nb IV, H Increasing. . . . .	73

Figure	Page
49. Coils H and V, Phase for Nb IV, H Increasing. . . . .	74
50. Coils H and V, Amplitude for Nb IV, H Decreasing. . . . .	75
51. Coils H and V, Phase for Nb IV, H Decreasing. . . . .	76
52. Coils H and V, Amplitude for Nb V, H Increasing . . . . .	77
53. Coils H and V, Phase for Nb V, H Increasing . . . . .	78
54. Coils H and V, Amplitude for Nb V, H Decreasing . . . . .	79
55. Coils H and V, Phase for Nb V, H Decreasing . . . . .	80

## ACKNOWLEDGMENT

The author would like to express his thanks to Dr. James Lange for his help and advice throughout the project, and to the National Science Foundation for their financial support. The shop crew of the Physics Department was also very helpful in constructing various pieces of equipment.



## CHAPTER I

### INTRODUCTION

The phenomenon of superconductivity is one which was not well understood until as late as 1961. Even at present there is no completely adequate theory of Type II superconductivity. The various theoretical treatments of Type II superconductivity rely mostly on phenomenological models and must therefore draw upon experimental data more heavily than upon "first principles." The magnetization is of importance because it is the parameter which fundamentally characterizes the superconducting state. For these reasons it is desirable to have ways of determining the magnetization state of a superconductor. This investigation was an attempt to measure the magnetic state of both Type I and Type II superconductors by exciting the specimens with an acoustic stress wave. In the following the results of these measurements are reported and compared with the known behavior of certain superconducting materials, an attempt is also made to correlate these results with a model of the system.

## CHAPTER II

### THEORY

#### Theory of Normal-State Magnetization in Solids

The term "normal state" means the non-superconducting state. In this region the gross aspects of magnetization in solids can be analyzed using Maxwell's equations. The relevant equations for the magnetic state are

$$\nabla \times \bar{H} = \bar{J}_c + \frac{\partial \bar{D}}{\partial t} \quad (1)$$

and

$$\nabla \cdot \bar{B} = 0 \quad (2)$$

where  $H$  is the magnetic intensity,  $B$  is the magnetic induction,  $D$  the electric displacement,  $J_c$  the "free" or "conduction" current density, and  $t$  the time. It is customary to make a distinction between two types of currents--the ohmic-type conduction currents  $J_c$  and the microscopic bound currents  $J_b$  which have their origin in the atomic and molecular motions. It should be emphasized that  $H$  is dependent only on  $J_c$  and  $D$ , not on  $J_b$ .

It is apparent that even if  $D(r,t)$  and  $J_c$  are known, equations (1) and (2) are not adequate to determine  $B$  and  $H$ , since a vector field is specified completely only if both its curl and divergence are specified. What is needed is a constitutive relationship between  $B$  and  $H$ . The usual procedure is to write

$$\bar{B} = \mu_0 \bar{H} + \bar{M} \quad (3)$$

where  $\mu_0$  is the free-space permeability and  $M$  is the magnetization vector. If the material is linear and isotropic, as is the case for most non-ferromagnetic materials, one can also assume that

$$\bar{M} = \mu_0 \chi_m \bar{H} \quad (4)$$

where  $\chi_m$  is independent of  $B$  and  $H$ . Then

$$\bar{B} = \mu_0 (1 + \chi_m) \bar{H} \quad (5)$$

which is the desired constitutive relationship. The factor  $\chi_m$  is called the relative susceptibility. If  $\chi_m < 0$ , the material is diamagnetic and if  $\chi_m > 0$  but  $\chi_m \ll 1$ , the material is paramagnetic.

There is one other approximation which will be made here--the so-called "quasi-static" or "low-frequency" approximation, which is simply  $\frac{\partial \bar{D}}{\partial t} = 0$ . All of the foregoing theory holds only if it is valid to make this approximation. We shall assume that it holds for all of the following work as well. A justification of this assumption is given in Appendix III. With these assumptions, the field equations becomes

$$\nabla \cdot \bar{H} = 0 \quad (6)$$

$$\nabla \times \bar{H} = \bar{J}_c \quad (7)$$

Equations (6) and (7), together with the boundary conditions, are sufficient to uniquely determine  $H$ , hence  $M$  and  $B$ . The physical interpretation of Equation (7) is that the conduction currents are the source of the field  $H$ . Similarly, the vector  $M$  has for its source the microscopic or bound charges, that is

$$\nabla \times \bar{M} = \mu_0 \bar{J}_b$$

By the superposition theorem, one obtains the total field by adding vectorially the fields due to all current sources. Hence

$$\begin{aligned}\nabla \times \bar{B} &= \mu_0 (\bar{J}_b + \bar{J}_c) \\ &= \nabla \times (\bar{M} + \mu_0 \bar{H})\end{aligned}\quad (8)$$

It is apparent that the relationship  $B = \mu_0 H + M$  satisfied Equation (8) and that B is the field due to all current sources. The field B is therefore generally regarded as more fundamental than H.

In the work which follows it will be of interest to calculate the voltage induced in a coil by some oscillating dipole distribution. The dipole distribution is induced by an applied magnetic field as illustrated below.

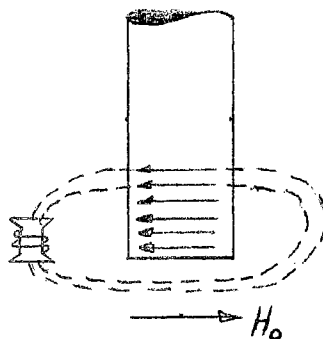


Figure 1. Induced Dipole Effects

The voltage induced in the coil will be given by Faraday's Law

$$V = -\frac{\partial \phi}{\partial t} = -N \frac{\partial}{\partial t} \int \bar{B} \cdot d\bar{s}$$

Where  $\phi$  is the flux linking the coil, N is the number of turns, and the surface integral is taken across a plane which cuts through the coil.

transverse to the axis. The principal difficulty in determining  $B$  is that one does not know the spatial distribution of the induced dipoles which are the sources for  $B$ . The distribution is assumed uniform throughout the material and directed parallel or anti-parallel to the field  $B$ . This assumption is quite often made in elementary discussions of magnetism, but it is not the case for a superconductor. Nor could one expect it to hold exactly even in the normal state if surface effects and end effects are important, as they are in the present case. We are therefore limited to a qualitative discussion of the coil voltage, based on rough assumptions about the dipole distributions in the normal state. In the superconducting state, one likewise assumes a certain general surface current configuration and attempts to make qualitative statements about the resulting voltage induced in the coils, although it is no longer proper to speak of an "internal dipole distribution." The details of this analysis for the two sets of coils are worked out in Chapter IV.

#### Superconductivity

If a metal is placed in a magnetic field and its temperature is then steadily lowered, a point is reached where the magnetic flux within the material is abruptly and completely expelled, so that below this temperature  $B = 0$  inside the specimen. The electrical resistance is also found to drop to zero, a phenomenon first observed by Kammerlingh Onnes in 1911. In the superconducting state we can formally write

$$\vec{B} = \mu_0 \vec{H} + \vec{M} = 0$$

or

$$\vec{M} = -\mu_0 \vec{H}.$$

Thus a graph of the magnetization vs. applied field would have the appearance shown below:

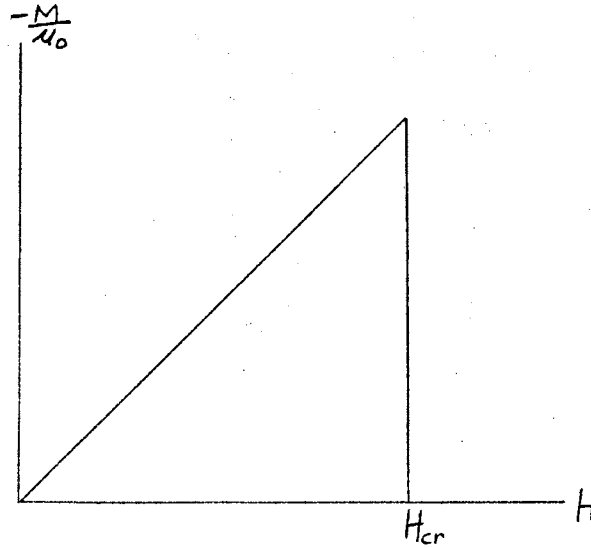


Figure 2. Magnetization Curve for Type I Material

It is apparent that the internal field  $M$  cannot continue to increase for  $H$  as large as we please. Indeed it is found that at a certain field  $H_{cr}$ , dependent on the temperature and type of material, the material suddenly reverts to the normal state, as shown. The critical field  $H_{cr}$  generally depends on the temperature according to

$$H_{cr}(T) = H_0 [1 - (T/T_c)^2]$$

where  $T_c$  is the so-called critical temperature. This function is plotted in Figure 3. The region enclosed by the curve is the superconducting region and  $H$  and  $T$  are considered independent variables which define

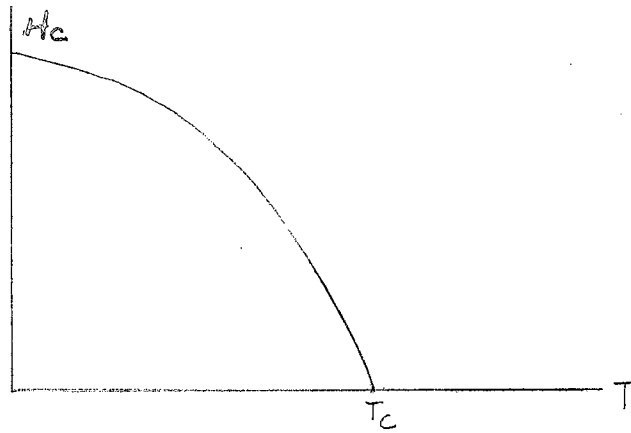


Figure 3. Graph of  $H_c$  vs  $T_c$ .

the state of the material. Figure 3 shows that the superconducting state is specified by  $H$  and  $T$ . The magnetic field is therefore the parameter which fundamentally characterizes the superconducting state, not the resistivity. In the superconducting region the material is perfectly diamagnetic ( $\bar{M} = -\frac{H}{\mu_0}$ ), while in the normal state the only contribution to  $M$  is that due to paramagnetic or diamagnetic effects which are slight except for ferromagnetic materials. We shall not consider these. Figure 2 shows that the flux which was excluded from the material in the superconducting state suddenly and completely penetrates into the material at  $H_{cr}$ . This is found to be the case for long cylindrical wires of certain pure metals where the field is applied longitudinally. These last two restrictions are of considerable importance. It is found that extremely small amounts of impurities, of the order of a few parts per million, are often sufficient to distort the magnetization curve considerably from the appearance of Figure 3. If the field is applied transversely instead of longitudinally, even for a pure metal the penetration is no longer abrupt and complete at  $H_c$ , but occurs

in a linear fashion, as illustrated in Figure 4.

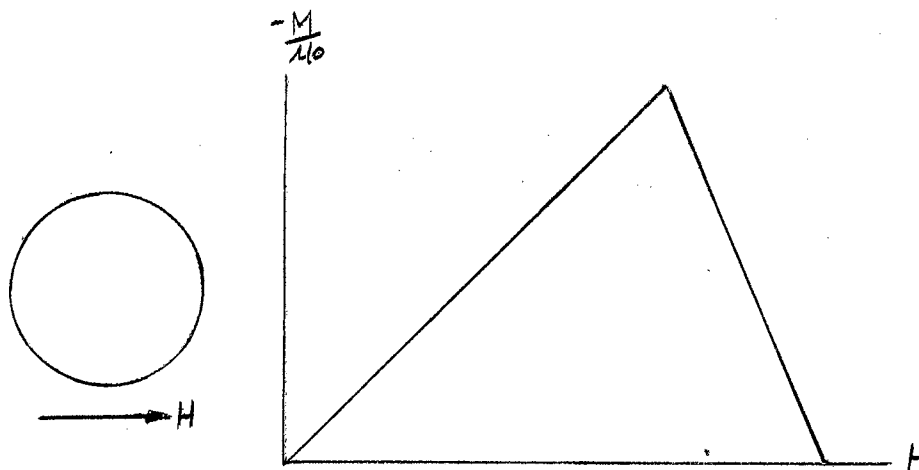


Figure 4. Graph of  $M$  vs  $H$  (Transverse Field)

Finally, it should be noted that there is a second class of materials whose magnetization curves exhibit two critical points, designated as  $H_{c1}$  and  $H_{c2}$ . At the point  $H_{c1}$  the flux begins to penetrate the specimen and at  $H_{c2}$  the penetration is complete, so that above  $H_{c2}$  the material is completely in a normal state and below  $H_{c1}$  it is in a completely superconducting state. The region between  $H_{c1}$  and  $H_{c2}$  is called the mixed state. The resistivity for small currents is zero below  $H_{c2}$ , returning to its normal-state value at fields above  $H_{c2}$ . A typical magnetization curve for a material in this second class is shown in Figure 5. Materials in the latter class are called "Type II," or "hard" superconductors, while those in the first class are called Type I, or "soft" superconductors. Lead and tin are two examples of Type I superconductors, while niobium and tantalum are two of the few elements



which, in pure form, exhibit Type II superconductivity. Most alloys and impure metals are Type II superconductors.

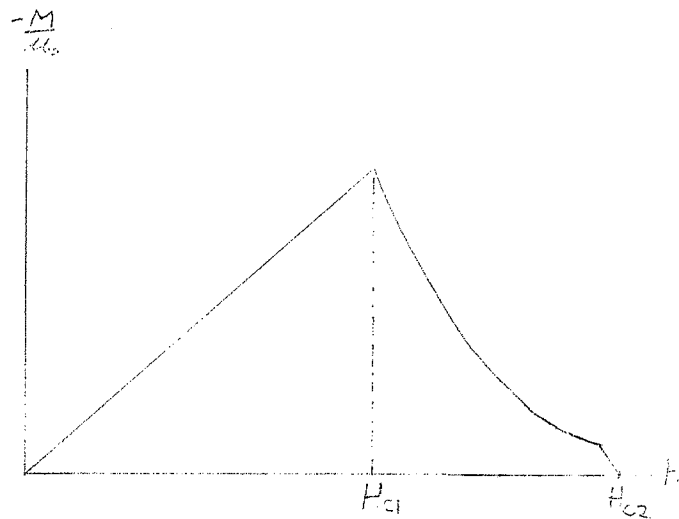


Figure 5. Graph of  $M$  vs  $H$  (Type II)

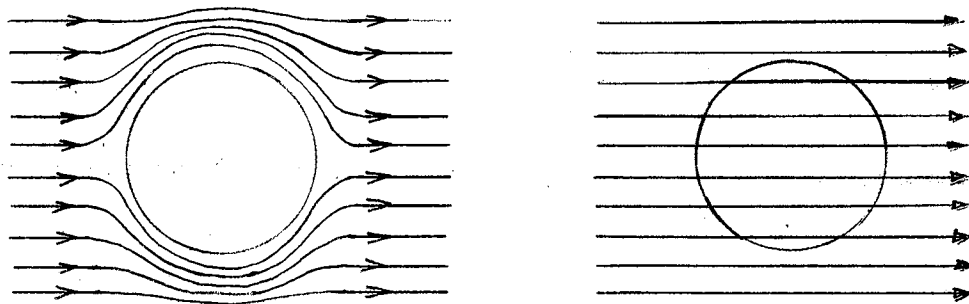
### Type I Materials

The behavior of a Type I superconductor in the superconducting region is due to the formation of surface currents. These surface currents are induced by the applied field, and are the origin of a field  $M$  such that  $B = \mu_0 H + M = 0$ . It should be emphasized that for an ideal Type I superconductor, there is no bulk magnetization--the opposing field has its source at the surface.

It is known from the classical field equations that if a material is placed in an external field, the field vector  $B$  at the surface obeys the relation

$$B_{n2} = B_{n1}$$

where the subscript  $n$  denotes the normal component and 1 and 2 denote the media. From this condition it follows immediately that for a Type I superconductor  $B$  is everywhere tangential at the surface, since otherwise it would not be possible to satisfy the condition  $B = 0$  within the material. If the field is applied transverse to an infinitely long cylinder, the flux pattern ( $B$ ) has the appearance shown in Figure 6.



Superconducting Region

Normal State

Figure 6. Flux Patterns in Superconducting and Normal States

In the region  $H_c/2 < H_0 < H_c$ , the material is in the intermediate state. In this region there is a partial penetration of the flux. The factor of  $1/2$  in the inequality is the demagnetizing factor for a cylinder in a transverse field. In general, this factor will depend on the geometry and orientation of the specimen. In the intermediate or mixed state the flux should penetrate more-or-less uniformly through

the specimen. According to Landau<sup>10</sup> the penetration is accomplished by the creation of discrete laminae of normal regions which increase in thickness as the field is increased. The laminae are parallel to the applied field, and in the intermediate state their volume increases linearly with applied field. At  $H_c$  they occupy the entire region. The fundamental difference between a Type I and Type II superconductor is not merely that Type I materials have a single, sharp discontinuity in the magnetization curve whereas Type II materials do not. Rather, one should say that a Type II material can exhibit the phenomenon of "flux trapping," while a Type I material cannot. Flux trapping is analogous in some respects to hysteresis in ferromagnetics, but is due in most cases to impurities. It is observed as a field which exists in the material after the applied field is removed. A typical curve for the complete magnetization-demagnetization cycle is shown in Figure 7. An associated effect in Type II materials is that of "flux jumping," i.e., sharp dips and/or rises in the magnetization as a function of applied field. These effects are believed to be due to impurity effects, though no quantitative theory has been formulated to account for them.

The presently accepted theory of superconductivity was first proposed by Bardeen, Cooper, and Schrieffer. It predicts the possibility of the formation of electron pairs which act like bosons, although the interaction which one electron sees from the other is not a direct one, but occurs through a phonon exchange, i.e., through the lattice. No attempt will be made to present or review this theory, since it is mathematically quite complex.

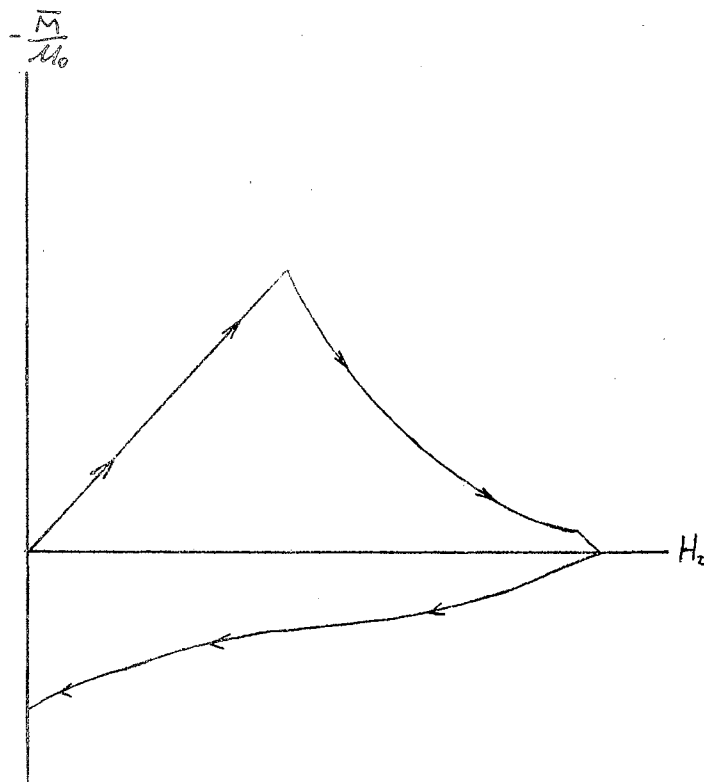


Figure 7. Graph of  $M$  vs  $H$  (Field Reversal)

### Ginsburg-Landau Equations

The distinctions and similarities between Types I and II superconductivity can be clarified by the Ginsburg-Landau Equations. These are a set of differential equations involving  $A$ , the magnetic vector potential, and a quantity  $\psi$ , which is closely related to the quantum state of the system. The equations are:

$$\left[ \frac{\nabla}{K} + \bar{A} \right]^2 \psi = \psi - \psi |\psi|^2$$

$$-\nabla \times \nabla \times \bar{A} = |\psi|^2 \bar{A} + \frac{i}{2K} [\psi^* \nabla \psi - \psi \nabla \psi^*]$$

The main point is that the constant  $K$  in large part determines the nature of the allowed solutions. If  $K < \frac{1}{\sqrt{2}}$ , then the equations predict

a positive surface energy between a superconducting and a normal region. This is equivalent to Type I superconductivity. If, however,  $K > \frac{1}{\sqrt{2}}$ , a negative surface energy is predicted. The solutions for this case turn out to have the form of flux filaments--small regions of magnetic flux which thread through the specimen and which are surrounded by a superconducting medium, for which  $B = 0$ . For  $K > \frac{1}{\sqrt{2}}$  the theory also predicts a second critical field at which the entire medium becomes normal. Most of the present theories of the mixed state are based on this idea of flux filaments, although there is considerable disagreement over the details. It is believed that the formation of flux filaments is governed by two factors:

- a) the non-uniformity of the field over the surface of the superconductor. Thus, for example, a transverse field applied across a Type I cylinder permits the formation of flux filaments, because the field is quite non-uniform around the surface.
- b) the impurity content and state of stress (dislocations). Type II superconductivity is due to effects such as these.

## CHAPTER III

### EXPERIMENTAL APPARATUS AND PROCEDURE

The sample was suspended at its midpoint at the end of a long cylinder and the detection coils were positioned near the lower end, as shown in Figure 8. The electronic network for exciting and detecting the stress wave is shown in Figure 9. The frequency synthesizer was capable of generating an AC signal in the acoustic range accurate to within  $\pm 0.005$  Hz. The gap between the terminating electrode and the sample acted as a transducer to change the electronic signal into a longitudinal stress wave. The FM detector sensed the amplitude of vibration of the end of the sample by using a variable-capacitance principle. This signal was then amplified and a read-out appeared on the oscilloscope or a recorder. The procedure was to vary the frequency until a sharp maximum appeared at the CRO. The lock-in amplifier was then tuned for a maximum reading by varying the phase and frequency controls. The uncertainty in the resonant frequency was never greater than a few parts per  $10^4$ , and at  $4^{\circ}\text{K}$  was a few parts per  $10^6$ .

When the magnetic field was applied, induced currents and/or dipoles were set up in the specimen. The wave imposed a time-varying oscillatory motion on these dipoles or currents, causing them to act as sources for a sinusoidal field  $B'$ . It was this field which the detection coils sensed. The applied field  $H_0$  had no direct effect on the coils, since it was constant in time. The voltages induced in the coil

were often as low as 50 u volts, much smaller than spurious noise signals, hence a rather sophisticated amplification technique was used. The amplifier was a PAR (Princeton Applied Research) Model HR-8 lock-in amplifier which works by comparing the signal to be measured against a reference voltage, and rejecting all frequencies except that of the reference. The bandwidth of such an amplifier is virtually zero, so it has good noise-rejection capabilities. An additional feature is that the amplifier is capable of measuring the phase difference between the reference voltage and the input signal. The phase of the signal proved to be as important as the amplitude since it was found that at  $H_{c2}$  (the second critical field) one set of the detection coils gave a well-defined phase shift.

The samples used were all of high-purity lead or niobium. Lead was chosen because it is very nearly an ideal Type I superconductor whose characteristics are well-known. Niobium is one of about three known elements which in a pure state is a Type II superconductor. Its characteristics have also been extensively studied although some of them are not very reproducible (in particular its behavior as the field is lowered from some point above  $H_{c2}$ ). The lead specimen was a polycrystalline cylinder. The Nb specimens were of different shapes and structures and included polycrystalline rods of cylindrical square, and "boat" shapes as well as a cylindrical single crystal. Data was taken for each of them under different orientations at He,  $N_2$ , and room temperatures, and the results were compared with the expected behavior as set forth in Chapter IV and Appendix I.

The detection coils and their relation to the specimen are shown in Figures 8, 10, and 11. The way in which each pair was connected

together is important since this determines whether the polarity of the voltage in one coil will add or oppose the voltage in the other.

The coils were attached near (but not touching) the lower end of the specimen. The reason for placing them near the end was that the amplitude of vibration is a maximum there and is zero at the mid-point.



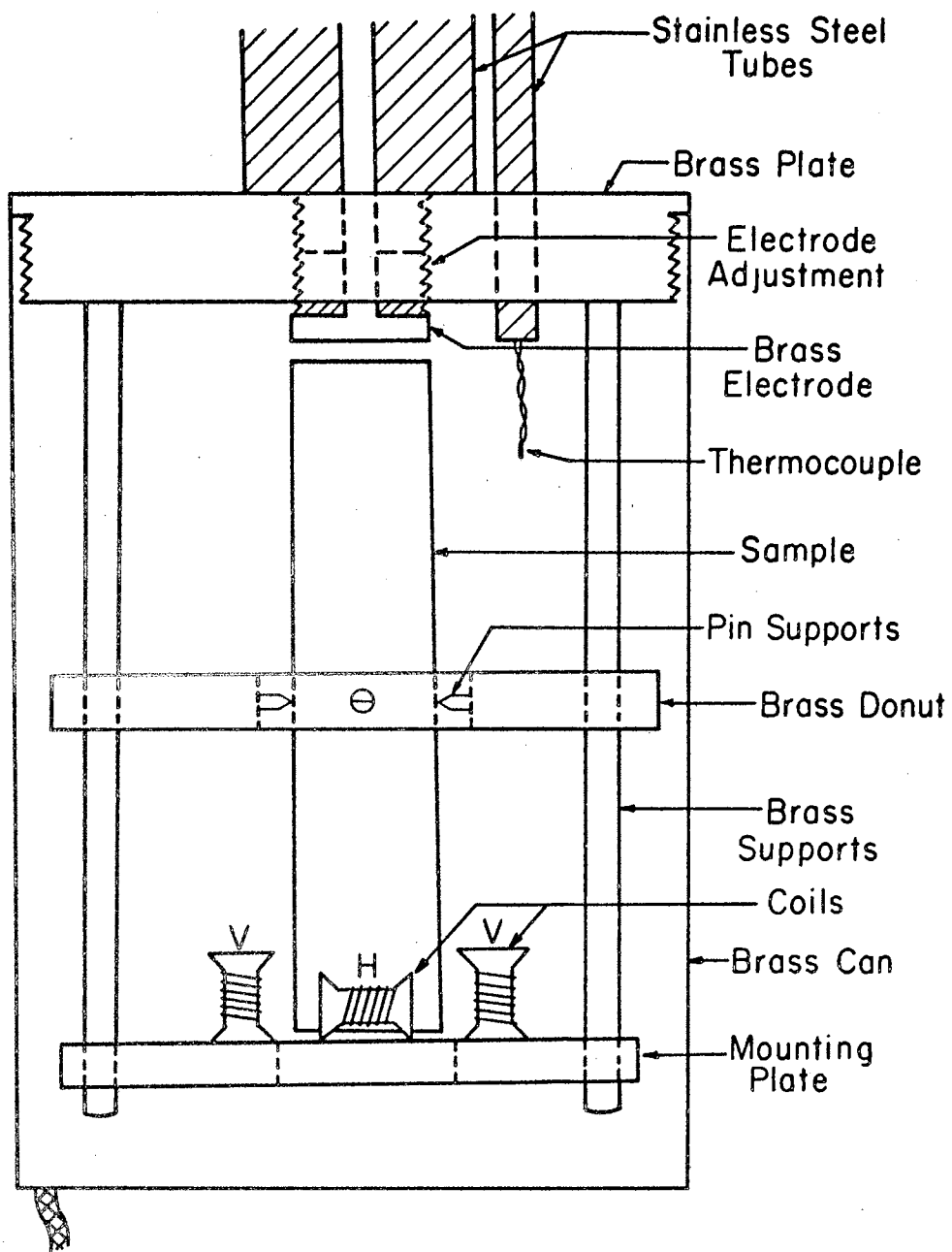


Figure 8. Method of Suspension and Coil Position

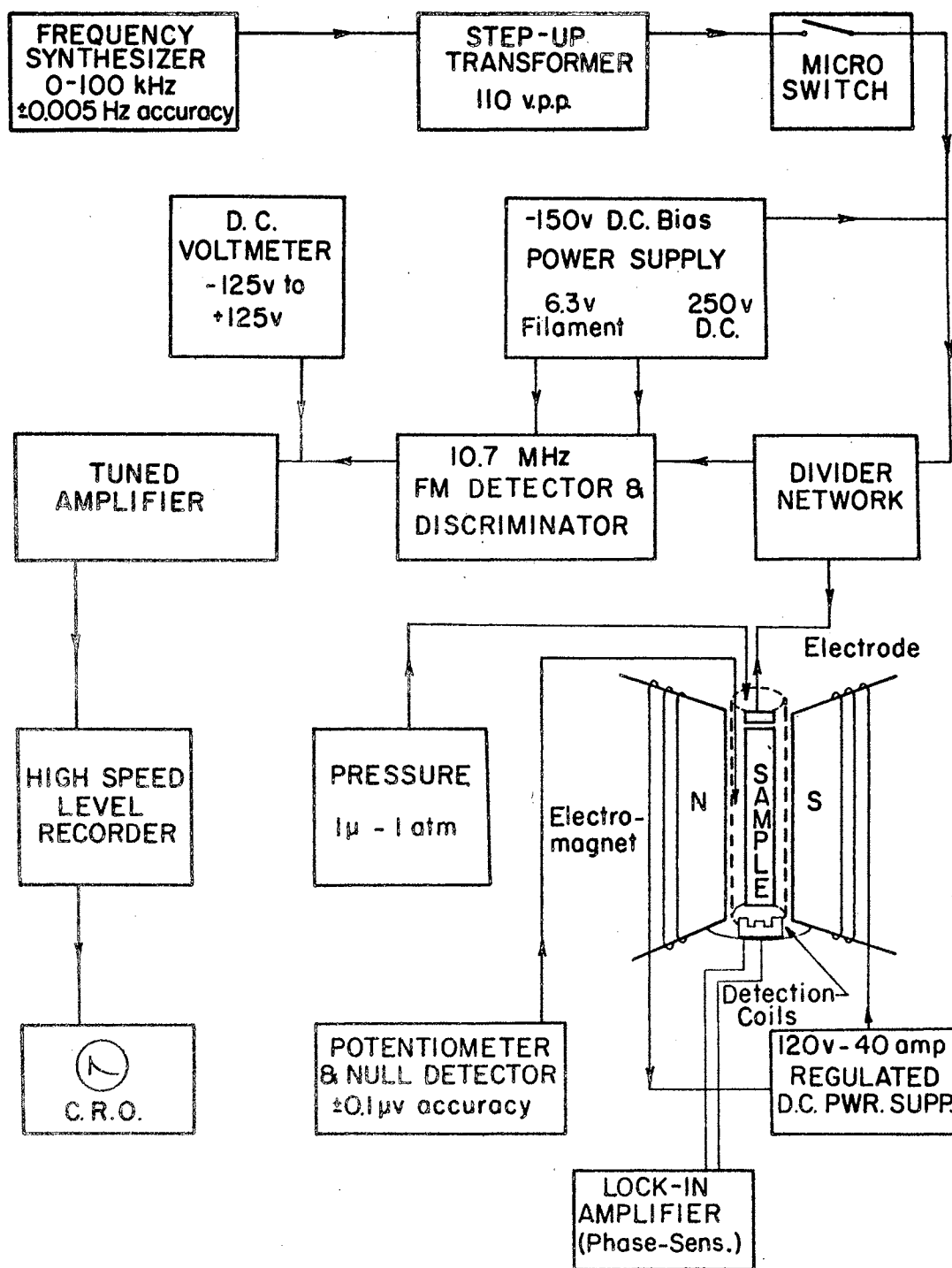


Figure 9. Electronic Exciting Network

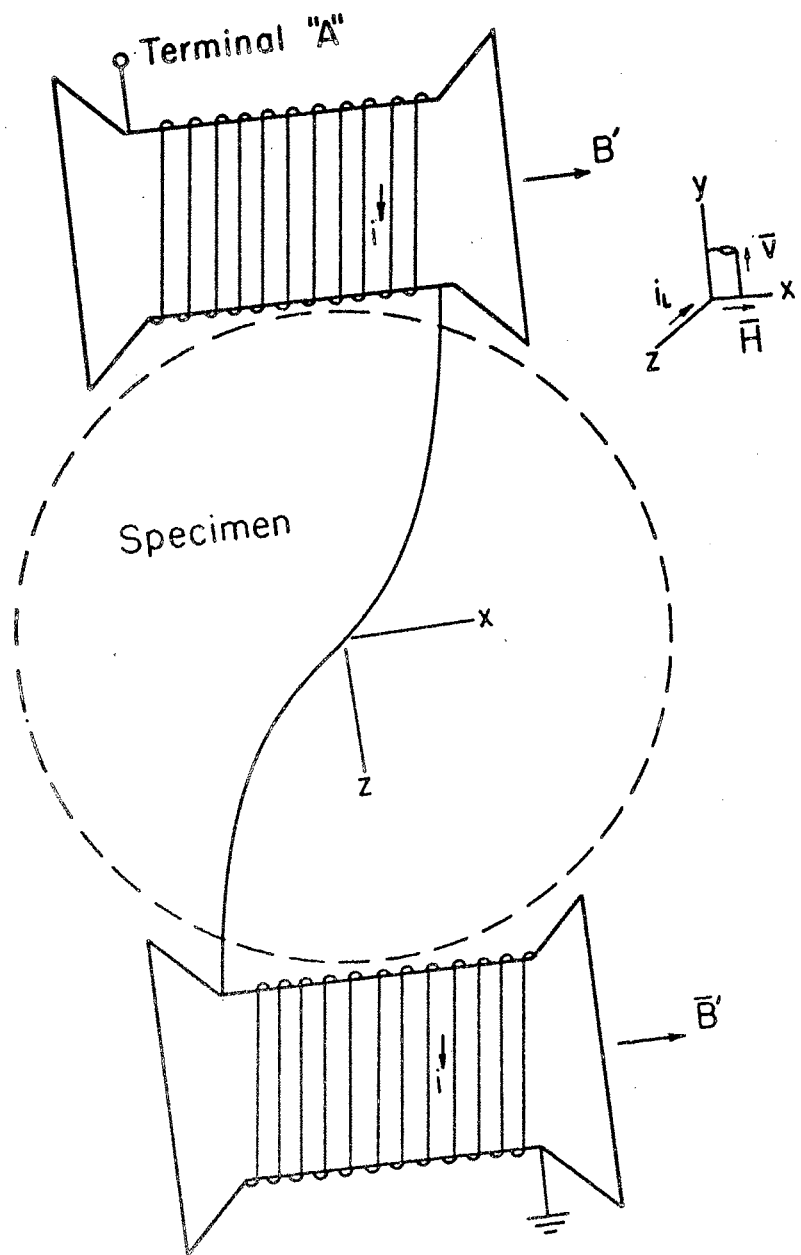


Figure 10. Horizontal Coils and Specimen

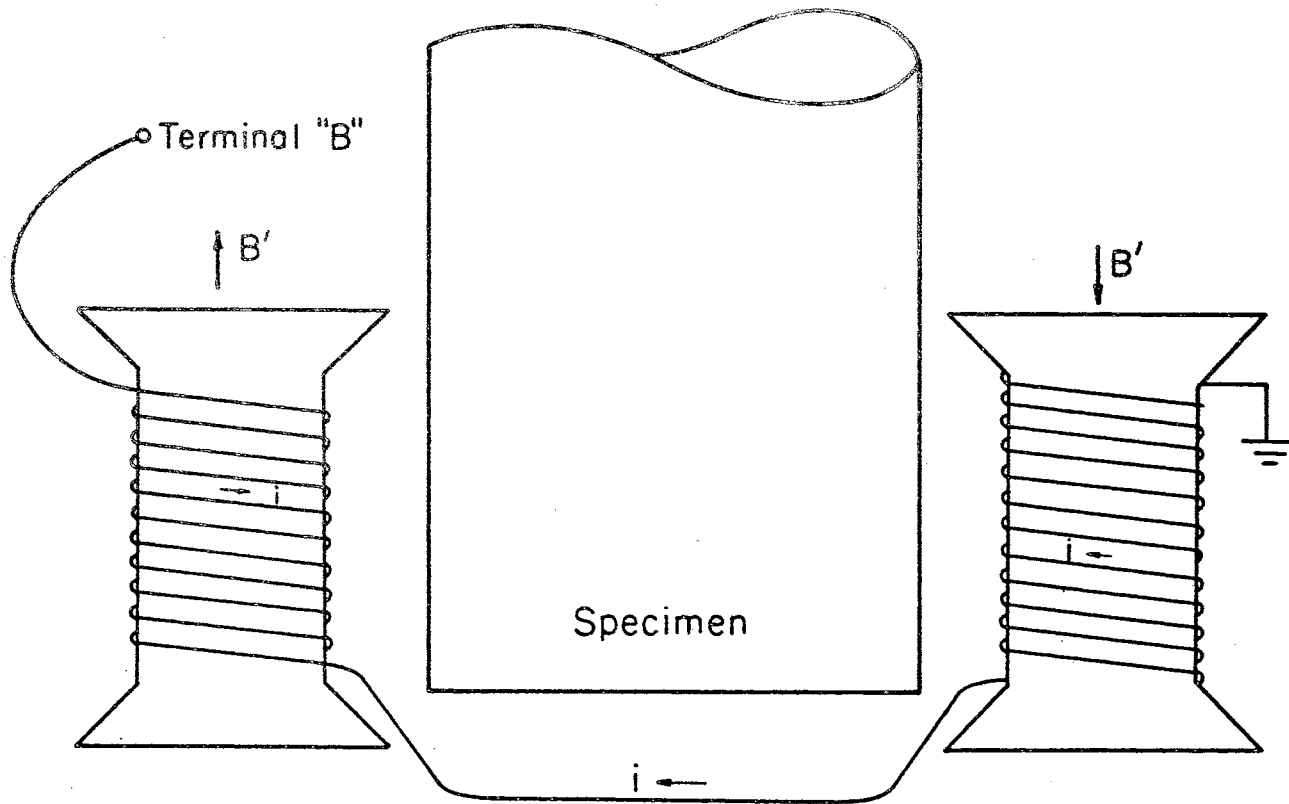


Figure 11. Vertical Coils and Specimen

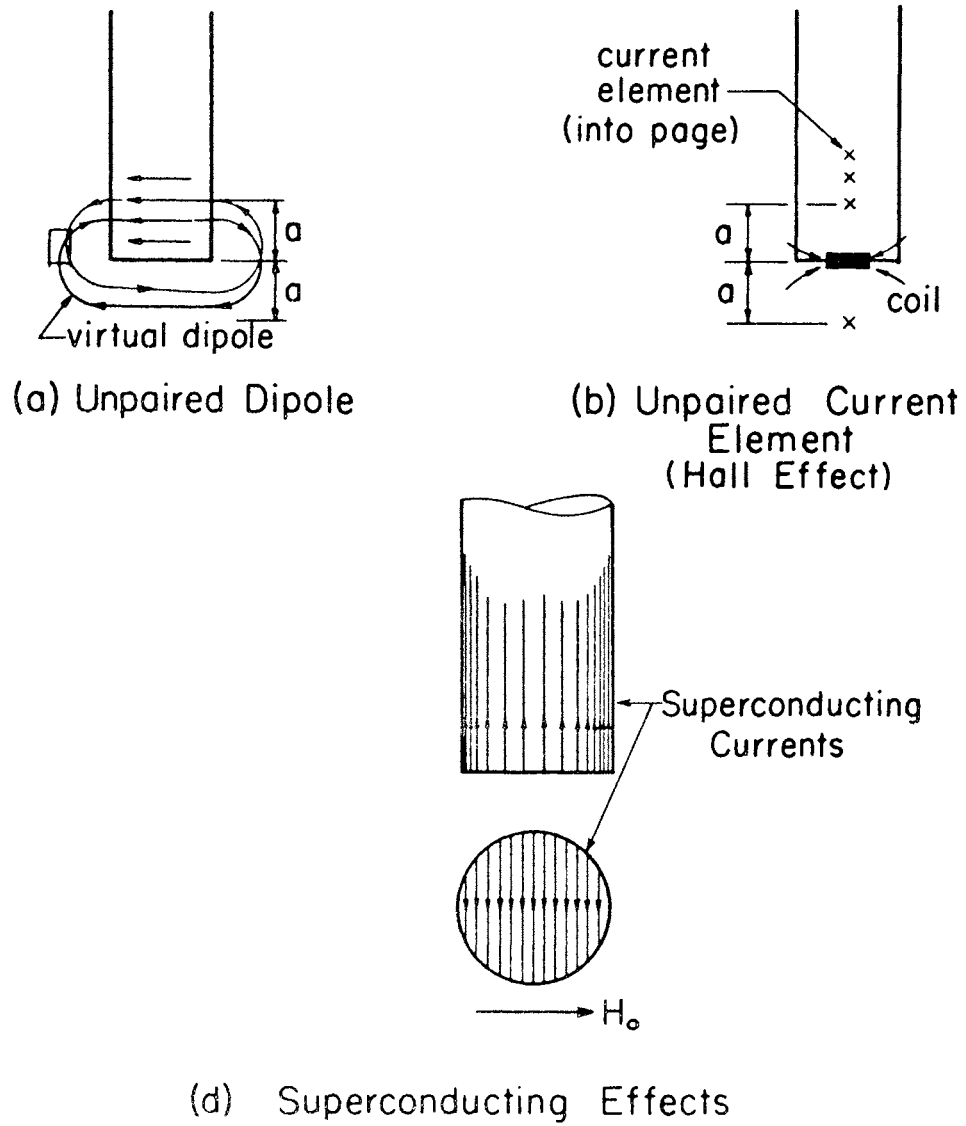


Figure 12 End Effects

## Lorentz Effects

(Normal, superconducting, and mixed states)

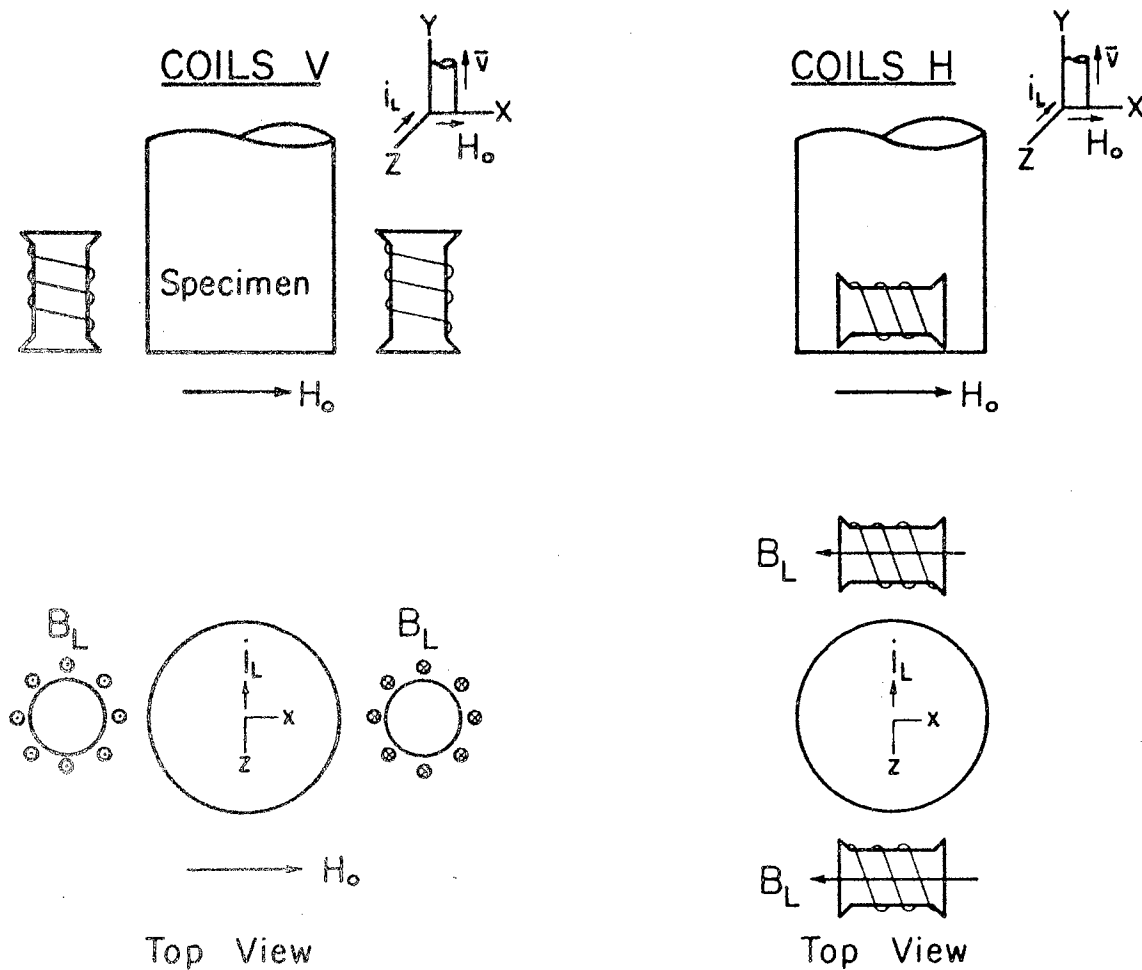


Figure 13. Lorentz Effects

# Magnetization Effects

(Superconducting State —  $\bar{B}_{int} = 0$ )

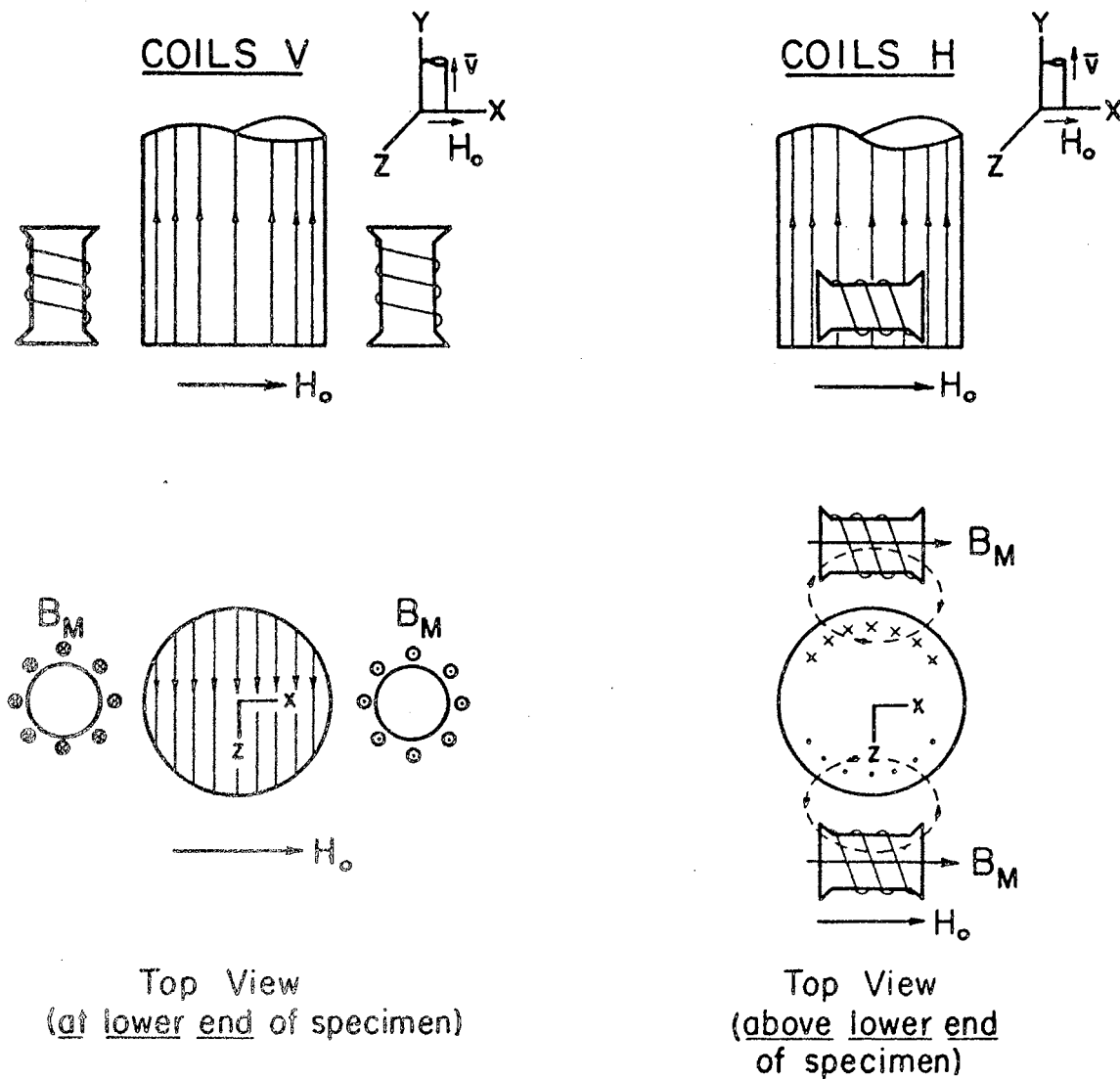
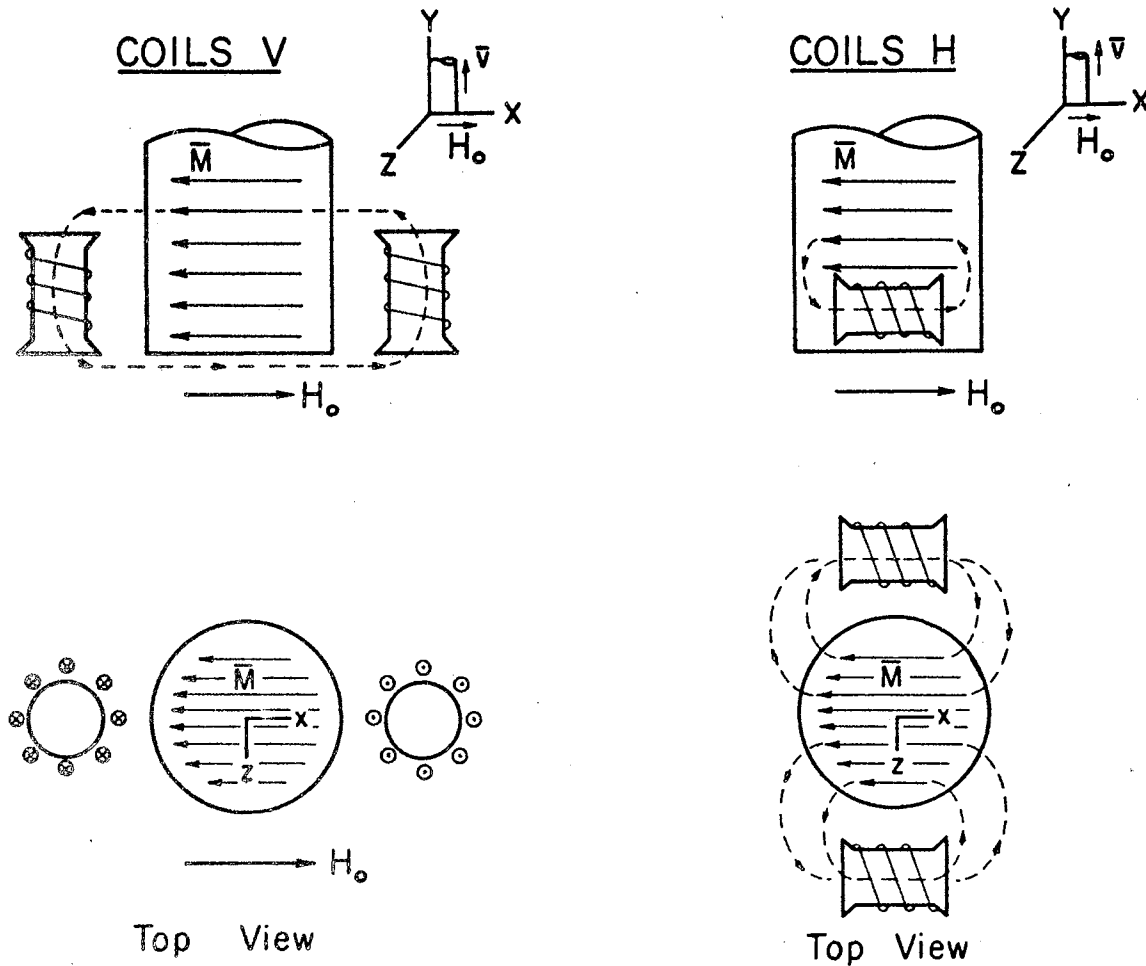


Figure 14. Superconducting Effects

## Magnetization Effects

(Normal State - Assume material to be diamagnetic.)



Magnetization effects in coils V are due to end effects, and are additive.

Magnetization effects in coils H are additive.

Figure 15. Normal State (A.C. Hall Effects)



## CHAPTER IV

### PREDICTIONS CONCERNING THE BEHAVIOR OF THE SYSTEM--A MODEL

#### Contributions to the Induced Field

It is desirable to be able to say at least qualitatively whether the induced voltage is due to free charge motion, to induced dipoles, to superconducting or to normal-state effects. For this reason an attempt will be made below to analyze the outputs and determine the contribution of these effects in each of the three states, normal, superconducting, and mixed. For simplicity we shall assume a Type I superconductor.

In general there are four effects which can combine to give the total voltage in the coils. These are as follows.

- 1) There is the diamagnetic or paramagnetic effects. These are generally very small since  $X_m$  is of the order of  $10^{-6}$ .
- 2) There is the contribution due to the A.C. Hall Effect, or Lorentz Effect. Since the conduction electrons have high mobilities, these might be expected to be significant. The analysis of Appendix I shows that the Lorentz Effect should be linearly dependent on the applied field. This was also verified experimentally. It is a point open to question as to whether the effect remains linear below the superconducting transition. It is known that the superconducting state is due

to a "condensation" of some of the conduction electrons into a lower energy state. The simplest assumption to make is that the effect remains approximately linear. The experimental data does not contradict this assumption. A straight line through points in the normal state generally extrapolates to the origin or a point close to it.

- 3) There are superconducting effects. These are due to surface currents which can exist only below the critical field. The superconducting effects are therefore best analyzed by assuming some general type of current distribution which will give rise to a field  $M$  in the interior which just cancels the applied field  $H_0$ . For a cylinder in a transverse field this can only be accomplished by current elements which form "loops" about the specimen, and which lie in planes perpendicular to the applied field.
- 4) There are "end effects." These are of four basic types as described below and illustrated in Figure 12.
  - a) The "unpaired dipole" effect is due to the fact that the cylinder is not infinitely long. If it were, and a probe or small coil were placed as shown, the flux from corresponding pairs would cancel. Since there are no dipoles to pair with those above the end, there is a finite contribution to the total flux linking the coil.
  - b) The "unpaired current element" effect is completely analogous to a), but involves currents which flow parallel to the end. It therefore applies to the Lorentz currents.
  - c) Eddy Currents. These are due to surface currents (not

superconducting currents) associated with the discontinuities at the boundary.

The primary effect of eddy currents is to render the internal field non-uniform near the end. The end effects should not necessarily be regarded as un-representative of the state of the material, for in the superconducting state, all currents are surface currents. The end of the specimen is then just as representative of the surface as is any other point. Also note that types a) and b) end effects are in fact not surface effects but are due to the volume distribution of dipoles or currents, i.e., to the bulk state of the material. The only atypical contribution is that due to eddy currents. These are probably quite small.

- d) Superconducting Effects. These are due to the surface currents which exist in the superconducting state, and are illustrated in Figure 12(d).

#### Analysis of Coil Voltages

The voltages induced in the coils due to the above effects will depend on their placement in the system and the way in which they are connected together. We shall consider each pair separately.

A. Coils H (Horizontally mounted at the end of the specimen--see Figures 8, 10, 13, 14, 15). Suppose the end of the sample to be moving upwards. Then the Lorentz currents will be in the  $-Z$  direction. The field from a single current element of any length is cylindrically symmetric about the axis of the element. Since most of the current

elements are above the coils, there will be a contribution  $B_L$  in these coils as shown. The coils H are connected so that if the field components along their axes are in the same direction, the induced voltages will add. This may be checked by assuming  $\vec{v}$  (the velocity) to be upwards and applying Lenz's Law. The contribution from the Hall Effect is therefore additive.

In the superconducting state (Figure 15) the surface currents will again induce voltages which add to each other. Coils H then can be expected to give a sum of two effects--one due to the Hall Effect, the other to the superconducting currents.

#### B. Coils V (Figures 1, 11, 13, 14, 15).

These coils are connected so that if the field components along the axis are in opposite directions, the voltages will add. If  $\vec{v}$  is upwards, the field due to Hall Effects is into the page on the right side and out of the page on the left. The Hall Effects are again additive.

In the superconducting state the surface currents down the side of the specimen cannot contribute to the flux through Coils V, since the direction of this field is perpendicular to the coil axis and so no flux links any of the coil loops. However at the end the currents can produce a flux contribution as shown in Figure 14. On comparing Figures 13 and 15 one might well ask what the relation is between the flux  $B_L$  and the flux  $B_M$  at any instant in time--do they add or subtract? The only answer that can be given is that there may well be some time lag, i.e., phase difference, between the maximums of  $V_L$  and that of  $V_M$ . It would be expected then that when superconducting effects vanish, there will be an apparent phase shift. The situation can be represented

in the complex plane as shown below.

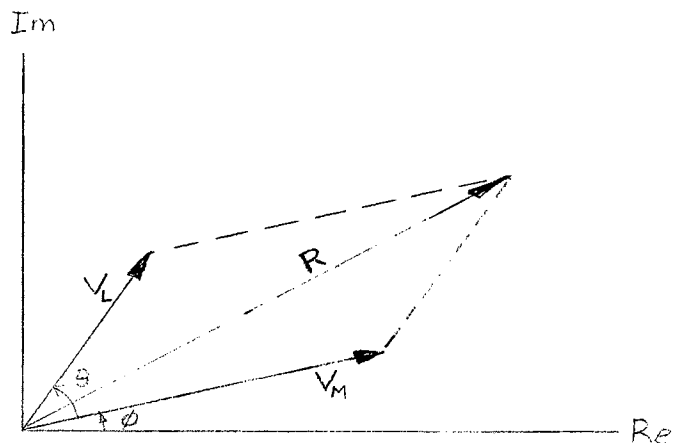


Figure 16. Superposition of Voltage Contributions

The vectors represent the voltages due to the two effects. As the applied field is increased through the critical field  $H_{c2}$  (or  $H_c$  for Type I materials) the vector  $V_M$  tends toward zero causing the resultant  $R$  to tend toward  $V_L$ , giving a phase shift.

One might also ask why a similar phase shift is not observed in coils H. The most plausible answer is that these coils see predominantly the superconducting currents down the sides. The currents here are distributed so that vibration along the Y-axis does not change the flux through coils H appreciably with respect to time. Indeed the voltage from coils H was consistently observed to be less than that of coils V in the superconducting state, usually by a factor of one-half or less.

## CHAPTER V

### EXPERIMENTAL RESULTS

#### Nitrogen ( $77^{\circ}\text{K}$ ) and Room Temperature Data

The graphs 1 through 7 show data taken at room temperature and liquid nitrogen temperatures. The coil signals for each coil were normalized by dividing all voltages for a given coil by the voltage at 10 KG, which was usually the maximum field. This enabled one to plot both coil voltages on the same scale, and makes the interpretation of the normal state easier, since any signal which is proportional to the applied field and is zero when  $H_0 = 0$  will plot as a straight line through the origin and the point (10 KG, 1). In all cases the expected linearity in the normal state was confirmed. The apparent deviation from a linear dependence at low fields (graphs 1 and 2) is due to a residual signal originating in the electronic exciting network. The phase data (graph No. 3) strongly suggests this since at low fields the phase is rapidly changing--the small residual signal is being overcome by the Hall Effects. Graphs 4 through 6 confirm the linearity for Nb for both temperature and nitrogen temperature. Graph No. 7 shows normal state data for a Nb specimen of boat-shaped cross-section.

#### Results in the Superconducting Region

As stated in Chapter II, the magnetization curve for high-purity lead is particularly simple since it is a Type I superconductor. We

shall show that the graph (No. 9) can be interpreted in terms of the assumptions put forth earlier. The critical field will be taken to be 575 gauss, the point at which the curve returns to the normal-state line. An infinitely long cylinder has a demagnetizing factor of  $1/2$ . Thus penetration effects should begin at approximately  $H_c/2$  or 288 gauss, or slightly higher according to the theory of Landau. The peak of the curve therefore coincides with the point at which the specimen enters the mixed state. This is what would be expected, since superconducting currents are being destroyed in the mixed state, allowing the field to penetrate. In the region 0.3-0.4 KG we shall assume that Hall Effects are negligible. This is certainly true at the beginning of the mixed state, since almost all of the material is still superconducting, so that the field in the interior is zero. A zero field implies that the Hall Effects are zero. Note that the slope in the mixed state does not change until  $H = 0.5$  KG. At this point the shielding currents have practically vanished, so that the Hall currents become significant and change the slope of the line. The penetration is not complete until  $H = 0.575$  KG. Thereafter the only effect is the normal-state Hall currents which have a linear dependence on the field. One must also remember that in the region 0.400 to 0.575 KG the phase of the resultant voltage is changing due to the changing ratio of the superconducting component to the normal-state component. The phase relationships may be clarified by a consideration of the phasor diagrams of Figure 16.

We shall assume that there are two components to any measured voltage--one due to the superconducting effect, the other due to the Hall currents. We shall also assume that  $\theta$  and  $\phi$  are constants. The

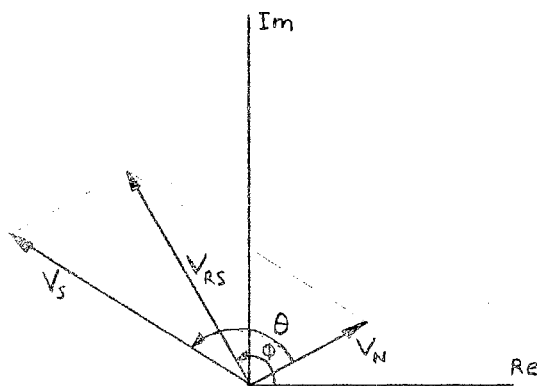
phase data indicates this is to be roughly true. We also assume that the Hall Effects have the same field dependence in both the superconducting and normal state, that above  $H_c$  the superconducting effects are zero, and that any measured voltage below  $H_c$  can be represented by

$$\bar{V}_{RS} = \bar{V}_S + \bar{V}_N$$

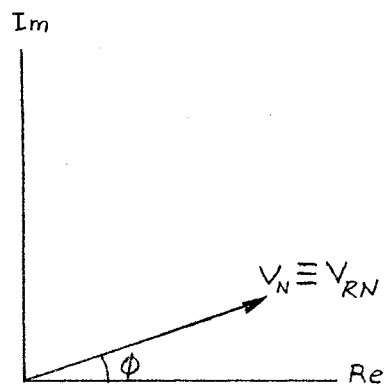
while in the normal state

$$\bar{V}_{RN} = \bar{V}_N.$$

the situation is illustrated below:



Superconducting



Normal

The voltage  $V_{RS}$  is the resultant voltage vector and is what is actually measured. In the normal state,  $V_N$  is measured. Thus, in the superconducting state the magnitude of  $V_{RS}$  is



$$|\bar{V}_{RS}| = [V_N^2 + V_S^2 + 2V_S V_N \cos\theta]^{1/2}$$

by the law of cosines.

In the superconducting state the magnitude of  $V_S$  should be given by  $V_S = K_1 H + S_0$ , assuming linear penetration. At  $H = H_c$  the superconducting effect must become zero, and remain there. Hence

$$V_S(H_c) = -K_1 H_c + S_0 = 0 ; \quad K_1 = -\frac{S_0}{H_c}$$

or

$$V_S(H) = S_0 \left(1 - \frac{H}{H_c}\right)$$

In the normal state,

$$V_N = K_2 H$$

and  $K_2$  must (under our assumptions) also be the same in the superconducting state. The expression for  $V_{RS}$  then becomes

$$V_{RS} = [C_1 H^2 + C_2 H + C_3]^{1/2}$$

where

$$C_1 = \left(\frac{S_0}{H_c}\right)^2 + K_2^2 - \frac{2K_2 S_0}{H_c} \cos\theta$$

$$C_2 = -2 \frac{S_0^2}{H_c} + 2K_2 S_0 \cos\theta$$

$$C_3 = S_0^2$$

The minimum for  $V_{RS}$  will occur at  $H_0 = \frac{-C_2}{2C_1}$  and

$$V_{RS}(H_0) = \left[\frac{1}{2} C_2 H_0 + C_3\right]^{1/2} = V_0$$

which gives

$$\begin{aligned} \cos\theta &= \left[ V_0^2 - S_0^2 \left(1 - \frac{H_0}{H_c}\right) \right] \frac{1}{K_2 H_0 S_0} \\ &= \frac{S_0}{K_2 H_0} \left[ \frac{V_0^2}{S_0^2} - \left(1 - \frac{H_0}{H_c}\right) \right] \end{aligned}$$

All of the constants may be determined graphically, and the result for  $\theta$  may be compared with the phase data. Evaluation of  $\cos\theta$  for Pb, graph No. 10, Coils V gives:

$$\cos\theta = \frac{S_0}{K_2 H_0} \left[ \left( \frac{V_0}{S_0} \right)^2 - \left( 1 - \frac{H_0}{H_c} \right) \right]$$

$$S_0 = 0.874 \times 0.445 = \underline{0.389}$$

$$K_2 = 0.0970$$

$$V_0 = 0.0173$$

$$H_0 = 0.450$$

$$H_c = 0.500$$

$$\begin{aligned} \cos\theta &= \frac{0.389}{0.097 \times 0.450} \times \left[ \left( \frac{0.0173}{0.389} \right)^2 - \left( 1 - \frac{0.450}{0.500} \right) \right] \\ &= 8.92 \left[ 4.44^2 \times 10^{-4} - (1 - 0.900) \right] \\ &= 8.92 \left[ 19.8 \times 10^{-4} - 0.100 \right] \\ &= 8.92 (-0.098) = -0.875 \end{aligned}$$

$$\theta = 120^\circ$$

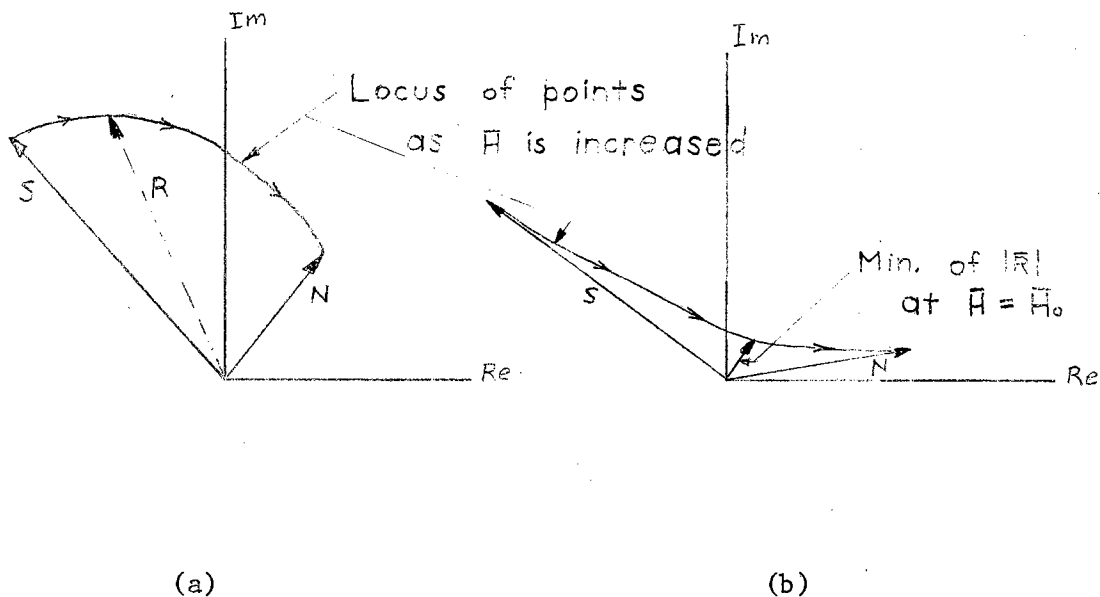
in fair agreement with the phase data:

$$\theta = 200^\circ - 50^\circ = 150^\circ$$

Now the minimum at  $H = H_0$  may or may not occur, because if  $H_0 > H_c$  the material has already gone into the normal state region when  $H = H_c$  and the expression for  $V_{RS}$  is no longer the assumed parabolic form, but is linear. The occurrence or non-occurrence of the minimum is therefore dependent on the physical parameters of the system. If  $H_0 < H_c$  the minimum will be observed--there will be a pronounced "dip" in the curve

just before it enters the normal state. If  $H_0 > H_c$  the minimum will occur at  $H_c$ , and will be observed as a discontinuity in the slope. This may be seen even more clearly by considering the following two cases.

Assume that two similar specimens are observed at some point  $H$  just into the mixed state.



In both cases we have shown the locus of points which the resultant vector  $V_B$  traces out as  $H$  is increased through  $H_c$  into the normal state. In case (a) the relationship between  $S$  and  $N$  is such that the magnitude of  $R$  steadily decreases until the specimen is completely normal, and no "dip" is observed. In case (b), however, there will be a minimum in the magnitude of  $R$  before the specimen is completely normal, after which the magnitude will increase until the specimen is completely normal. This was observed in lead (graph No. 10) for coils V. This was the value used in calculating  $\cos\theta$ .

What has been shown so far is that by assuming a linear penetration in the mixed state one can derive a function that has the general shape of the amplitude curve, and that the phase data roughly agrees with this assumption.

In Tables I, II and III all fields are given to KG.  $H_M$  is the point at which there was a maximum in the signal, and the following column gives the normalized value of the signal. Similarly,  $H_0$  is the occurrence of a minimum, and the signal is normalized. The sign of the phase shift is taken to be positive if it shows a marked increase with increasing field otherwise it is negative. The last column gives the coil outputs at 10 KG in micro-volts, thus permitting one to convert the normalized values to voltage values. Table III summarizes the factors which were considered in determining the critical fields.

The data for lead (run No. 1) shows that penetration effects begin at 280 G. The demagnetizing factor for the cylinder is about 1/2, and on the basis of Landau's theory one would expect the peak to occur at  $1/2(500) = 250$  G or slightly higher. This agrees well with the observed value. The data for decreasing field (No. 1) follows closely the curve for increasing field. This is characteristic of Type I materials.

For the second run with Pb the same behavior was observed. Penetration began at 300 G and  $H_c$  occurred at 0.510. These coils were not the same as those used in run No. 1.

The square niobium specimen shows typical Type II behavior in that the curve for H decreasing does not retrace itself, due to trapped flux within. Even at  $H = 0.0$  there is a residual field due to these trapping effects. This is also true of the other three niobium samples.

We next consider similarities and differences between different

specimens and different orientations. The signal in coils V is consistently higher than in coils H. The ratio between the two is even greater in the superconducting state. This is probably because the superconducting currents at the end induce an appreciable voltage in coils V while those along the sides do not contribute greatly.

The phase change in coils V occurred in all cases except the single crystal with H// [111] axis. The reason it did not occur here is not known--it could be due to some experimental anomaly or it may be a true orientation effect. One difficulty was that the specimen sometimes tended to move as the field was increased.

The minimum in voltage in all cases appeared before  $H_{c2}$ , though sometimes quite close to it. The Hall Effect is also quite linear with respect to applied field, as predicted. The greatest non-linearity was for the niobium single crystal, run No. VI. The return of the curve toward a straight line was very gradual and non-linear. The reason for this behavior is not known.

It is of interest that critical fields for niobium apparently depend on the geometry and orientation.  $H_{c1}$  varies from 0.600 to 1.35 KG while  $H_{c2}$  varies from 2.20 to 3.10. The data presented here are of a rather preliminary sort for purposes of making such comparisons, because the specimens were not made from a common rod, and because there is not enough data. Also, the structures are different, being either polycrystalline or single crystal.

TABLE I  
SUMMARY OF DATA FOR  $\bar{H}$  INCREASING

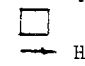
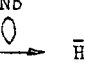
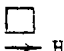
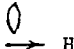
Run Number	Spec.	$H_c$ or $H_{cl}$ KG.	$H_{c2}$ , KG.	Peak Sig. $H_M$ , KG.	Peak Sig. at $H_M$	Min. in Sig. $H_o$	Min. Sig. at $H_o$	Phase Shift (coils V) KG.	Sig. at 10 KG. $\mu$ Volts
29 Aug.									
I <sup>H</sup> <sub>V</sub>	Pb-Cyl.	0.500	----	0.280	0.0770	0.475	0.0360	0.450 to 0.500 -	185
				0.280	0.140	0.450	0.010		210
9 May									
II <sup>H</sup> <sub>V</sub>	Pb-Cyl.	0.510	----	none	none	none	none	0.500 -	82
				0.306	0.260	0.500	0.000		135
III <sup>H</sup> <sub>V</sub>	Nb - Sq. 	0.950	2.60	none	none	none	none	2.20 to 2.60 +	1820
				1.00	0.393	2.4	0.00		2500
IV <sup>H</sup> <sub>V</sub>	Nb 	1.35	3.10	1.76	1.63	2.90	0.329	2.4 to 2.8 -	243
				1.76	1.28	2.90	0.0338		4050
V <sup>H</sup> <sub>V</sub>	Nb Single Crystal $\bar{H}$ 111	0.600	2.60	none	none	none	none	1.1 (dip)	180
				0.650	0.0355	1.02	0.0775		1830
VI <sup>H</sup> <sub>V</sub>	Nb Single Crystal $\bar{H}$ 100	0.619	2.20	0.619	0.360	1.10	0.226	0.900 to 1.50 +	2500
				0.711	0.178	1.10	0.0489		4600

TABLE II  
SUMMARY OF DATA FOR  $\bar{H}$  DECREASING

Run Number	Spec.	$H_c$ or $H_{c1}$ KG.	$H_{c2}$ (From Table I)	Peak Sig. $H_M$ , KG.	Peak Sig. at $H_M$	Min. in Sig. $H_o$	Min. Sig. at $H_o$	Phase Shift (coils V) KG.	Sig. at 10 KG. $\mu$ Volts
29 Aug.									
I	Pb-Cyl	0.500	----	0.275	0.0713	0.471	0.0368	0.450 to 0.400 +	185
				0.285	0.131	0.442	0.0119		210
9 May									
II	Pb-Cyl	0.510	----	none	none	none	none	0.540 to 0.470 +	82
				0.280	0.248	0.470	0.0148		135
III	Nb-Sq. 	0.950	2.60	none	none	0.900	0.0067	0.960 to 0.900 +	1820
				1.85	0.344	0.900	0.281		2500
IV	Nb 	1.80	3.10	0.510	1.32	2.50	0.096	2.80 to 2.0 +	243
				0.510	1.59	2.84	0.341		4050
V	Nb Single Crystal 111	0.600	2.60	0.550	0.244	0.240	0.011	none	180
				none	none	none	none		1830
VI	Nb Single Crystal 100	0.619	2.20	none	none	none	none	none	2500
				none	none	none	none		4600

Type	$H_{c1}$ , KG (or onset of nonlinear magnetization)	$H_{c2}$
I	0.280 - Sharp peak in coils H, peak in coils V.	Coils H are nearly coincident with normal-state line at 0.470. Coils V reach normal state at 0.580. Phase change is complete at 0.500.
II	0.300 - Peak in coils V. Data is insufficient to determine the linearity.	Sharp phase change - complete at 0.510 Coils V are past the minimum at 0.510
III	0.960 - Sharp peak in coils H. Coincides with peak in coils V.	Sharp phase change - complete at 2.60 Amplitude of both coils has reached normal-state line.
IV	1.35 - Jumps in the curve suggest nonlinearities below the peak. There is also a jump in the phase curve.	Phase is changing rapidly. Both curves lie on the normal-state line at 3.10.
V	0.600 - Peak in coils V.	Minimum in coils V occurs considerably before material is normal. Amplitude nearly coincide with normal-state line at 2.60. There is no phase change.
VI	0.620 - Sharp peak in coils H.	2.80 - Quite ambiguous since the return to the normal state is gradual and fluctuates.

TABLE III

INTERPRETATION OF DATA



## CHAPTER VI

### SUMMARY AND CONCLUSION

The above work shows that the method of measurement described above has at least three advantages over more conventional methods.

- 1) It gives a sharp discontinuity in the phase of the voltage at  $H_{C2}$ .
- 2) It can give information about relative phases between the forcing function, the Hall Effect, and superconducting effects.
- 3) There are no leads in contact with the specimen. This is significant because in more conventional methods it is necessary to wrap a wire around the sample or even to make a metal-to-metal junction, either of which can distort the surface currents in the superconducting region.

We have also shown that the voltages induced in the coils can be fairly well explained by assuming a superposition of voltages in the intermediate state which must be combined vectorially.

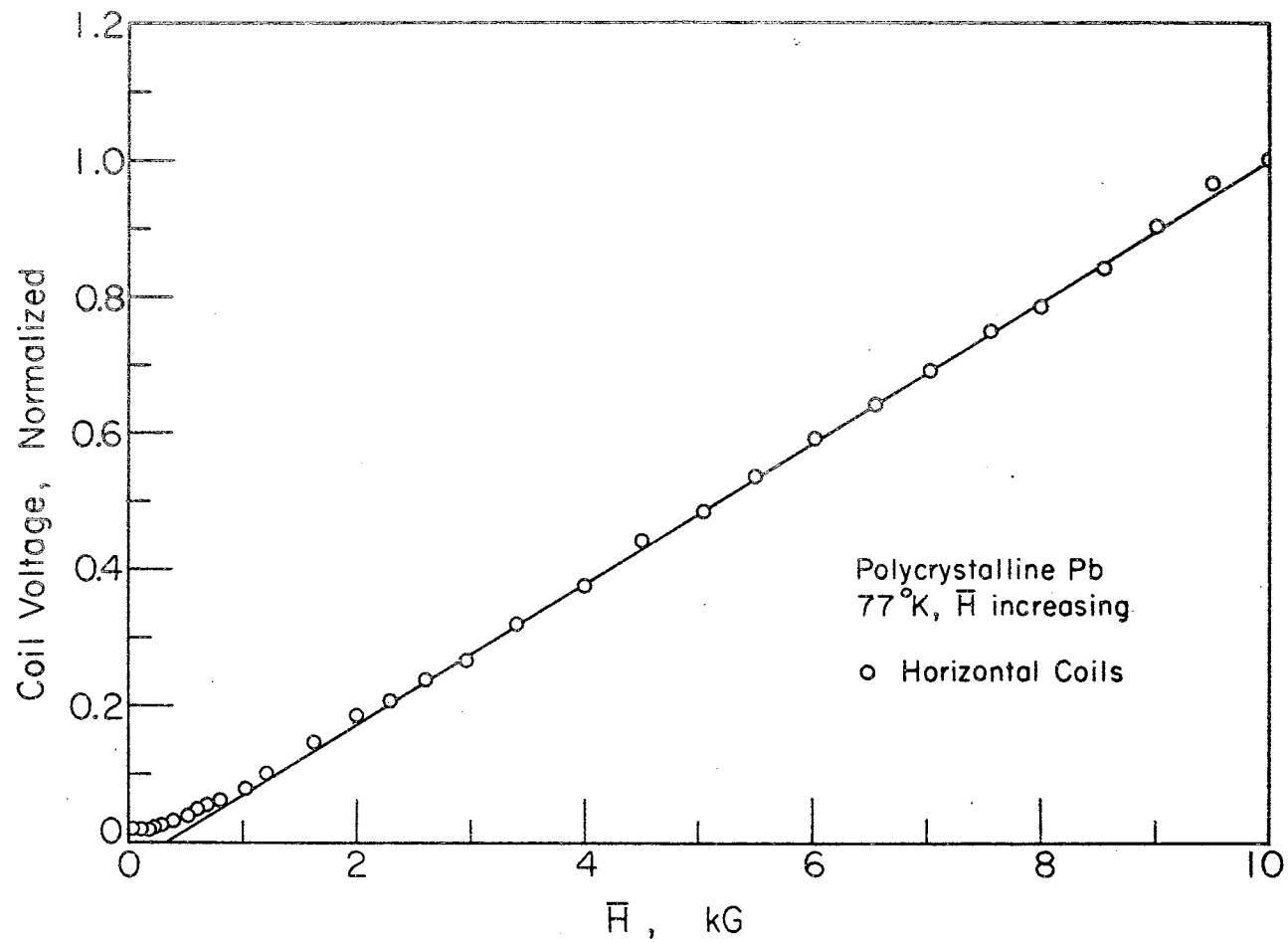


Figure 17. Coils H, Amplitude for Pb

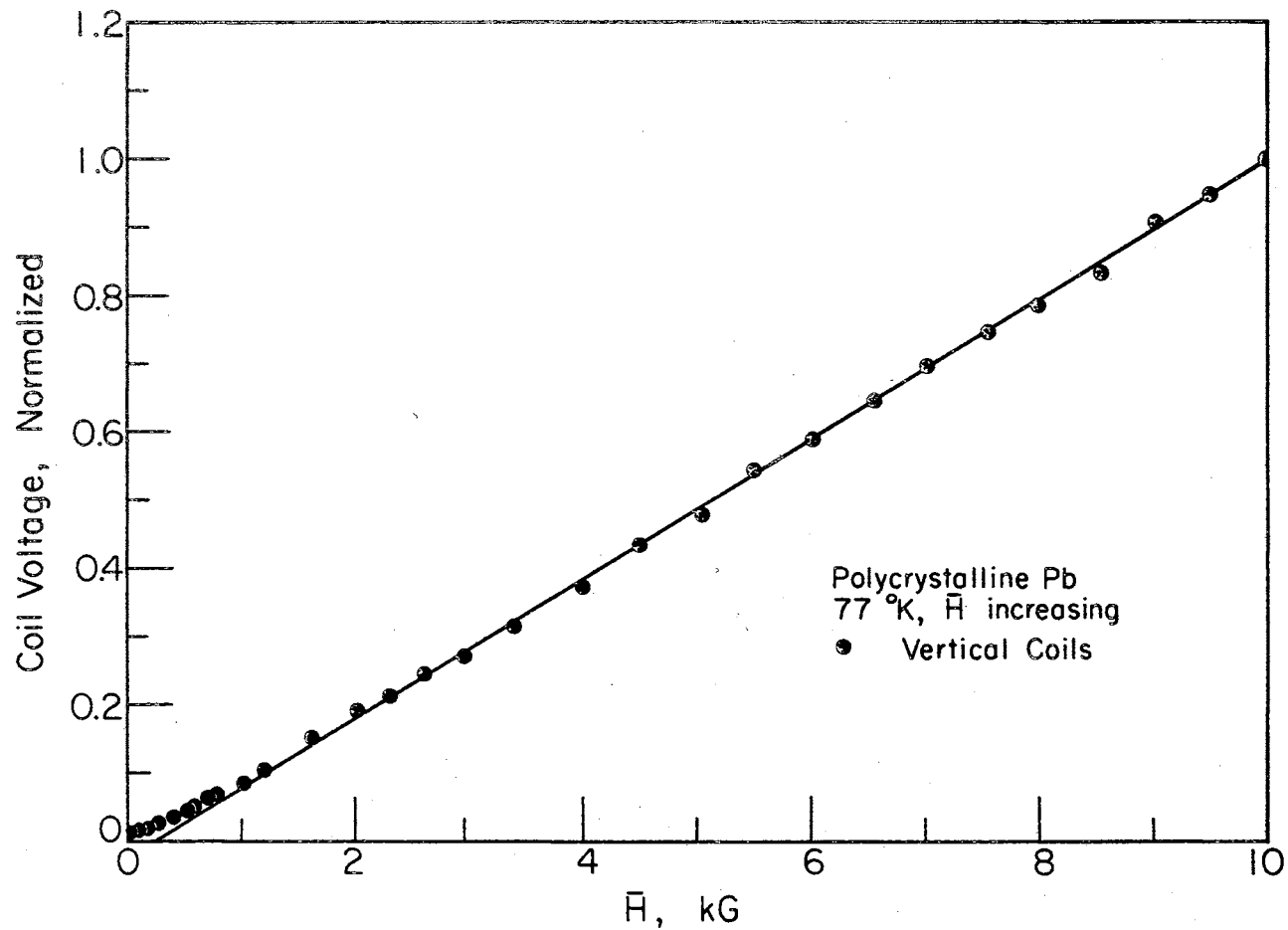


Figure 18. Coils V, Amplitude for Pb

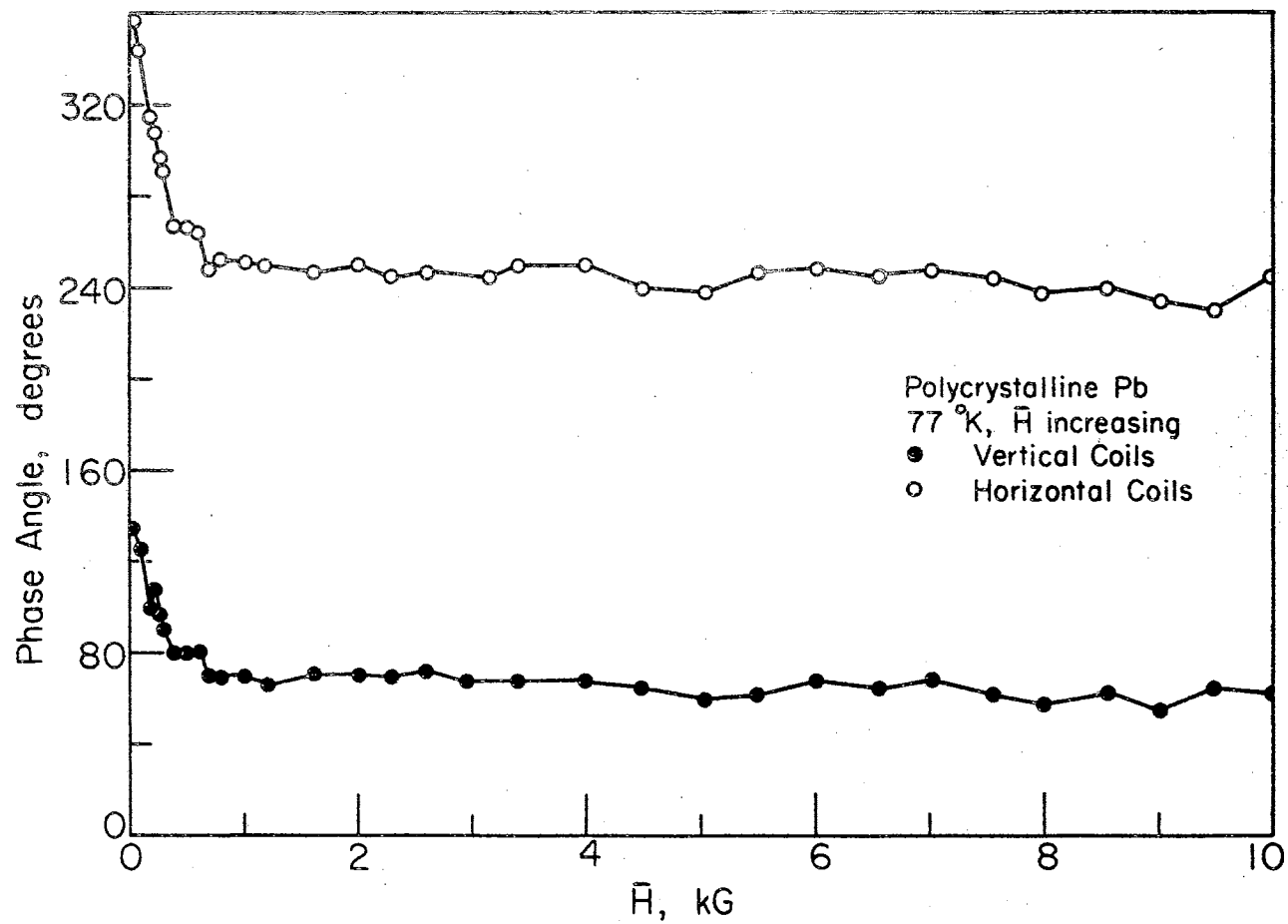


Figure 19. Coils H and V, Phase for Pb

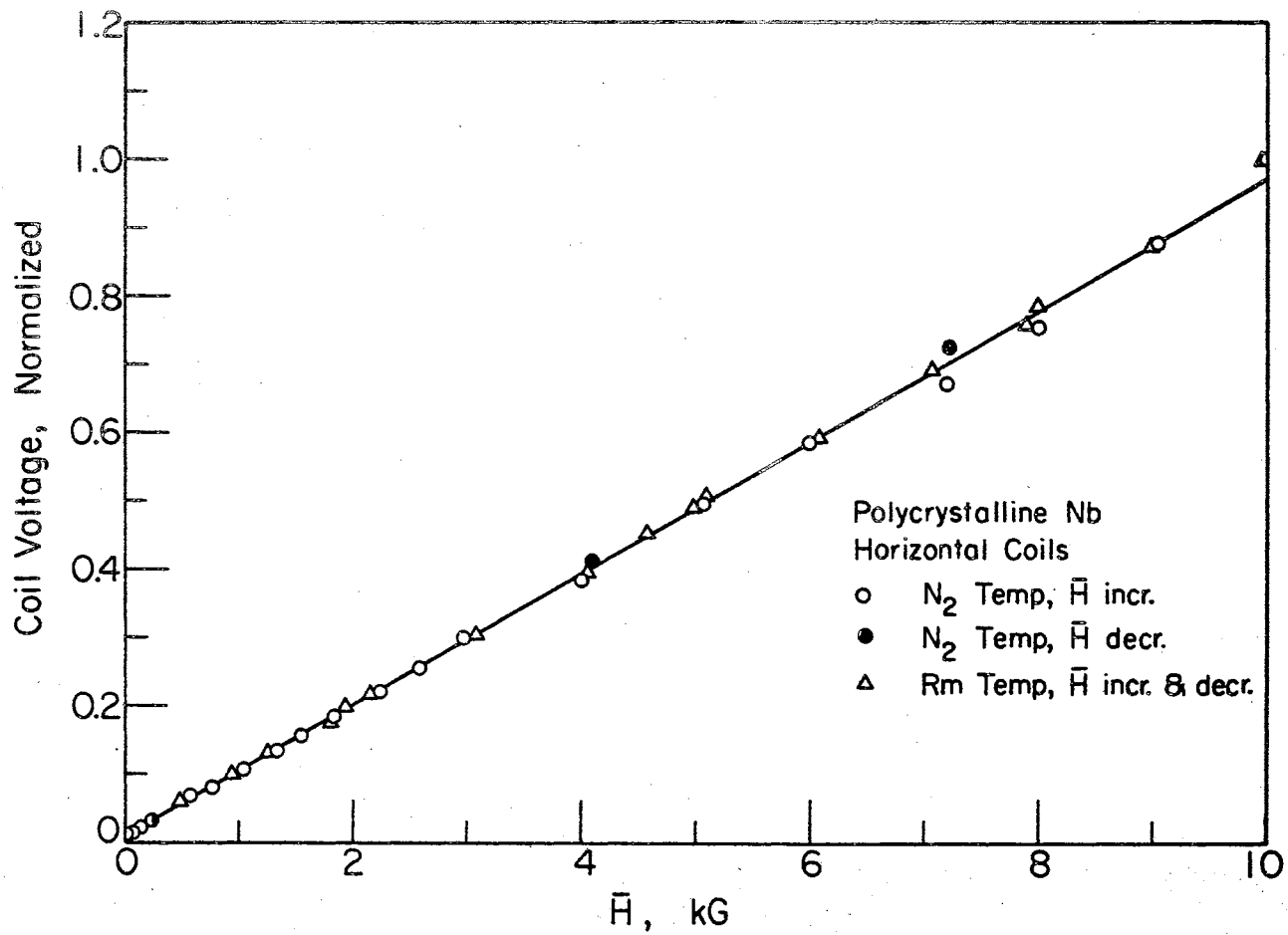


Figure 20. Coils H, Amplitude for Nb I

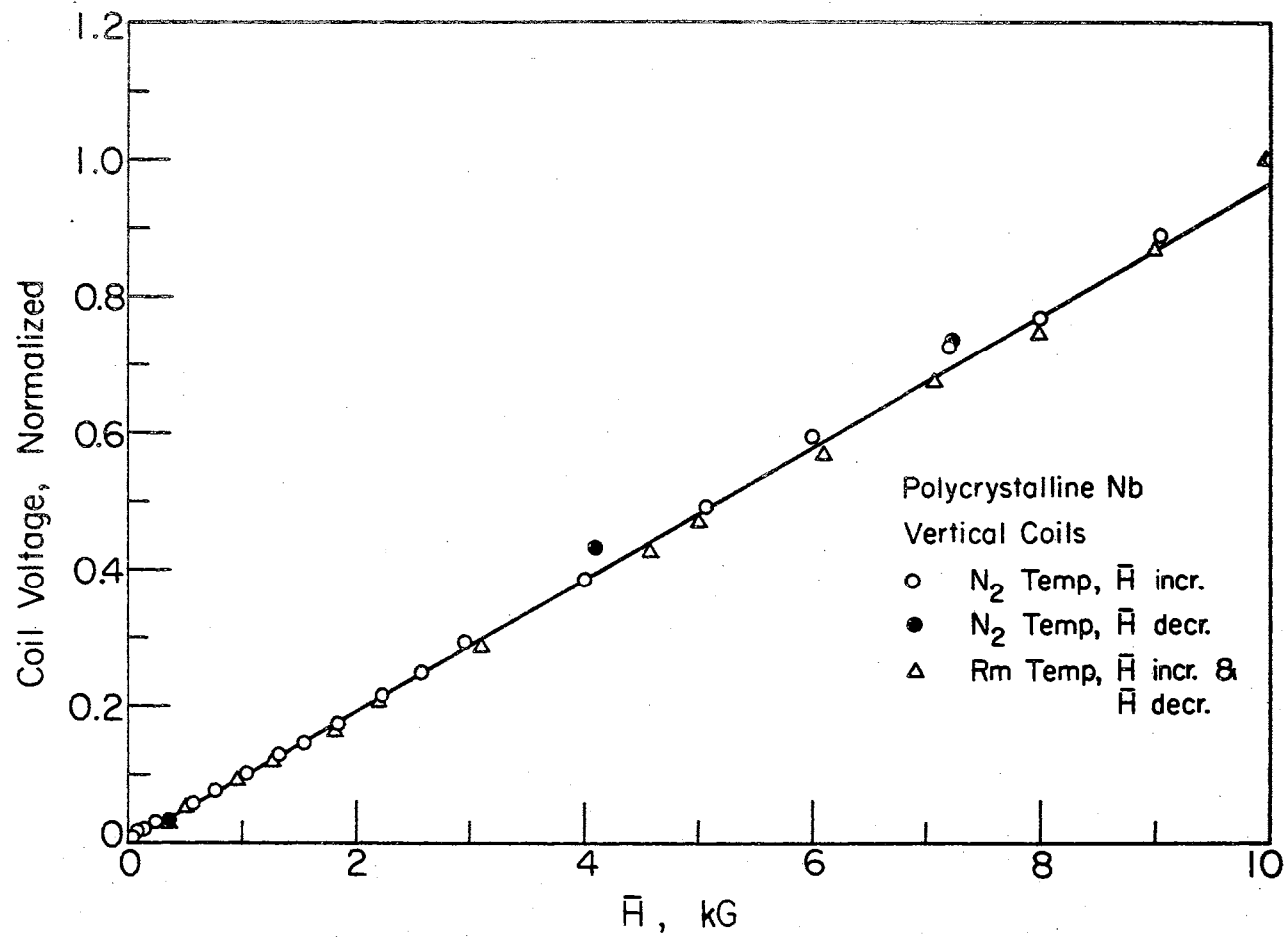


Figure 21. Coils V, Amplitude for Nb I.

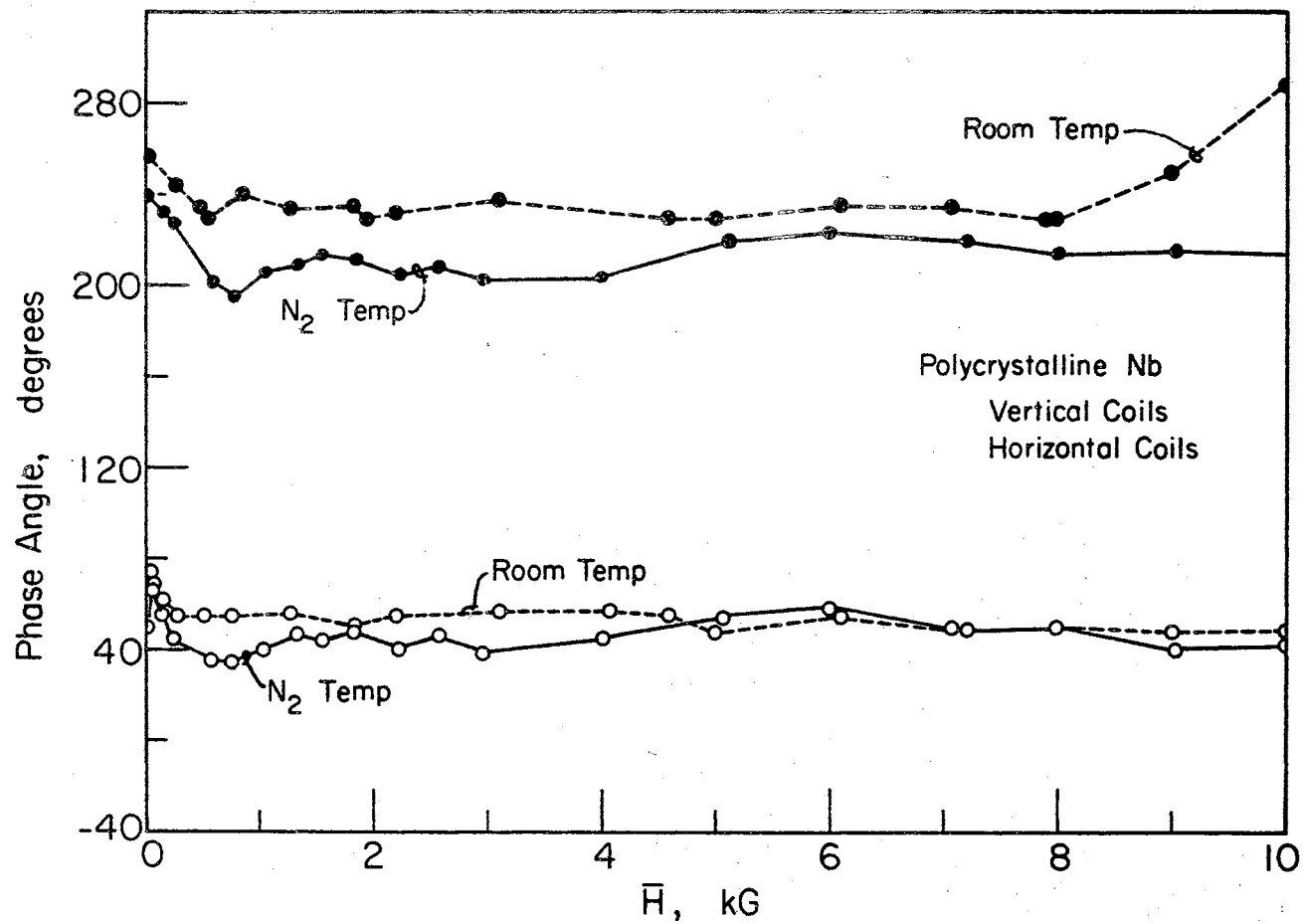


Figure 22. Coils H and V, Phase for Nb I

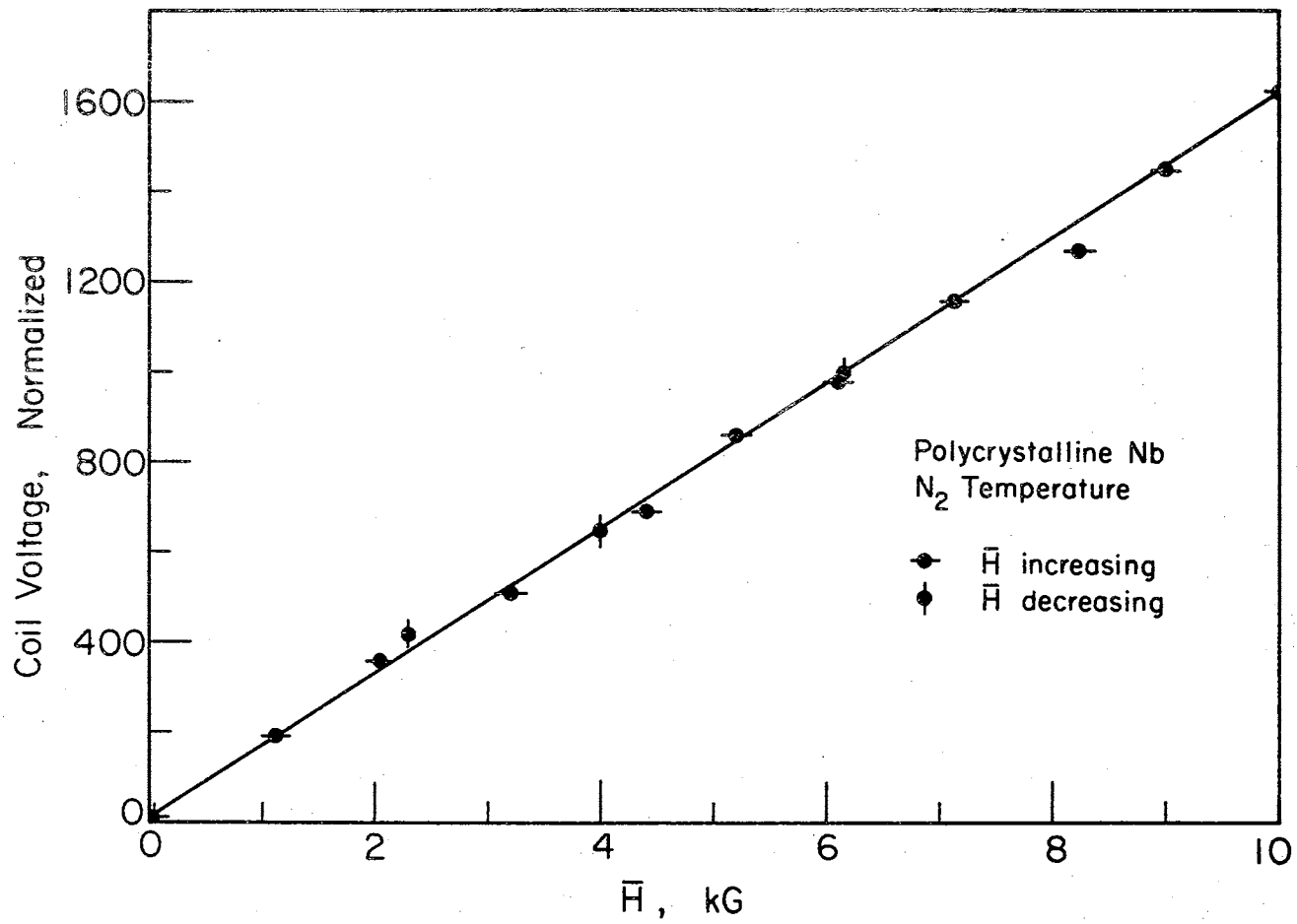


Figure 23. Coils V, Amplitude for Nb II



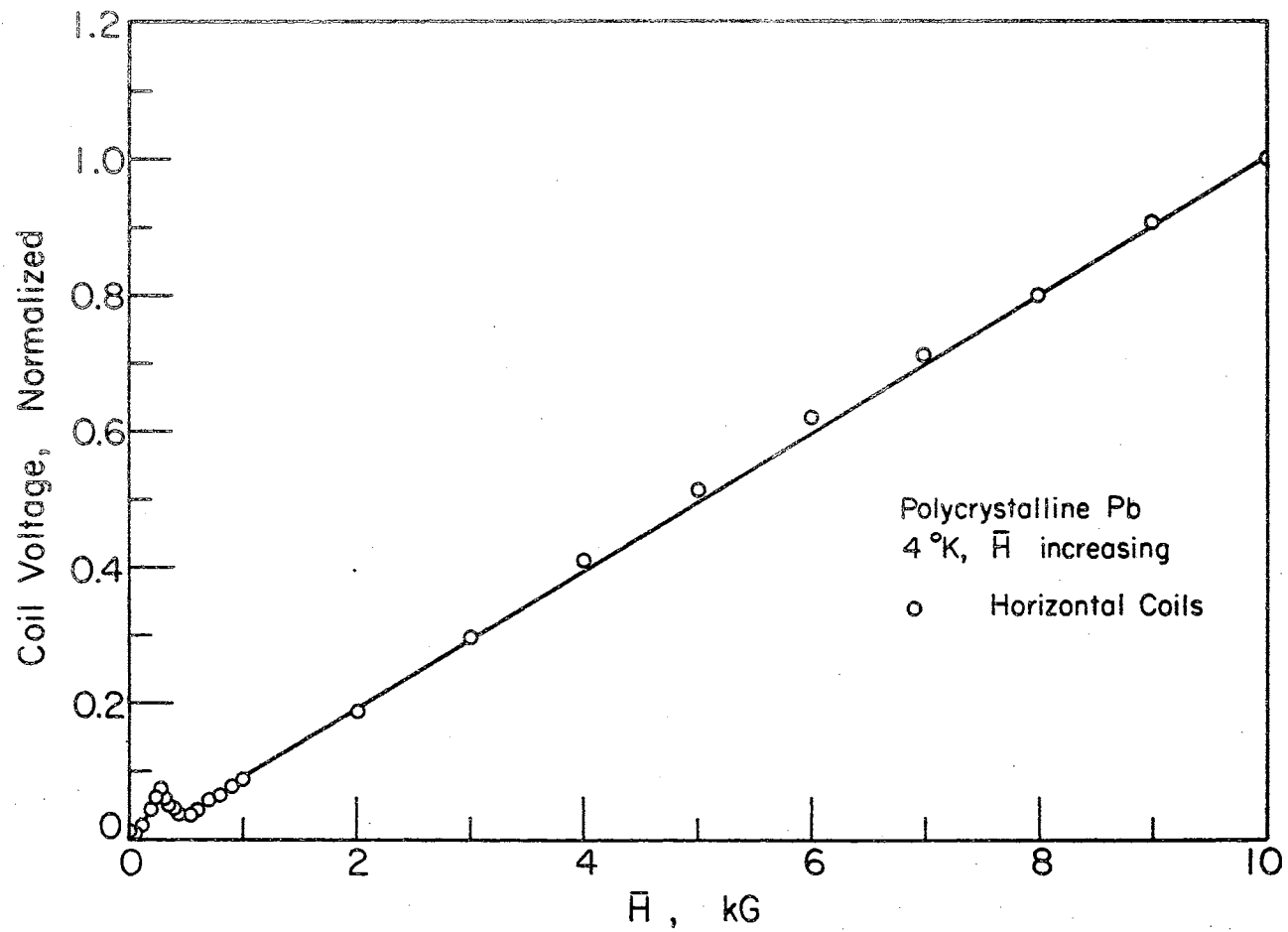


Figure 24. Coils H, Amplitude for Pb I, H Increasing

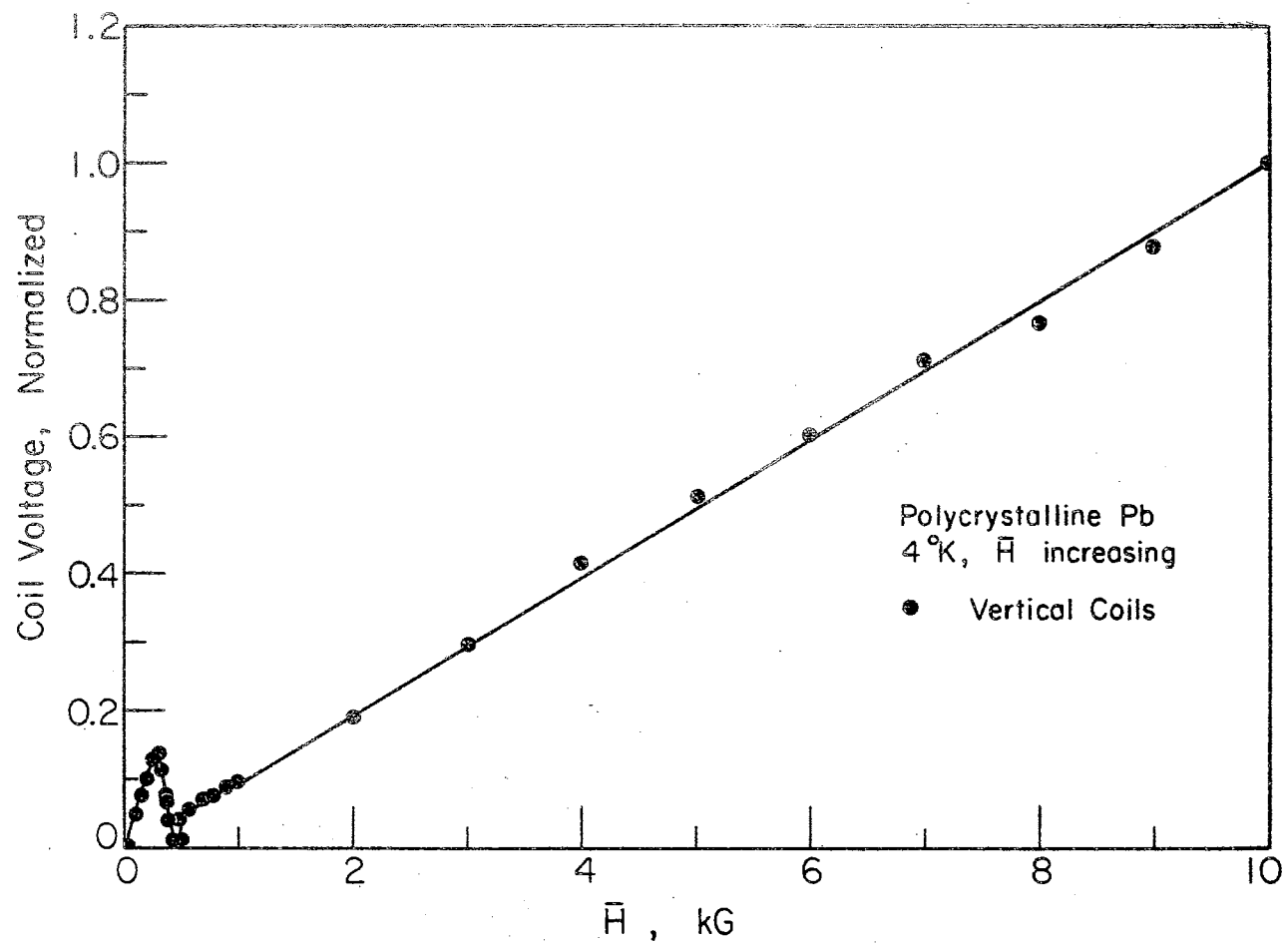


Figure 25. Coils V, Amplitude for Pb I, H Increasing

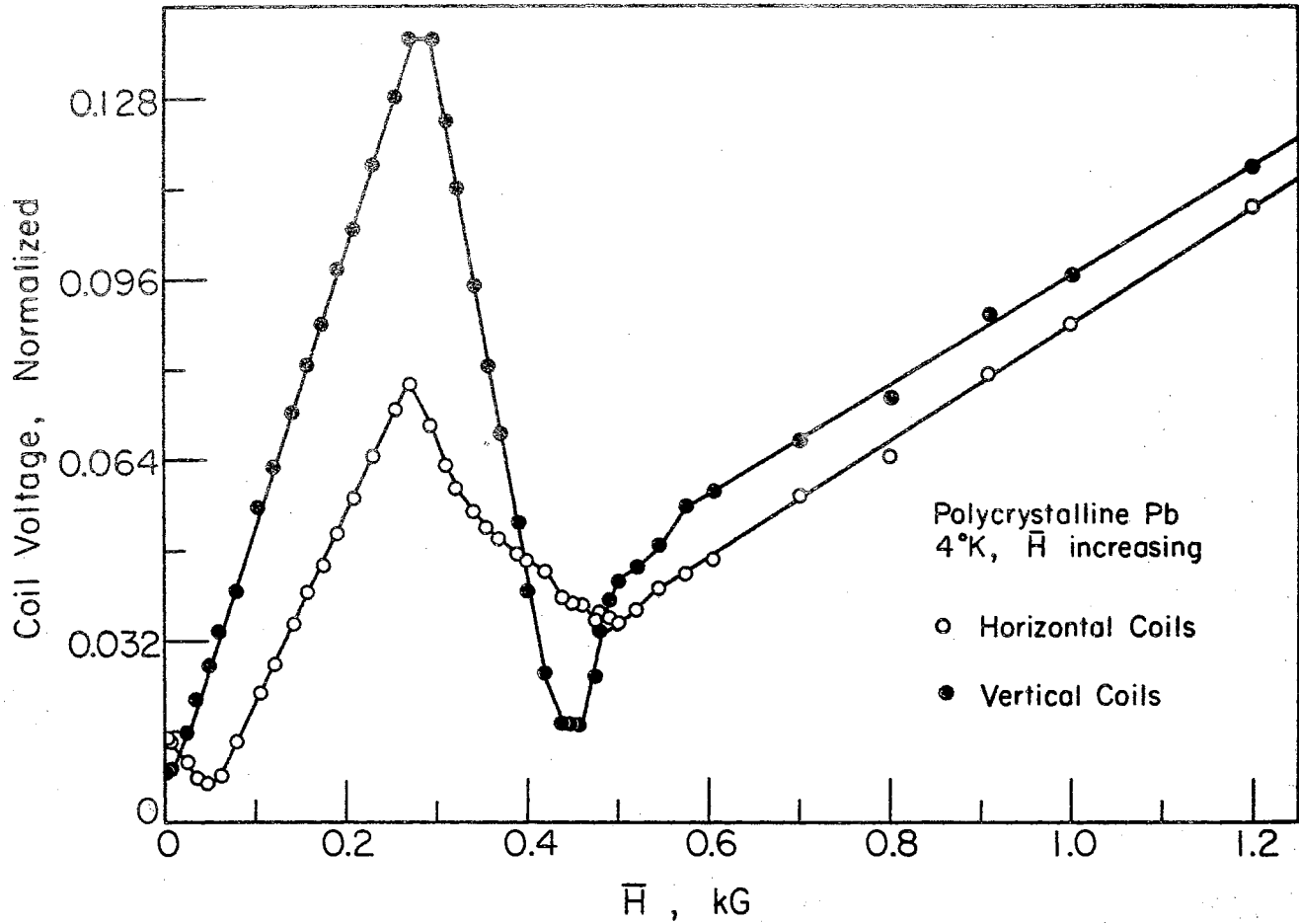


Figure 26. Coils H and V, Amplitude for Pb I, H Increasing

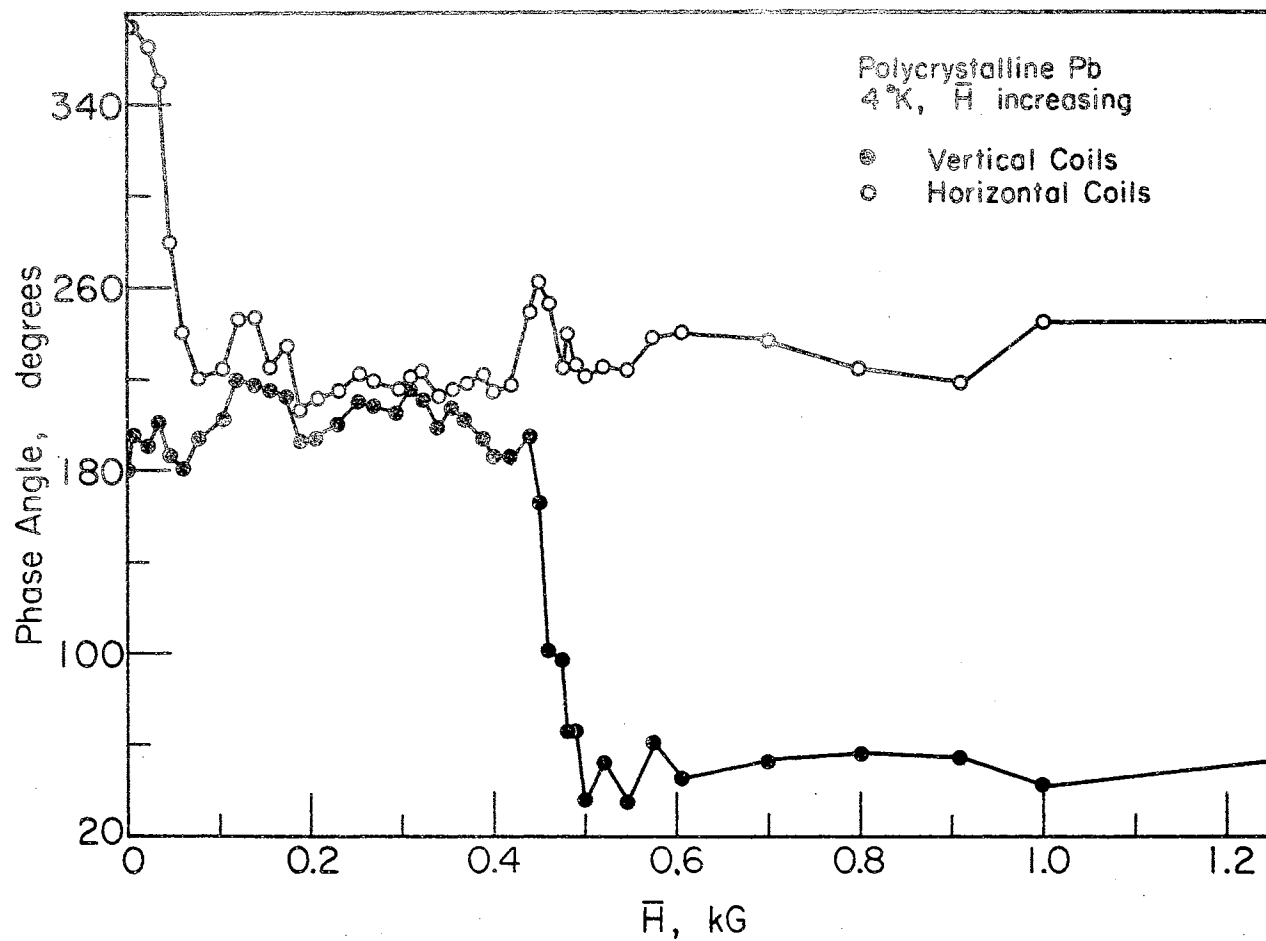


Figure 27. Coils H and V, Phase for Pb I, H Increasing

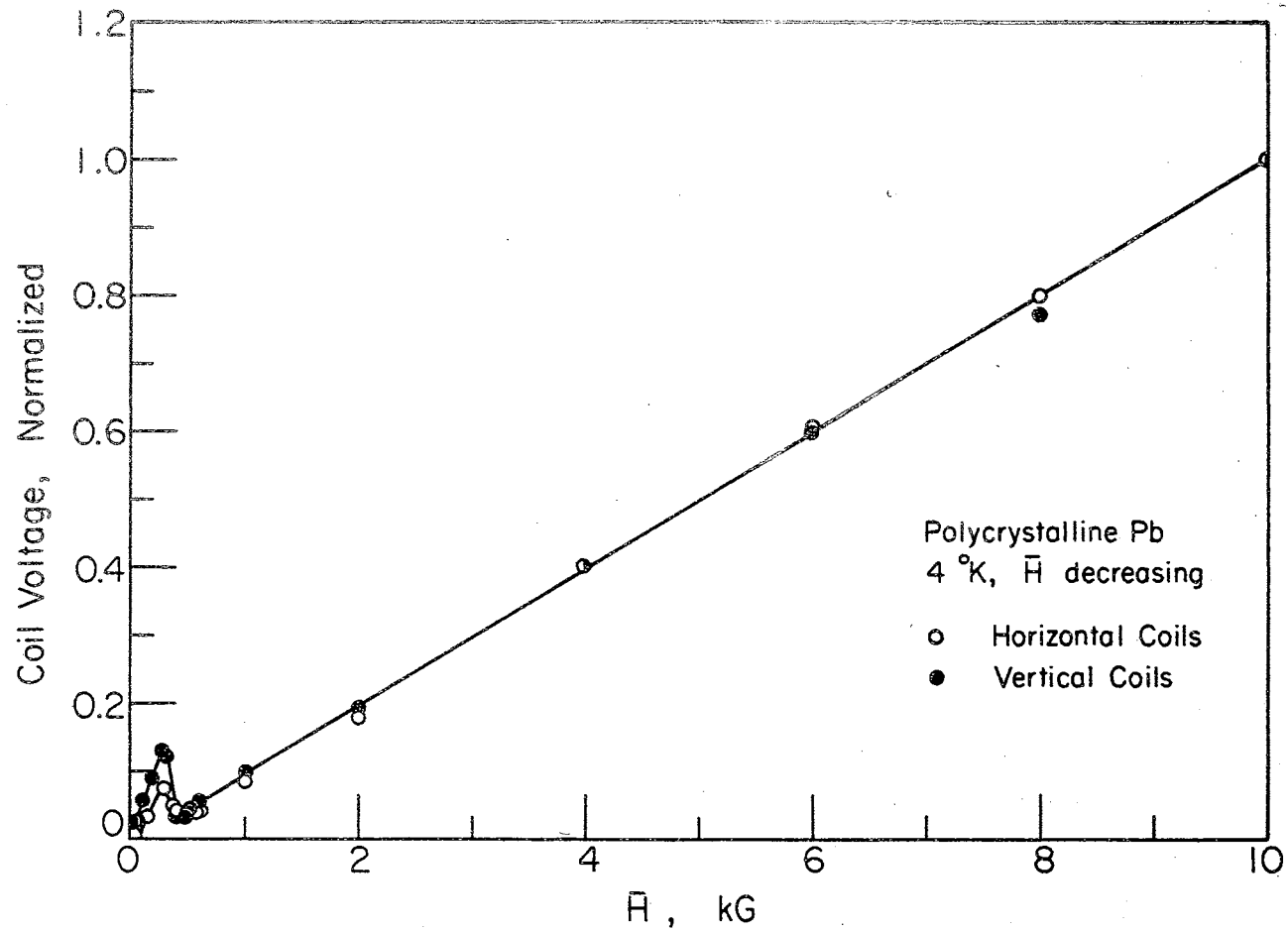


Figure 28. Coils H and V, Amplitude for Pb I, H Decreasing

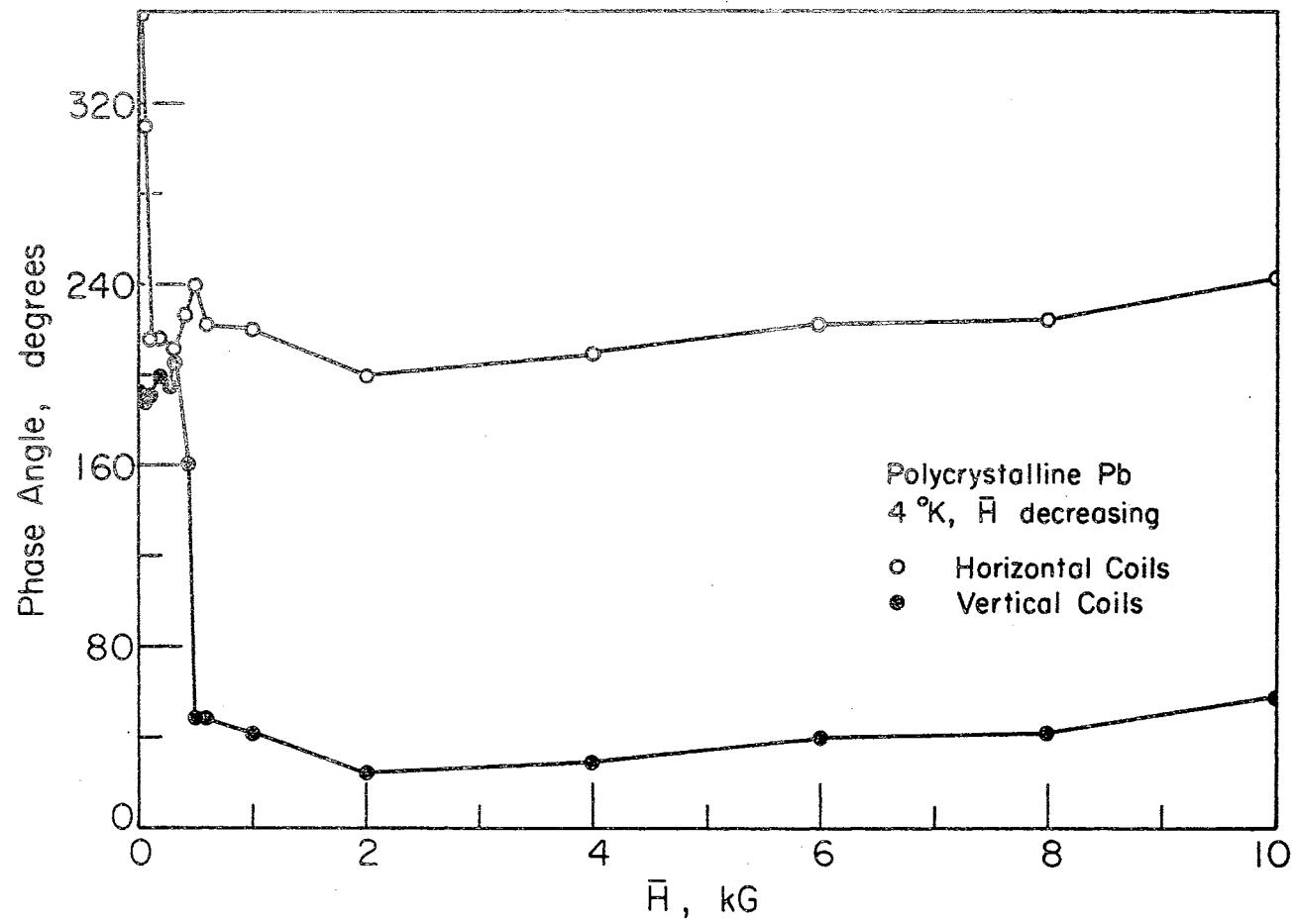


Figure 29. Coils H and V, Phase for Pb I, H Decreasing

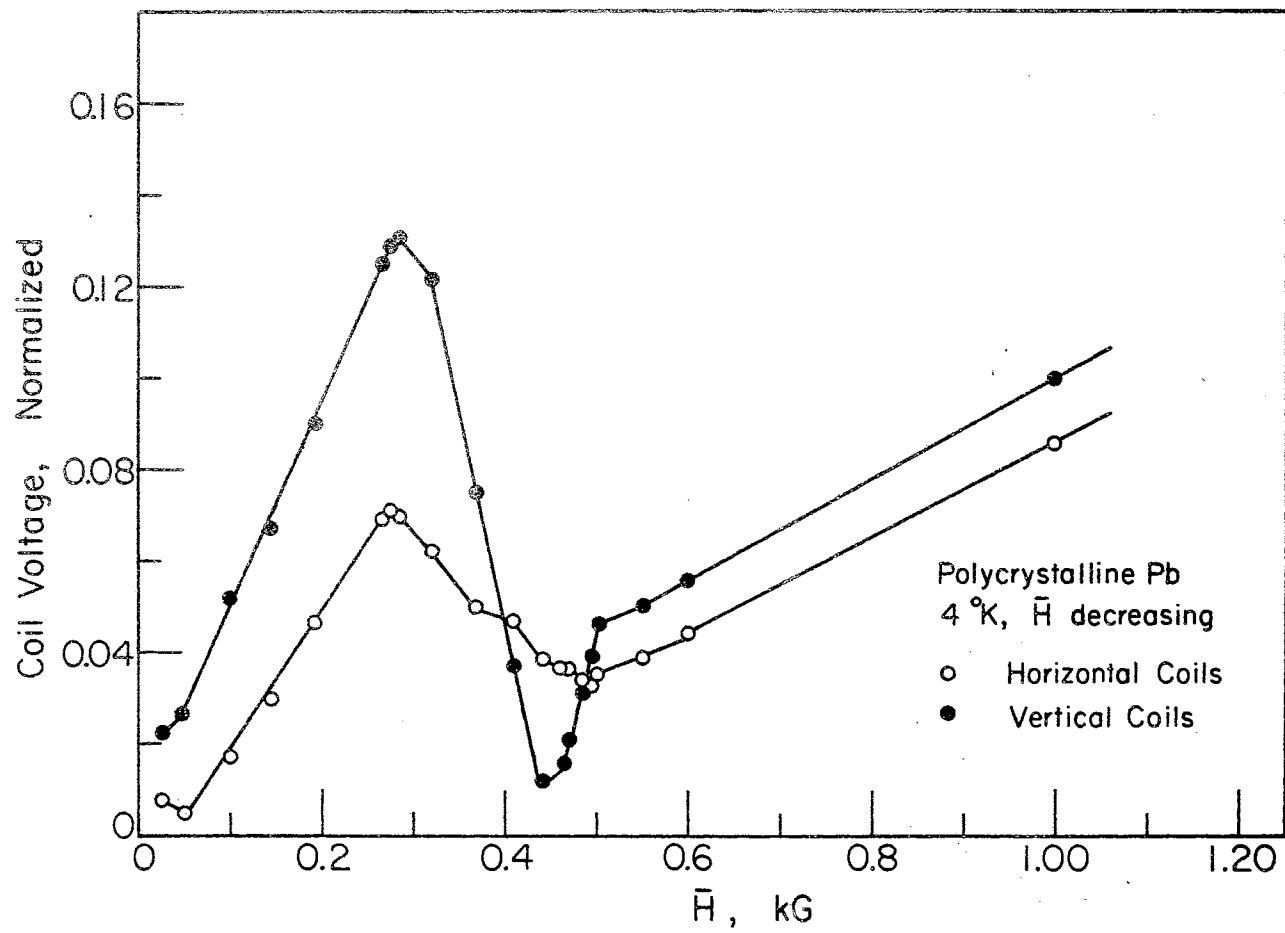


Figure 30. Coils H and V, Amplitude for Pb I, H Decreasing

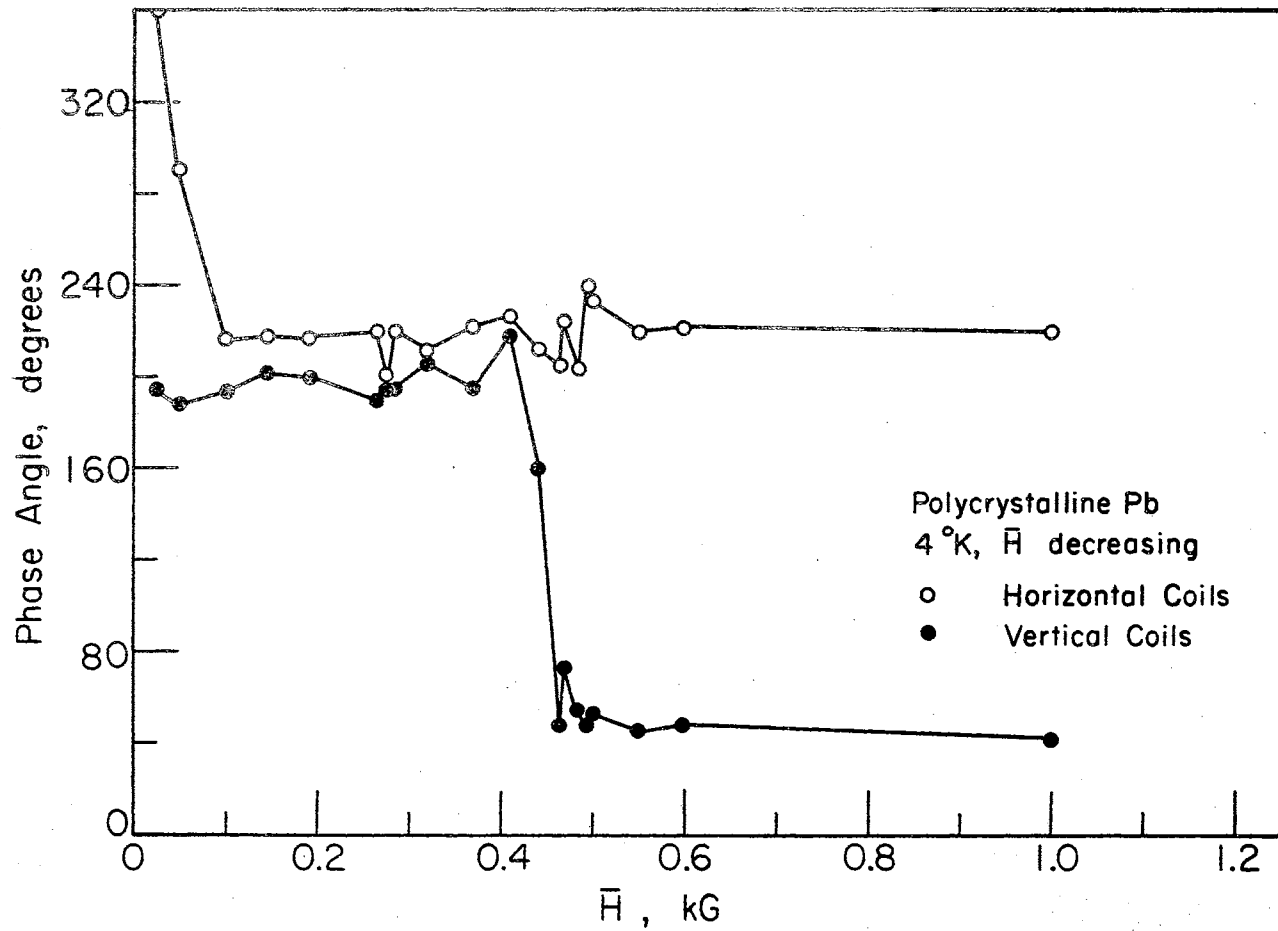


Figure 31. Coils H and V, Phase for Pb I, H Decreasing



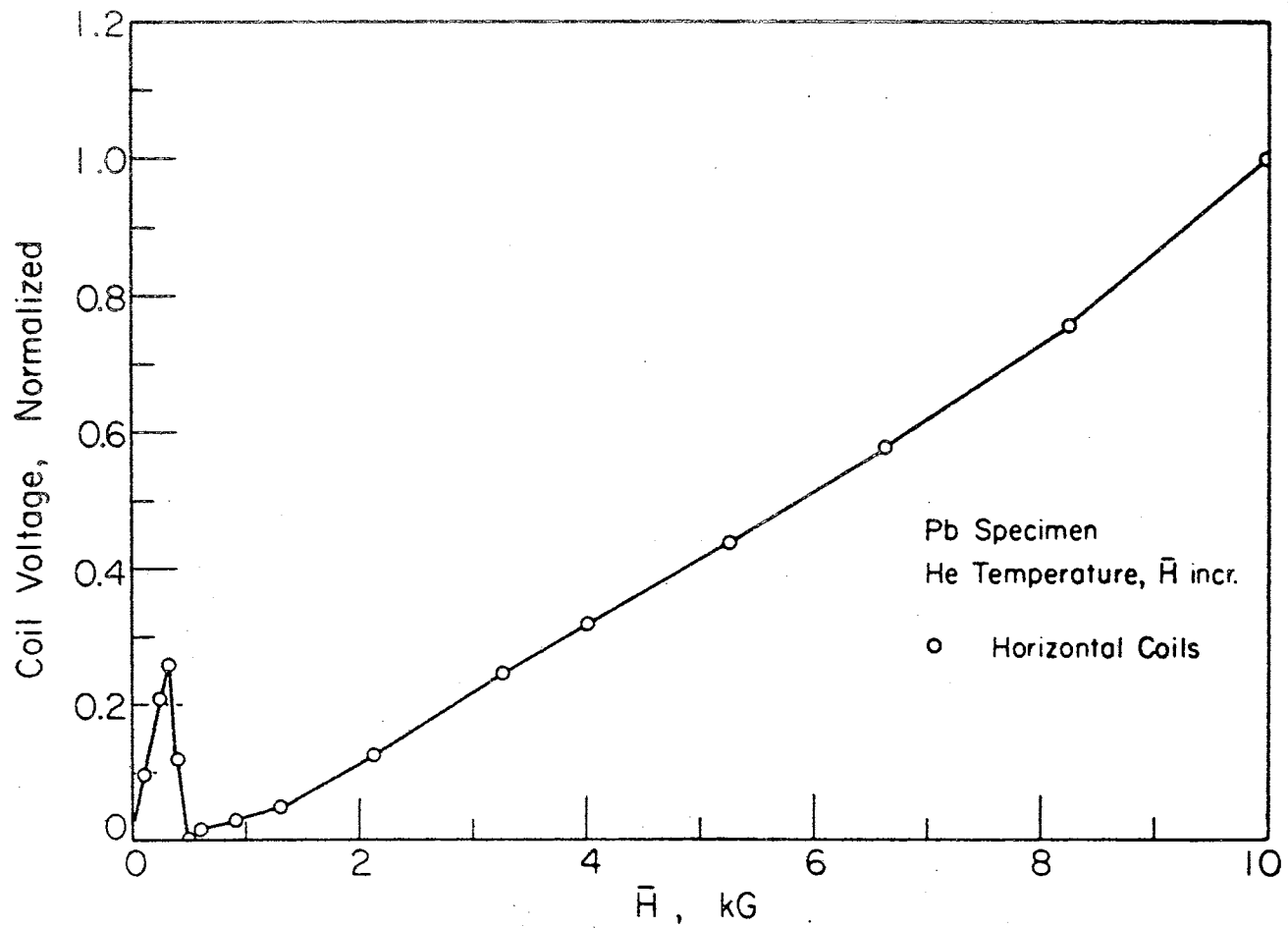


Figure 32. Coils H, Amplitude for Pb II, H Increasing

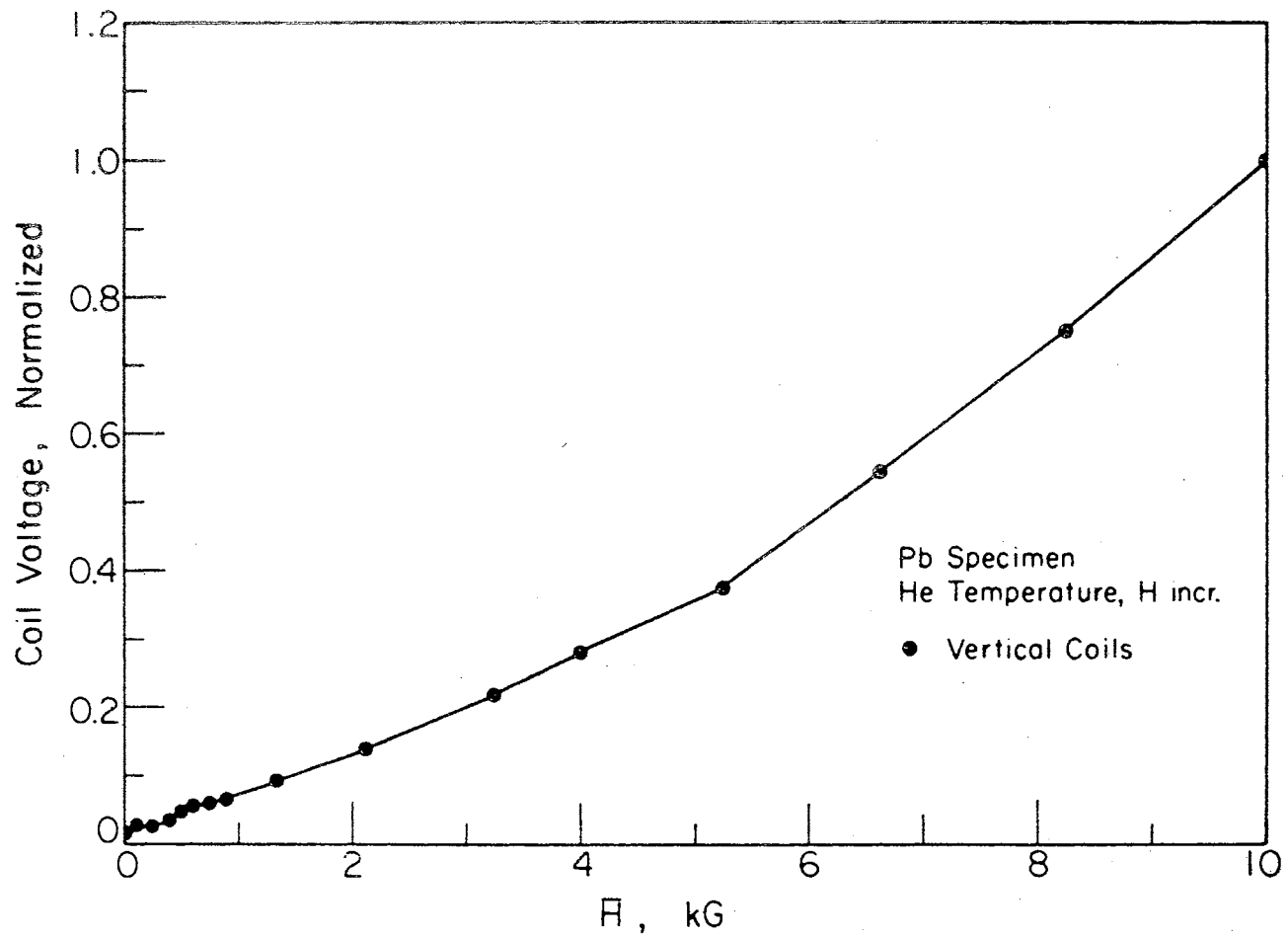


Figure 33. Coils V, Amplitude for Pb II, H Increasing

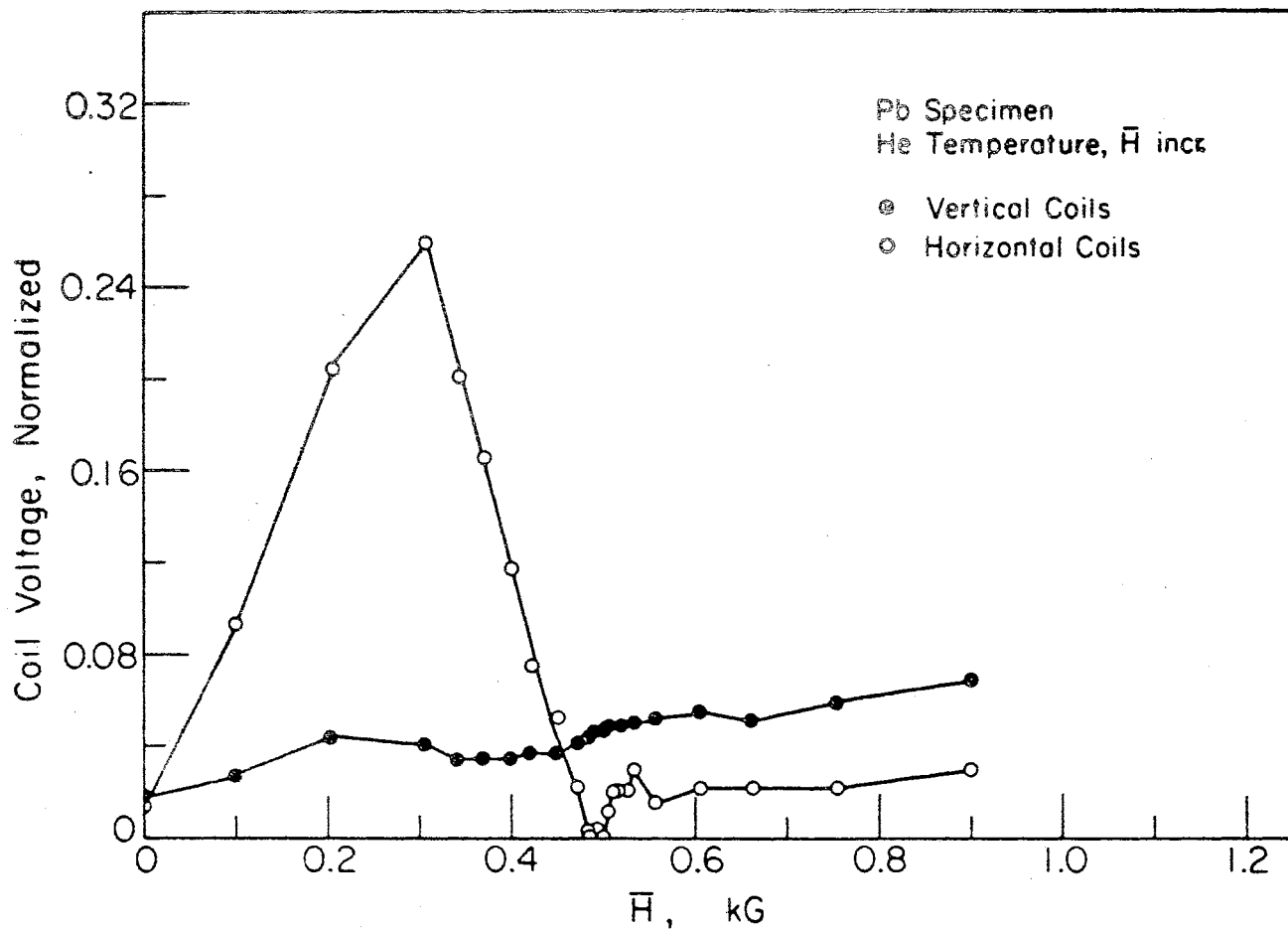


Figure 34. Coils H and V, Amplitude for Pb II, H Increasing

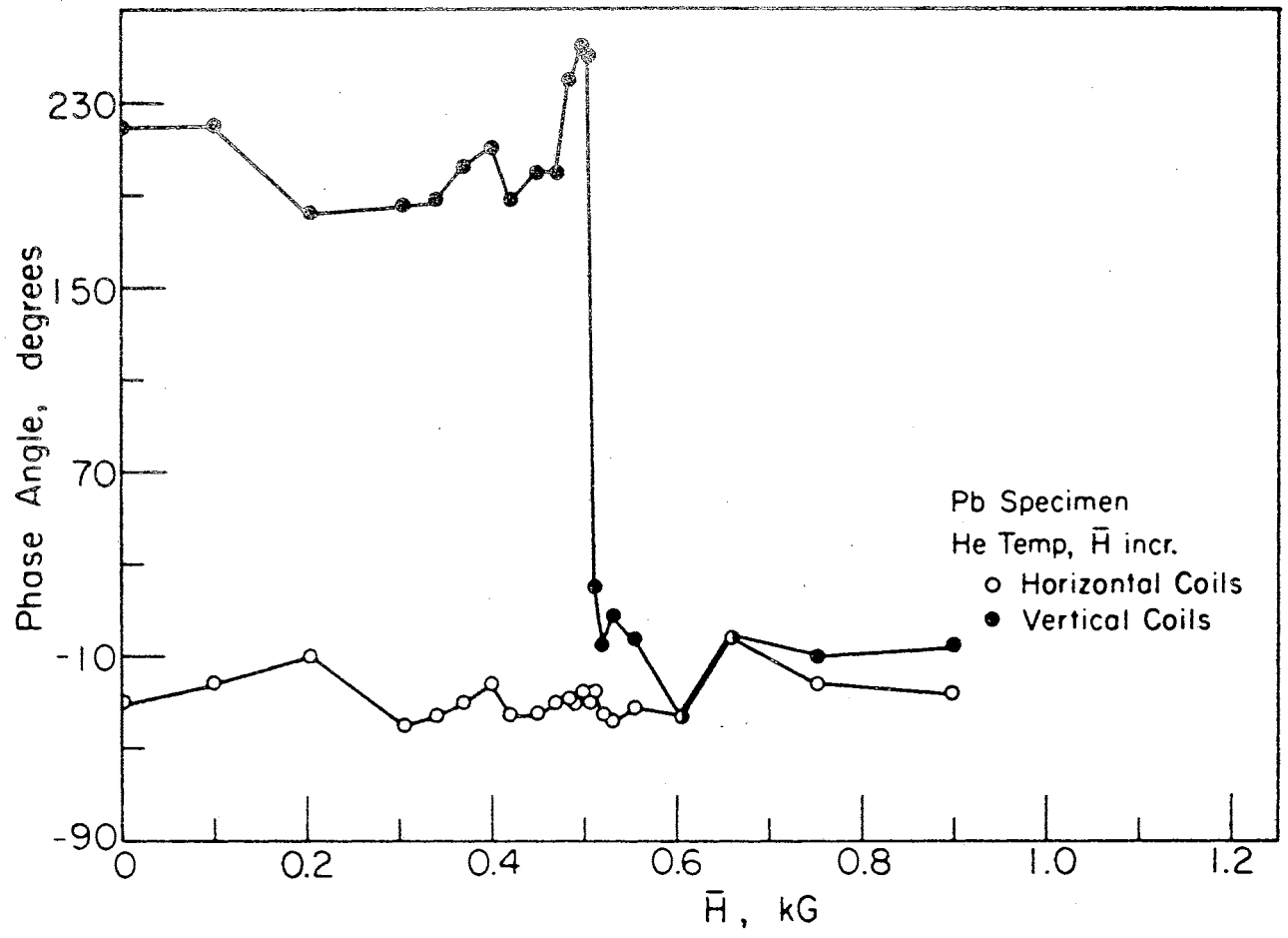


Figure 35. Coils H and V, Phase for Pb II, H Increasing

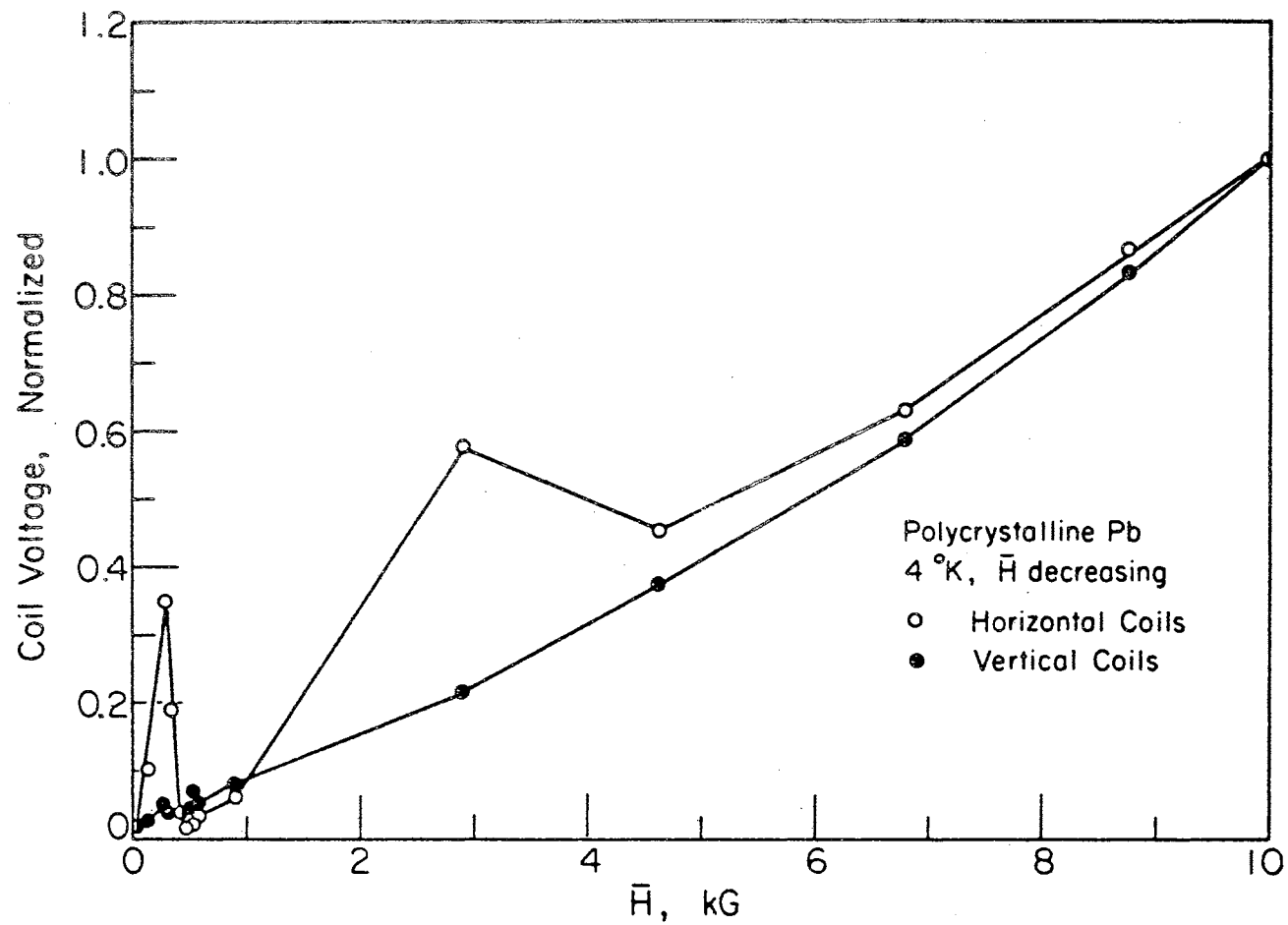


Figure 36. Coils H and V, Amplitude for Pb II, H Decreasing

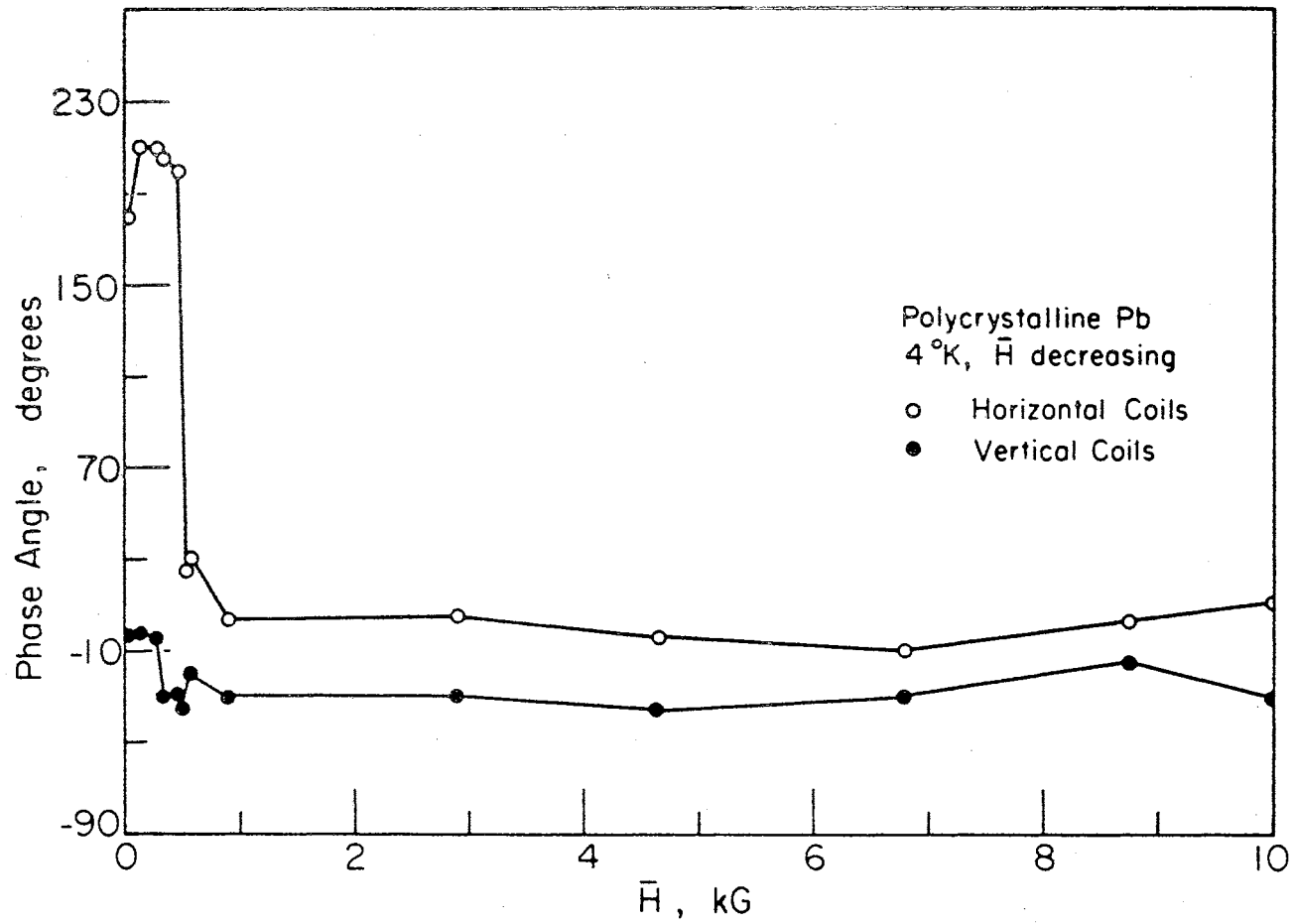


Figure 37. Coils H and V, Phase for Pb II, H Decreasing

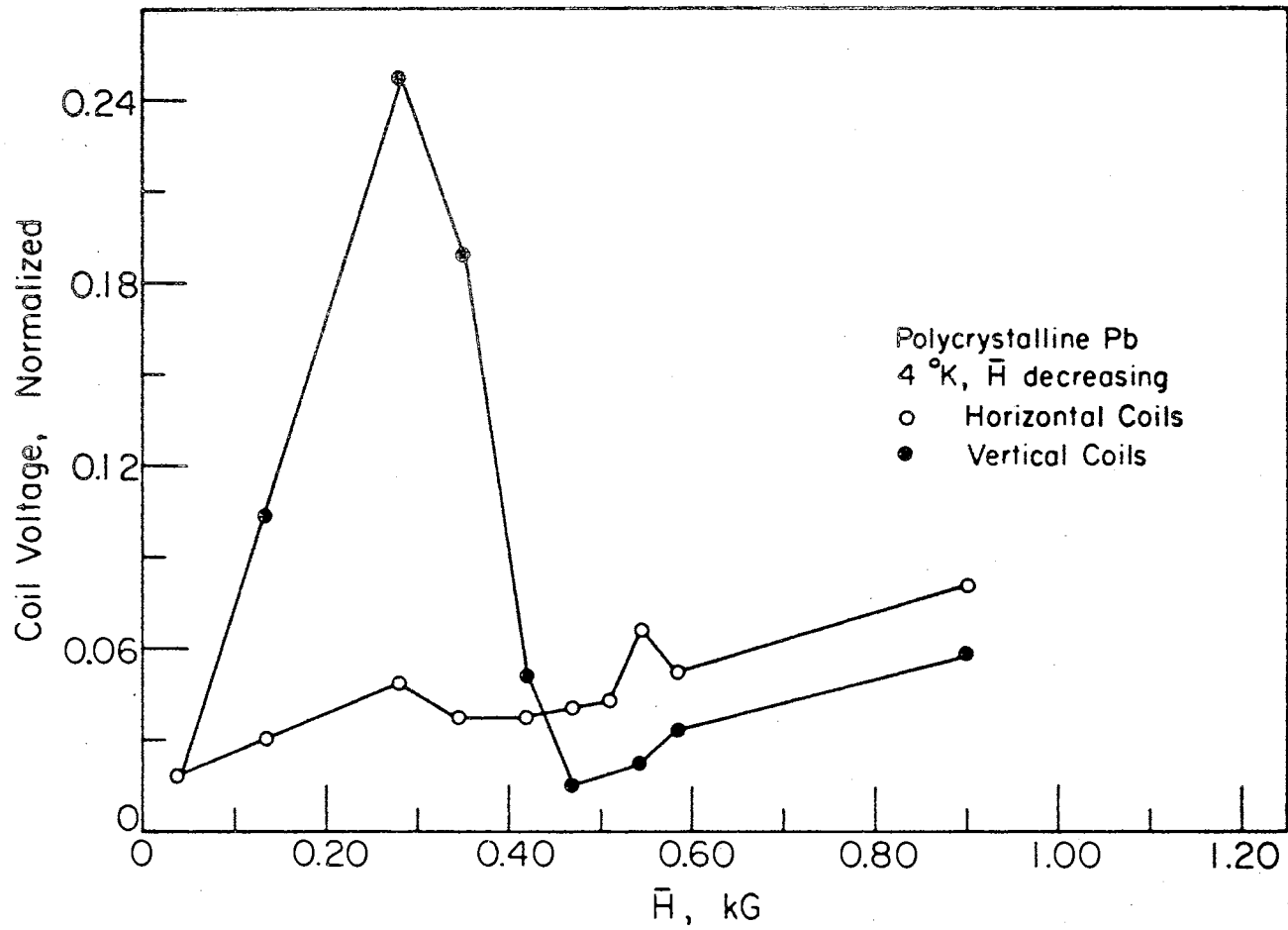


Figure 38. Coils H and V, Amplitude for Pb II, H Decreasing

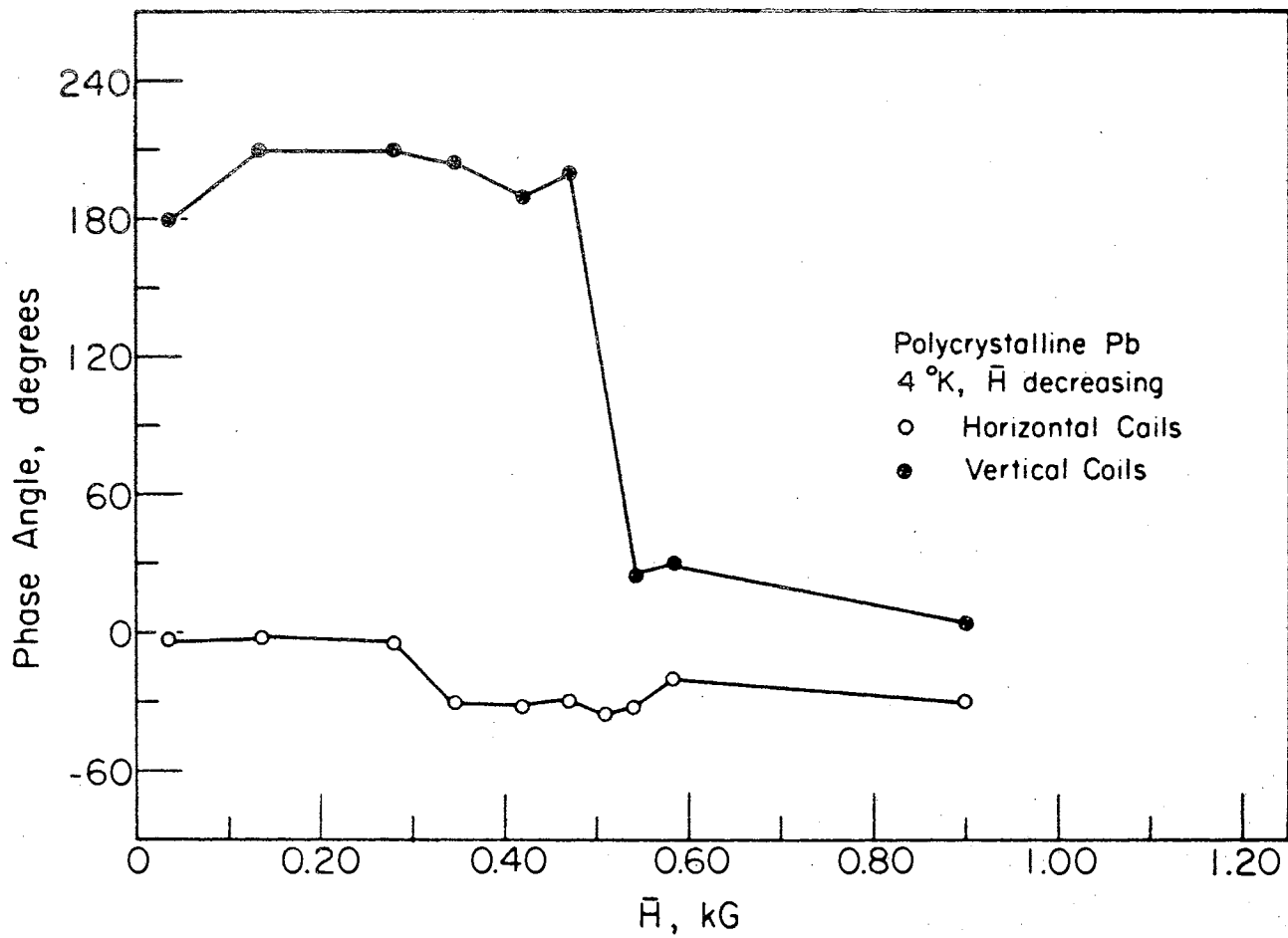


Figure 39. Coils H and V, Phase for Pb II, H Decreasing



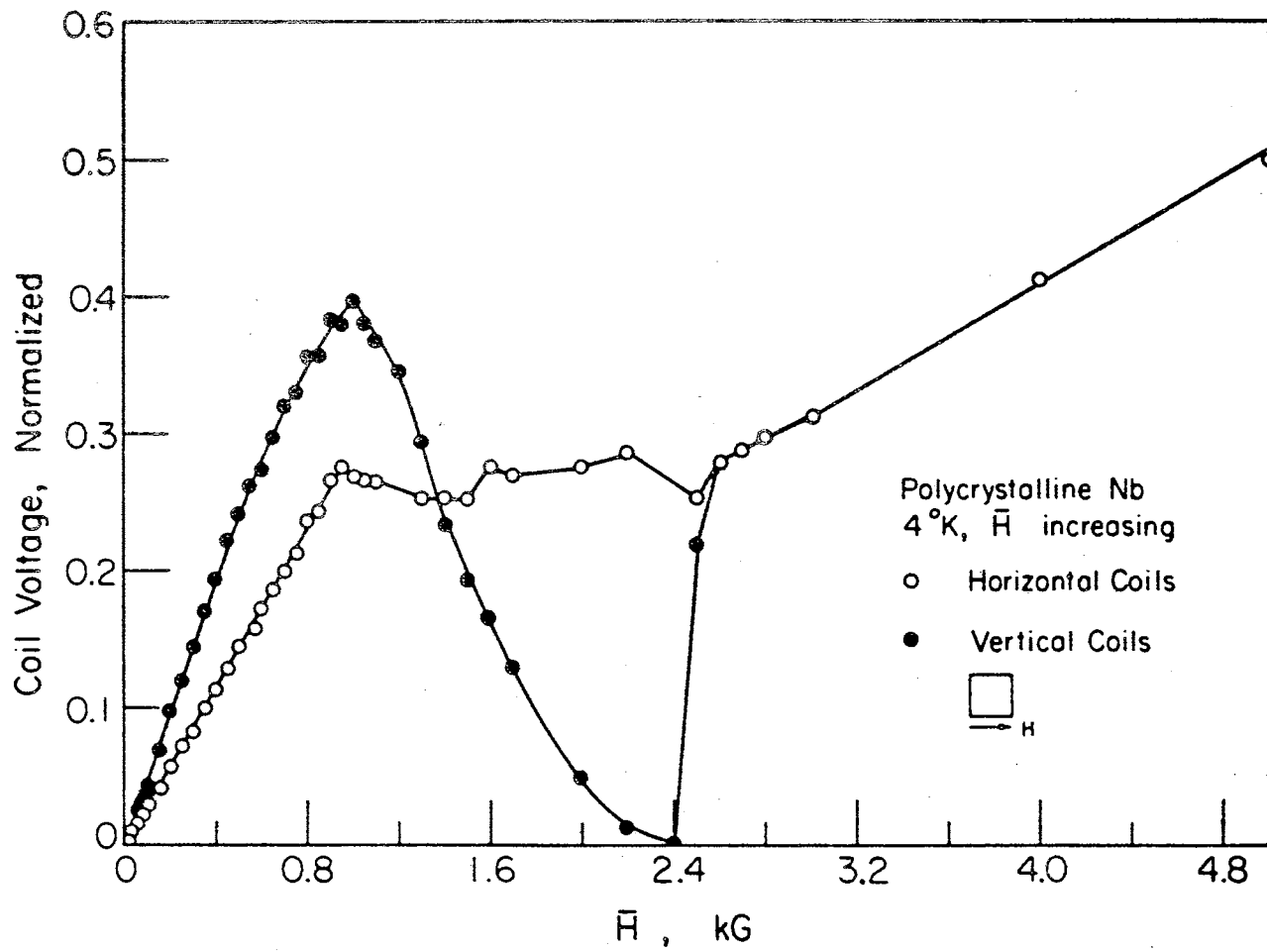


Figure 40. Coils H and V, Amplitude for Nb II, H Increasing

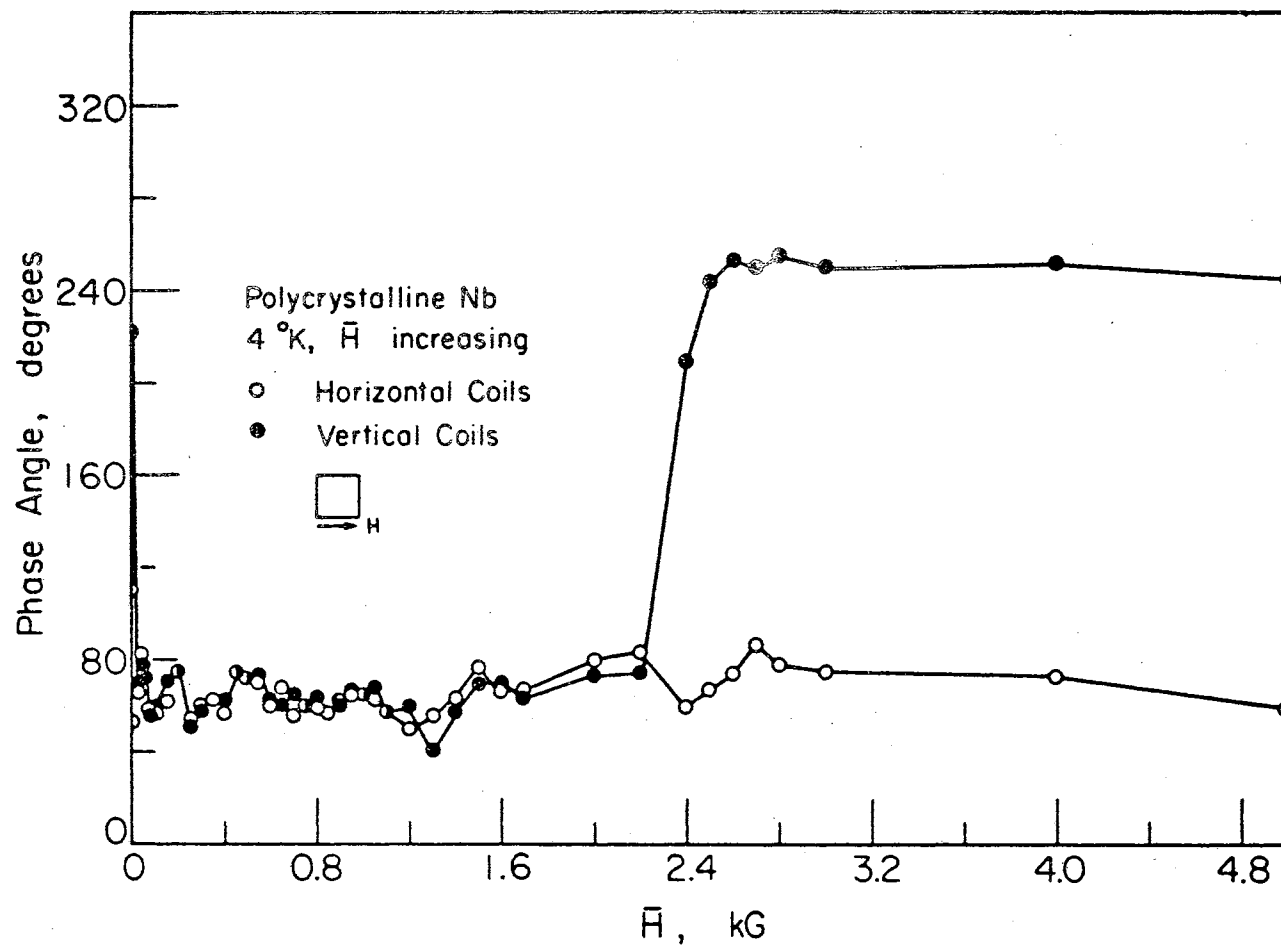


Figure 41. Coils H and V, Phase for Nb II, H Increasing

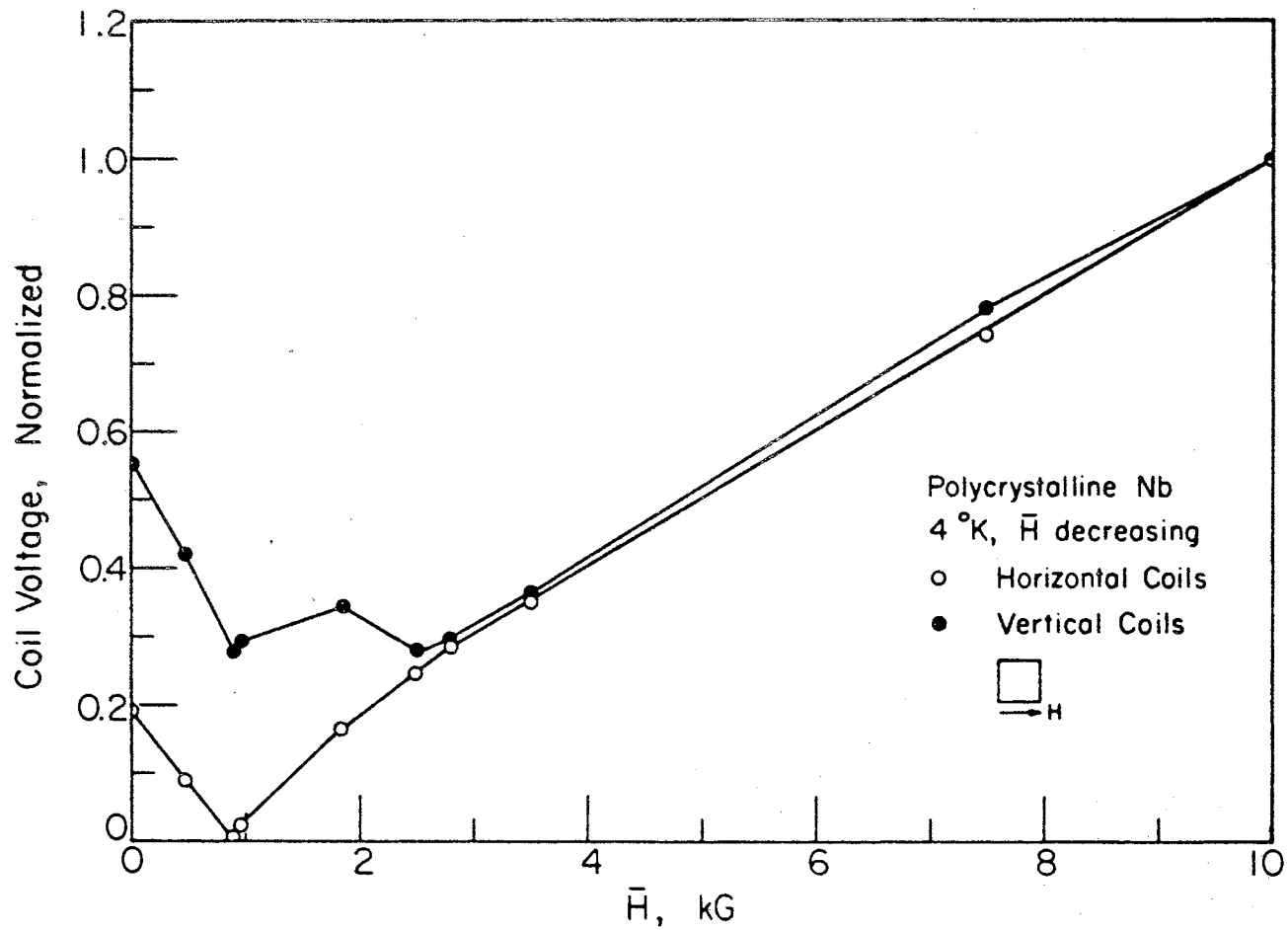


Figure 42. Coils H and V, Amplitude for Nb II, H Decreasing

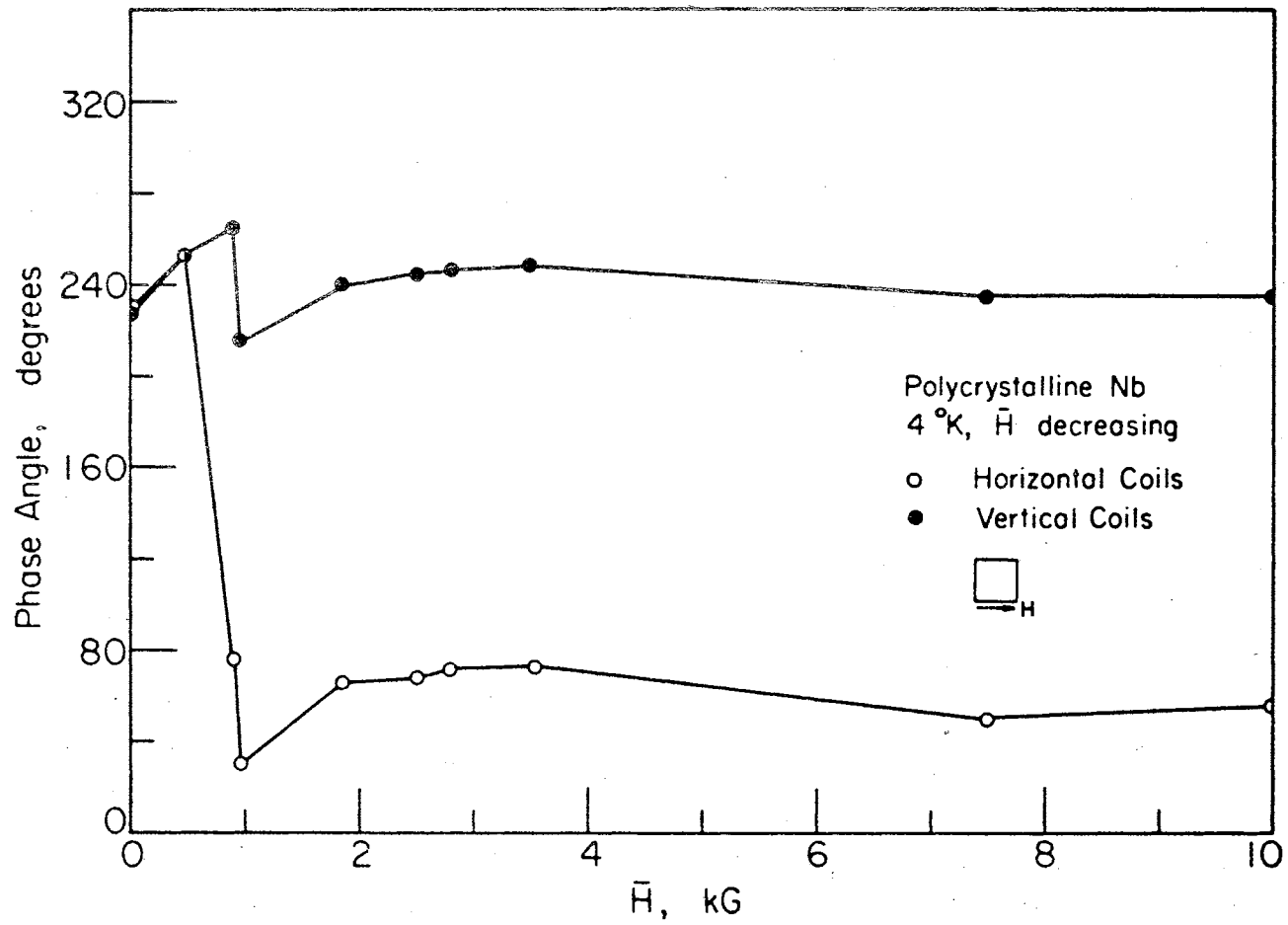


Figure 43. Coils H and V, Phase for Nb II, H Decreasing

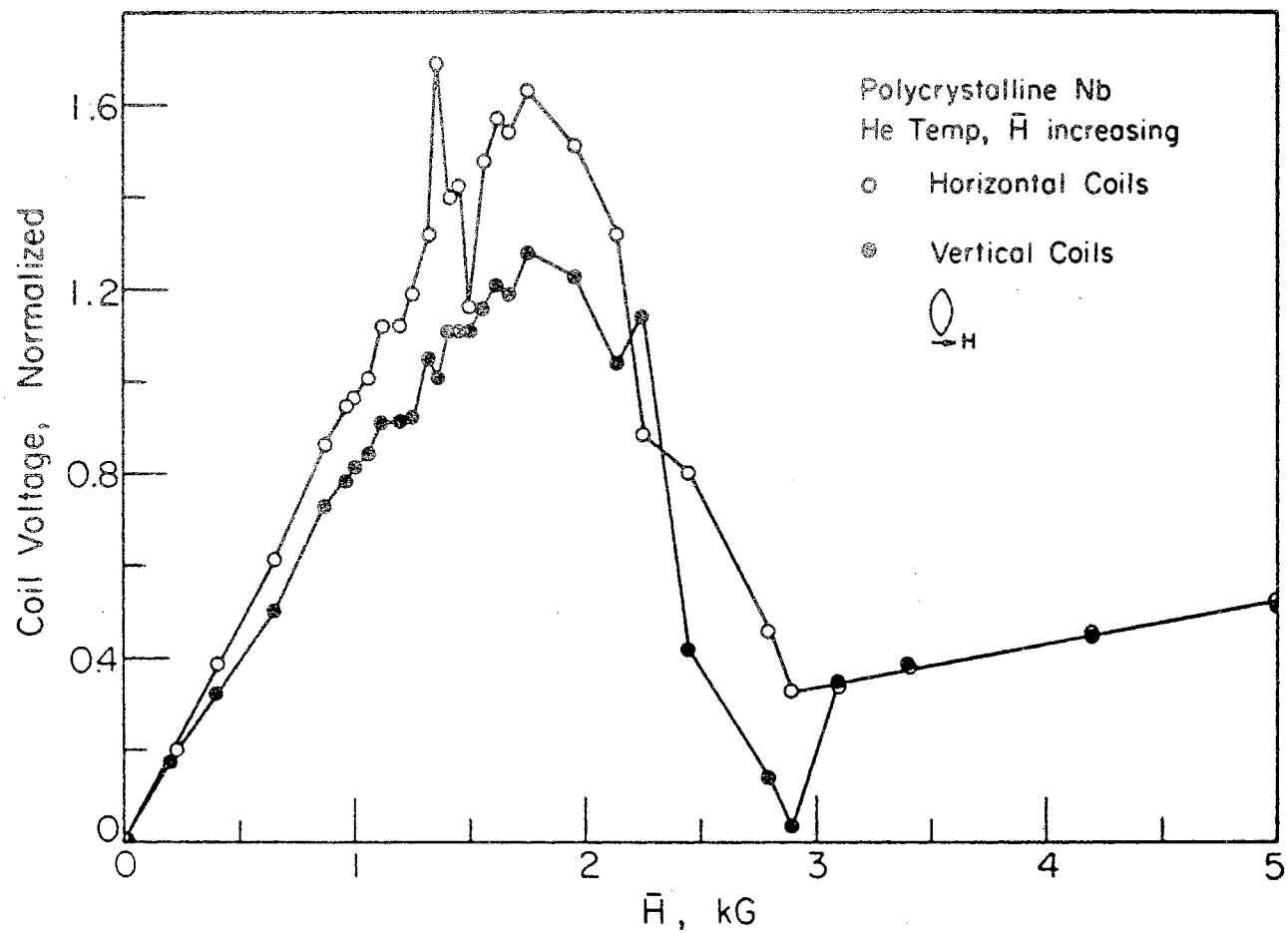


Figure 44. Coils H and V, Amplitude for Nb III, H Increasing

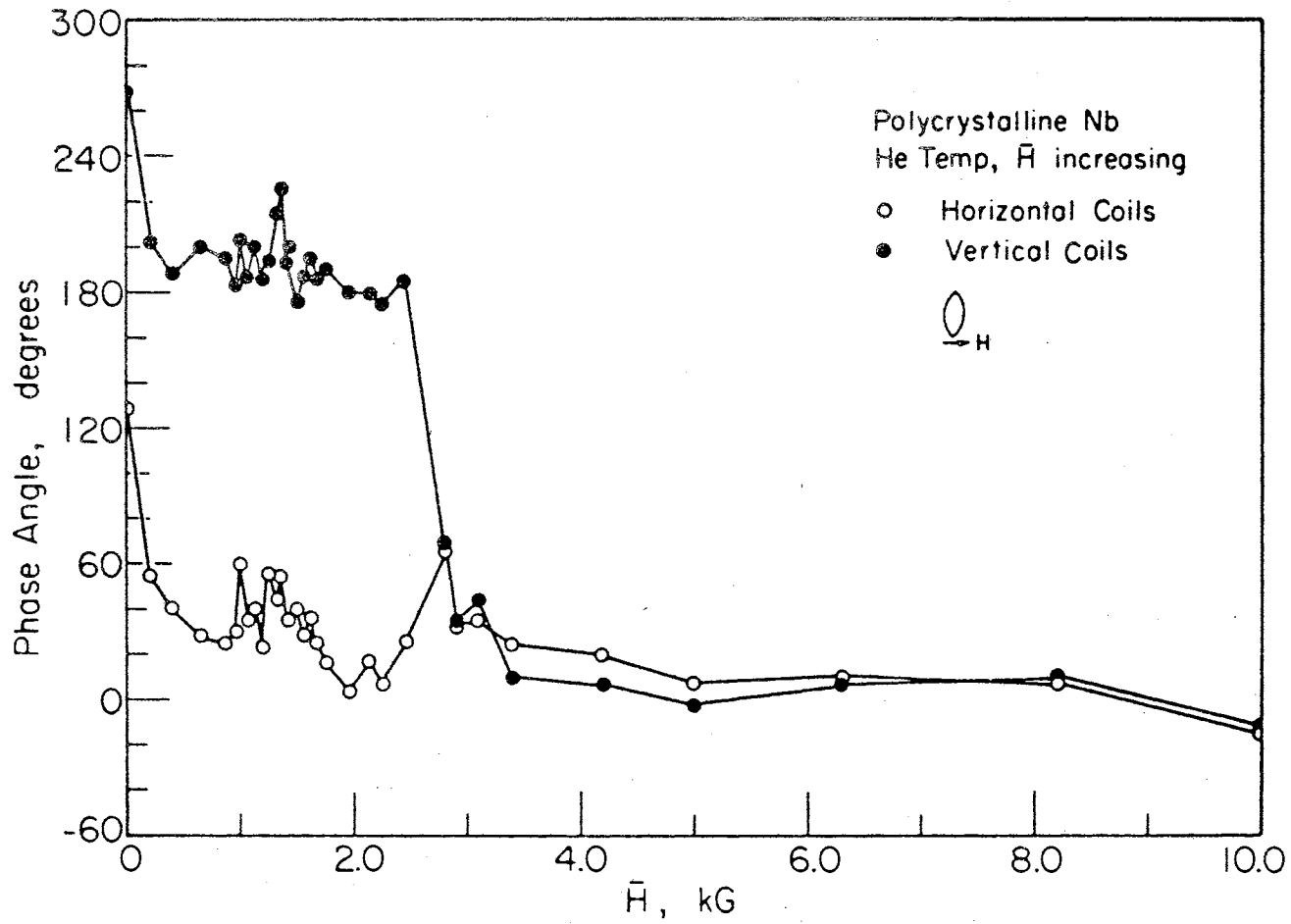


Figure 45. Coils H and V, Phase for Nb III, H Increasing

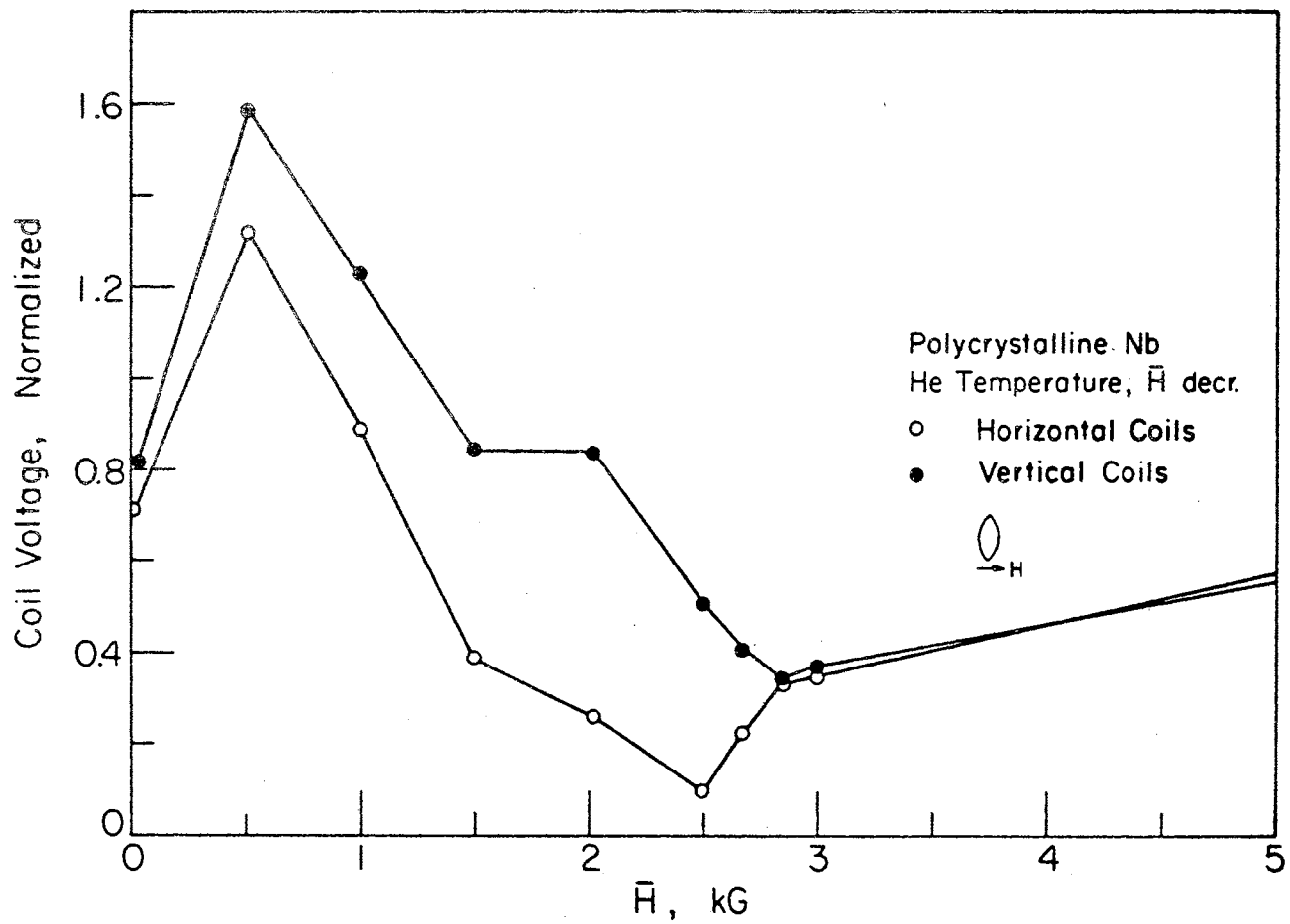


Figure 46. Coils H and V, Amplitude for Nb III, H Decreasing

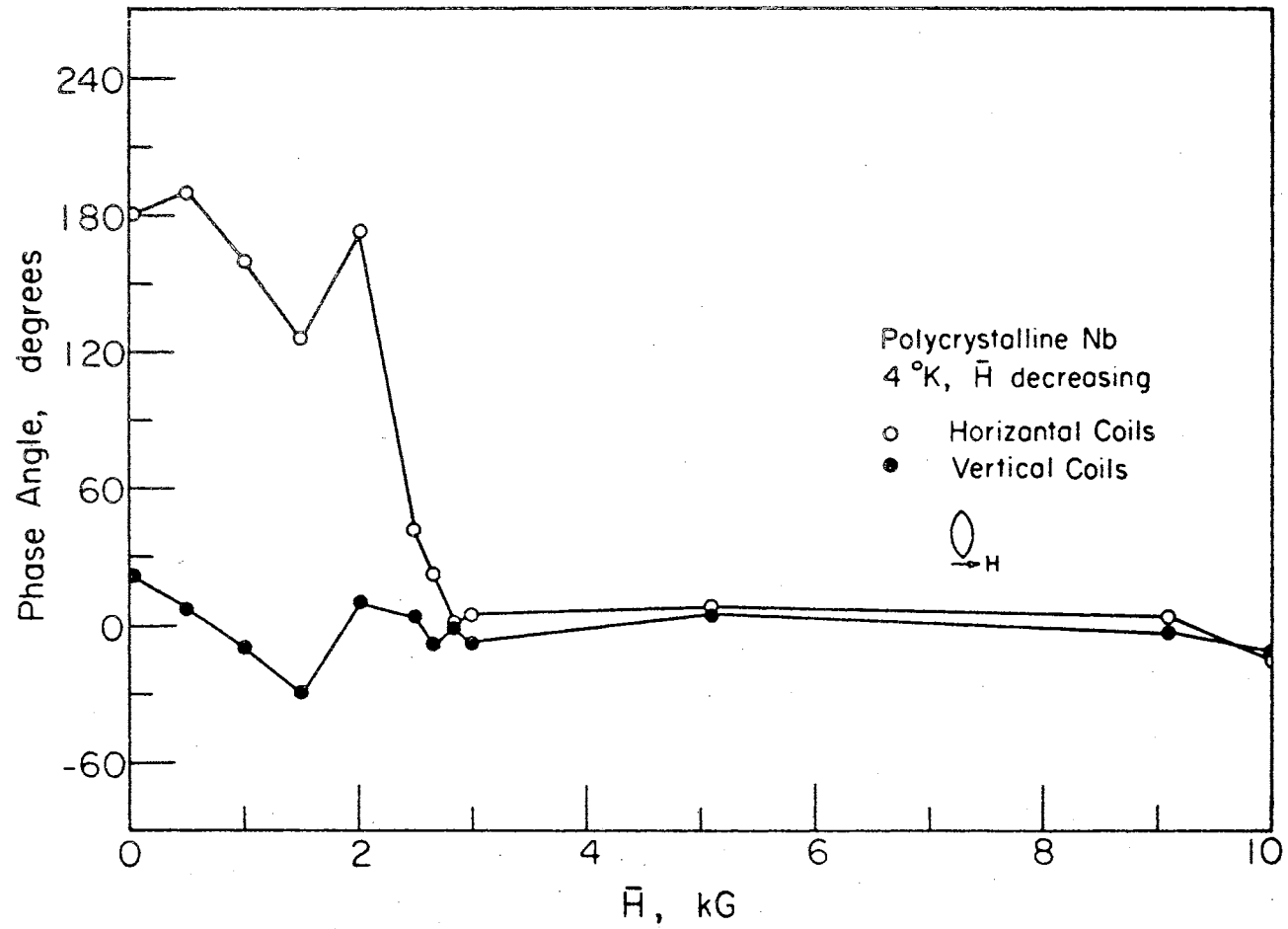


Figure 47. Coils H and V, Phase for Nb III, H Decreasing



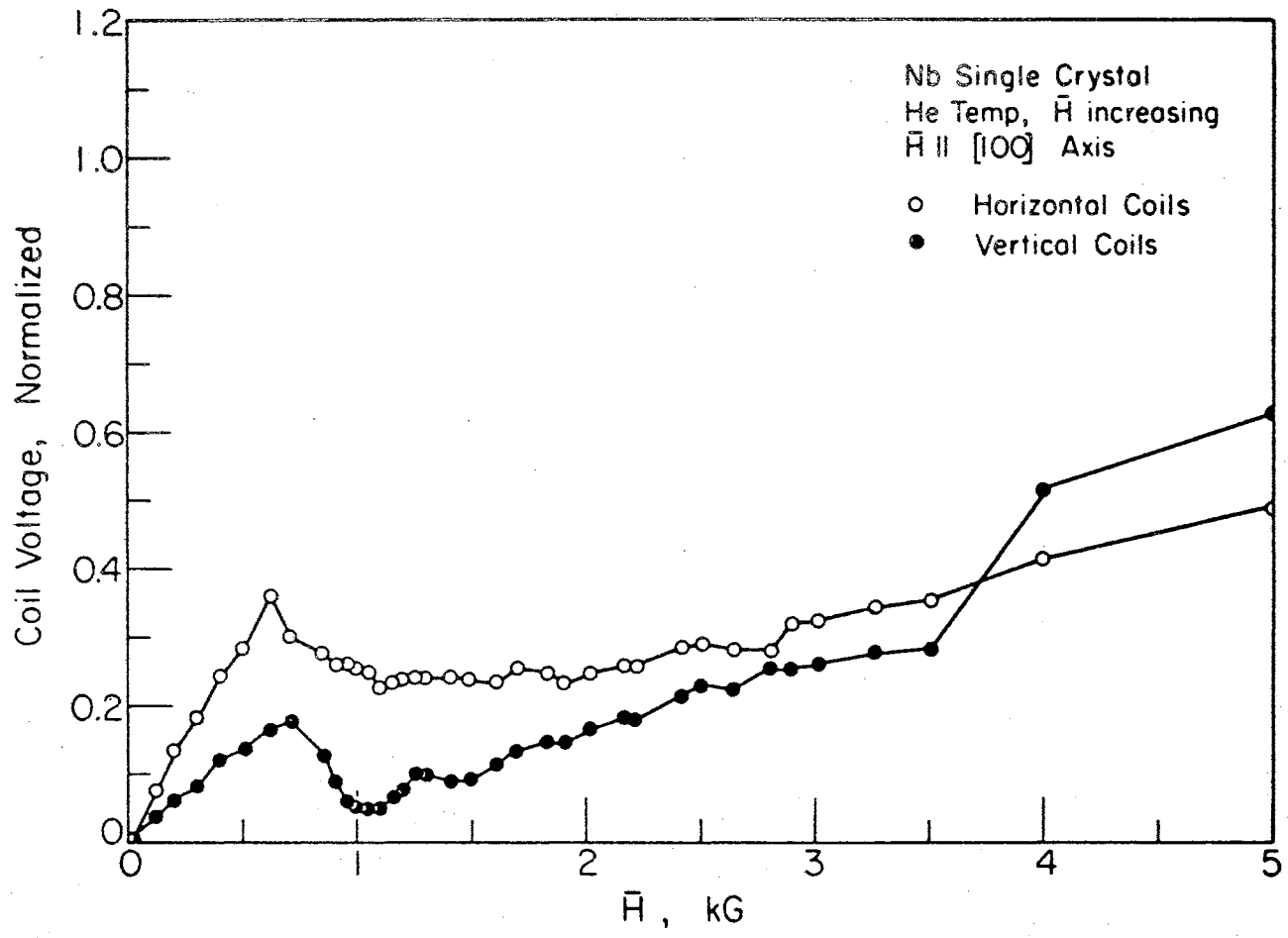


Figure 48. Coils H and V, Amplitude for Nb IV, H Increasing

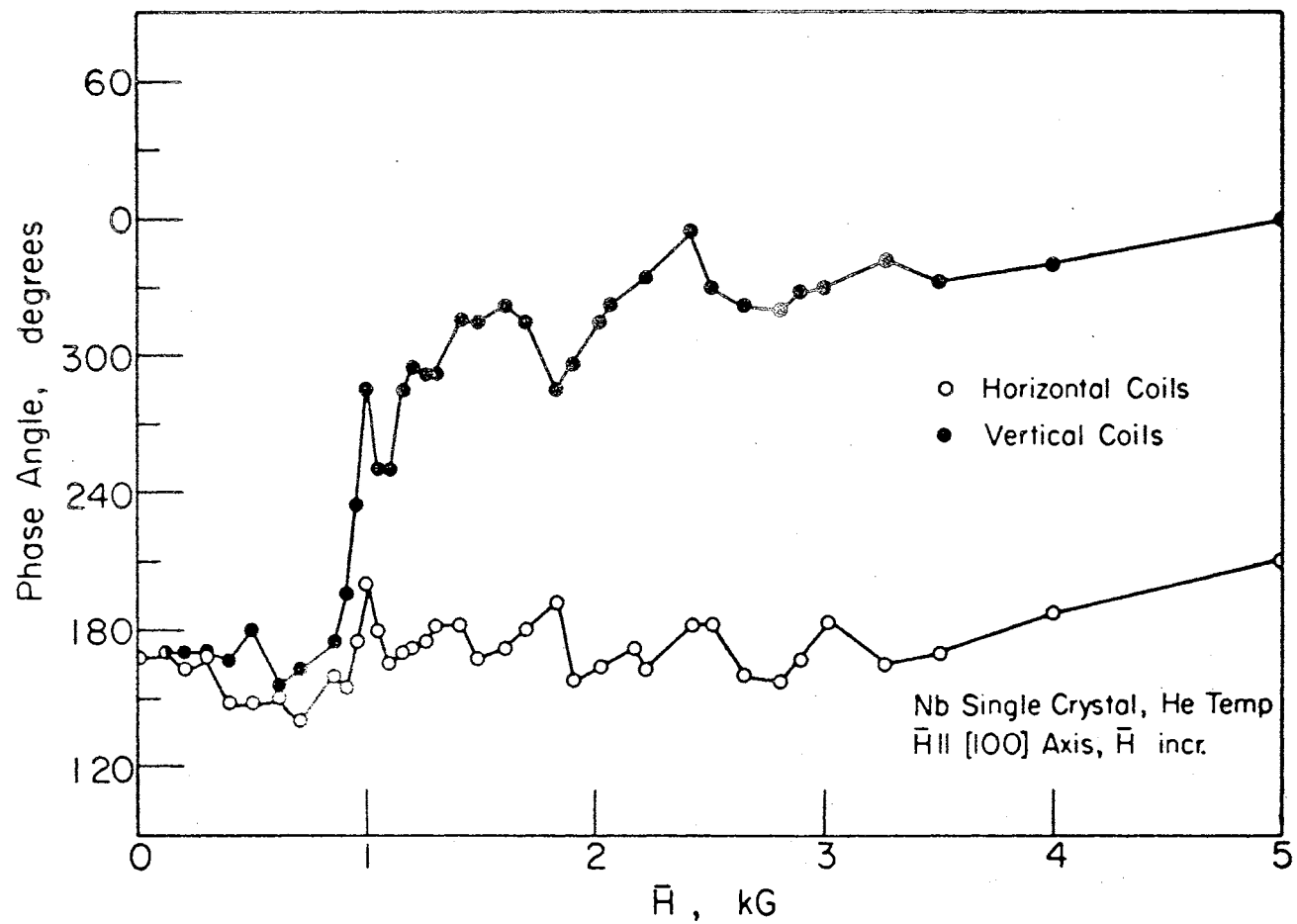


Figure 49. Coils H and V, Phase for Nb IV, H Increasing

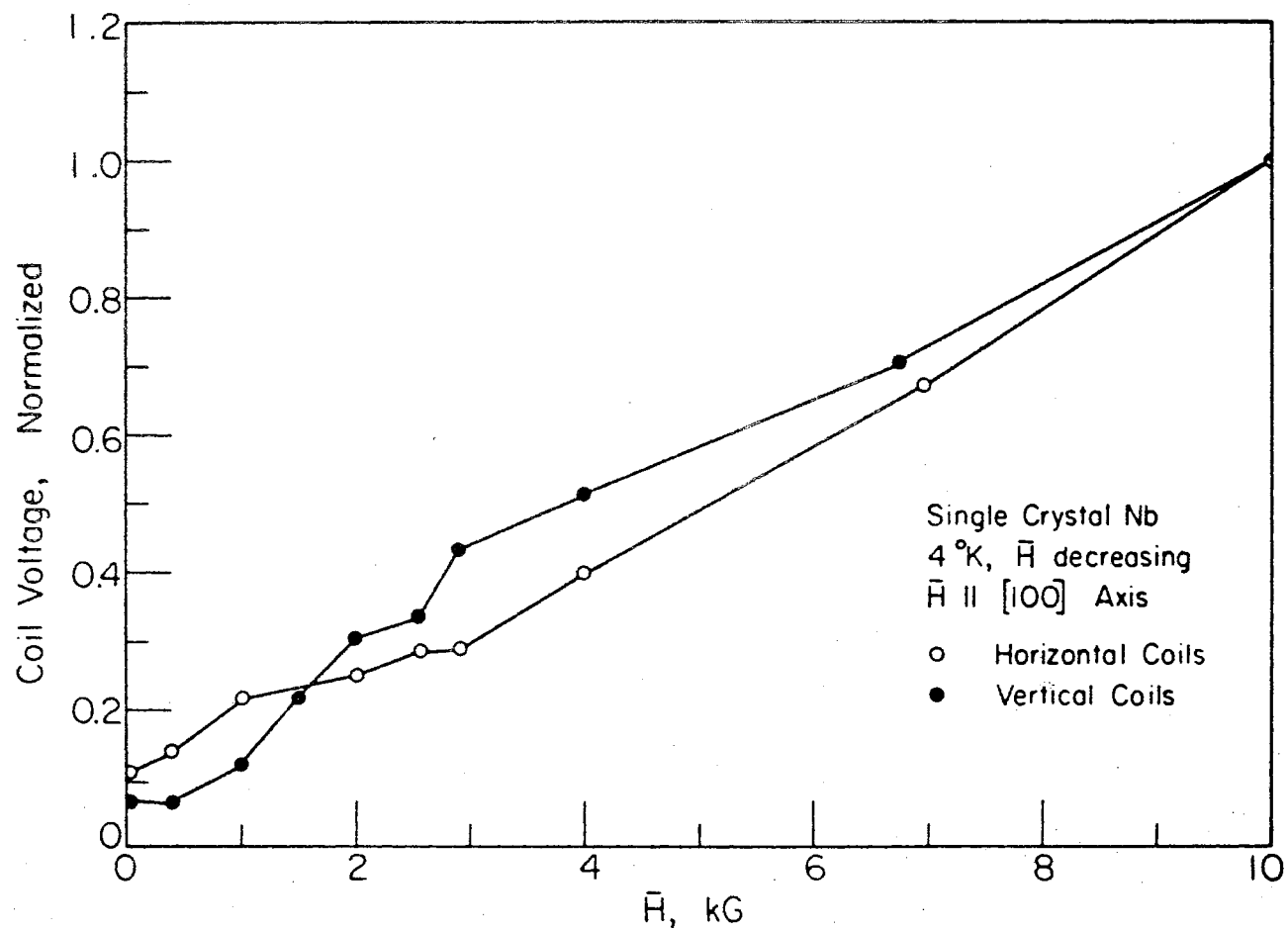


Figure 50. Coils H and V, Amplitude for Nb IV, H Decreasing

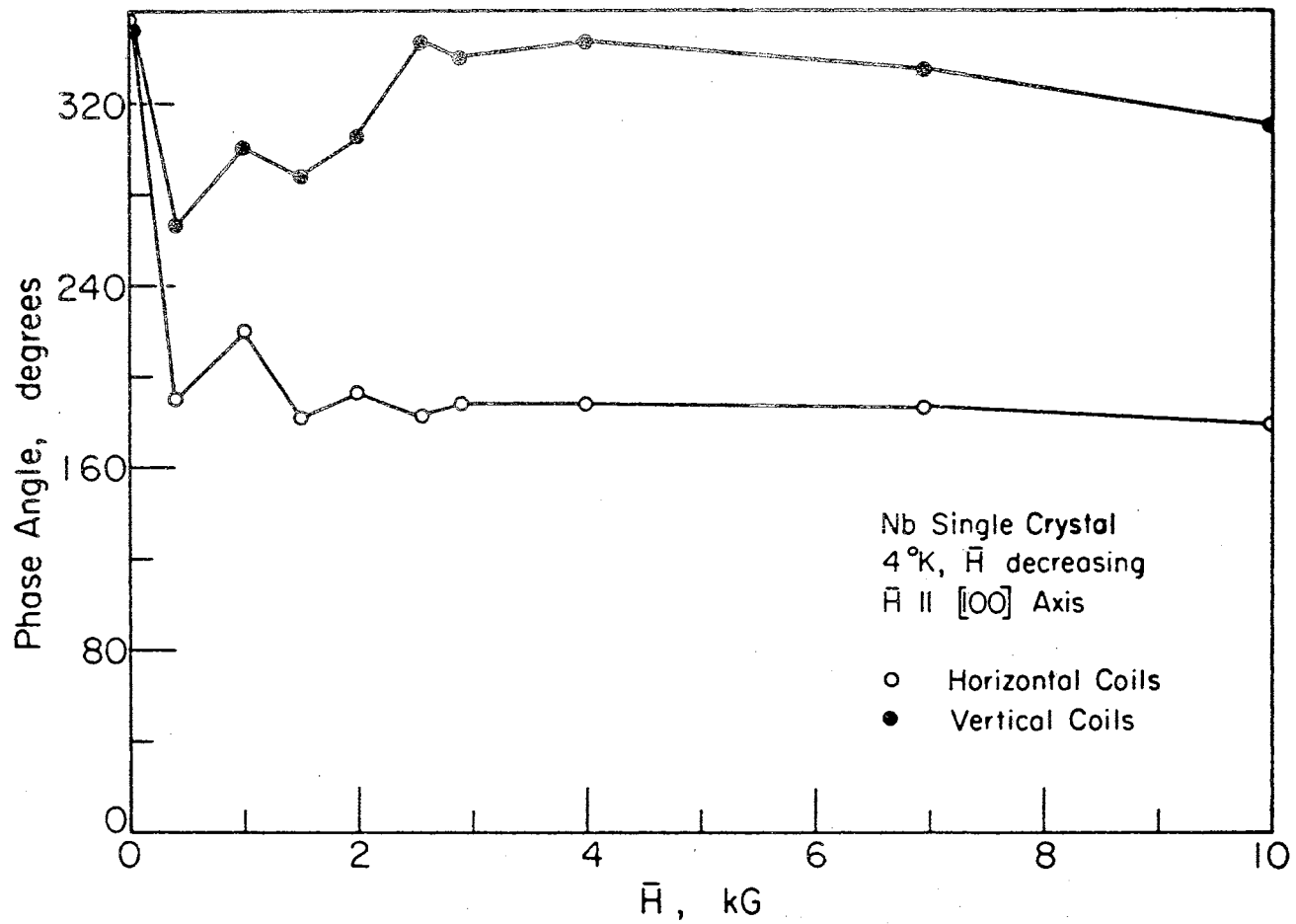


Figure 51. Coils H and V, Phase for Nb IV, H Decreasing

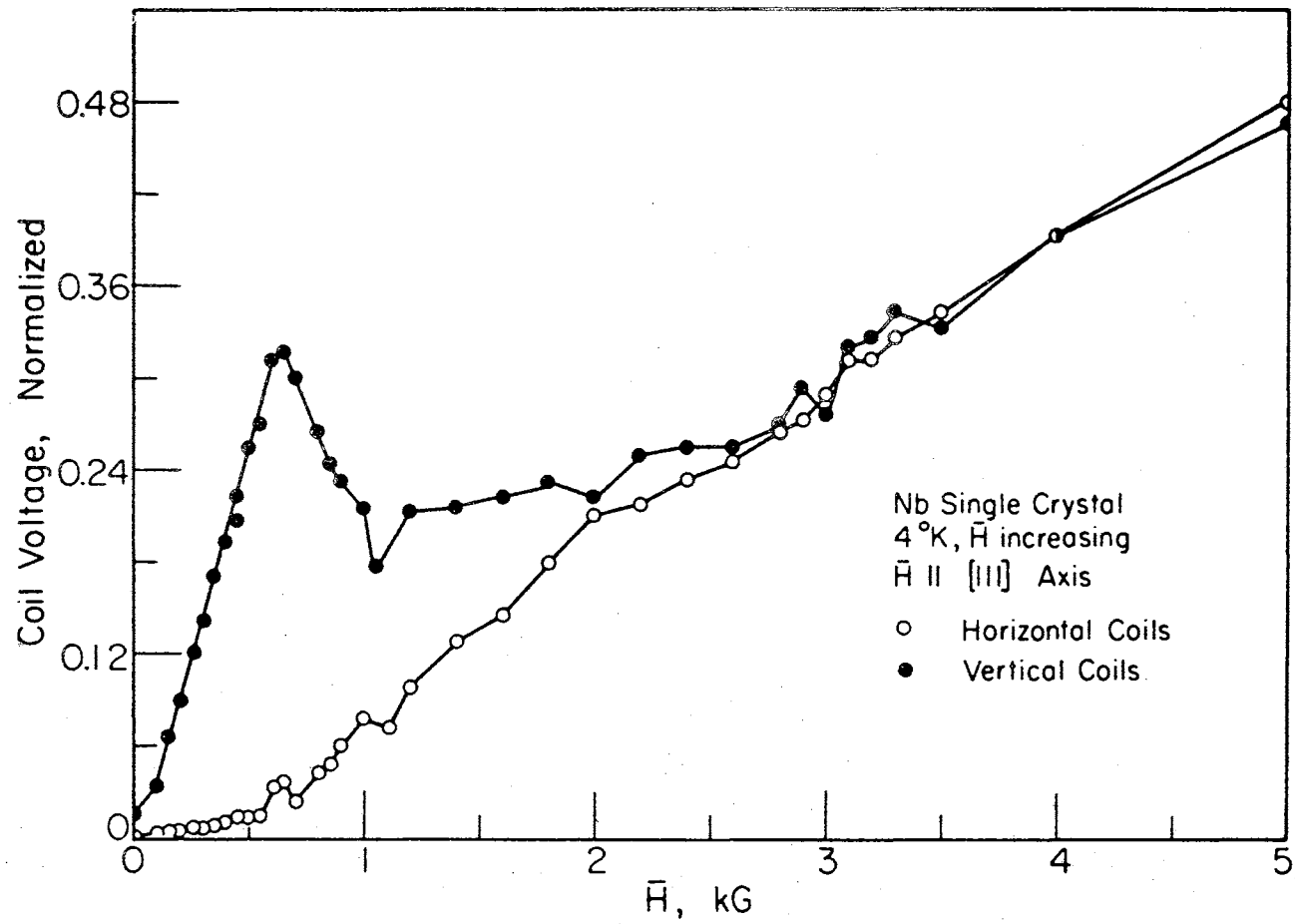


Figure 52. Coils H and V, Amplitude for Nb V, H Increasing

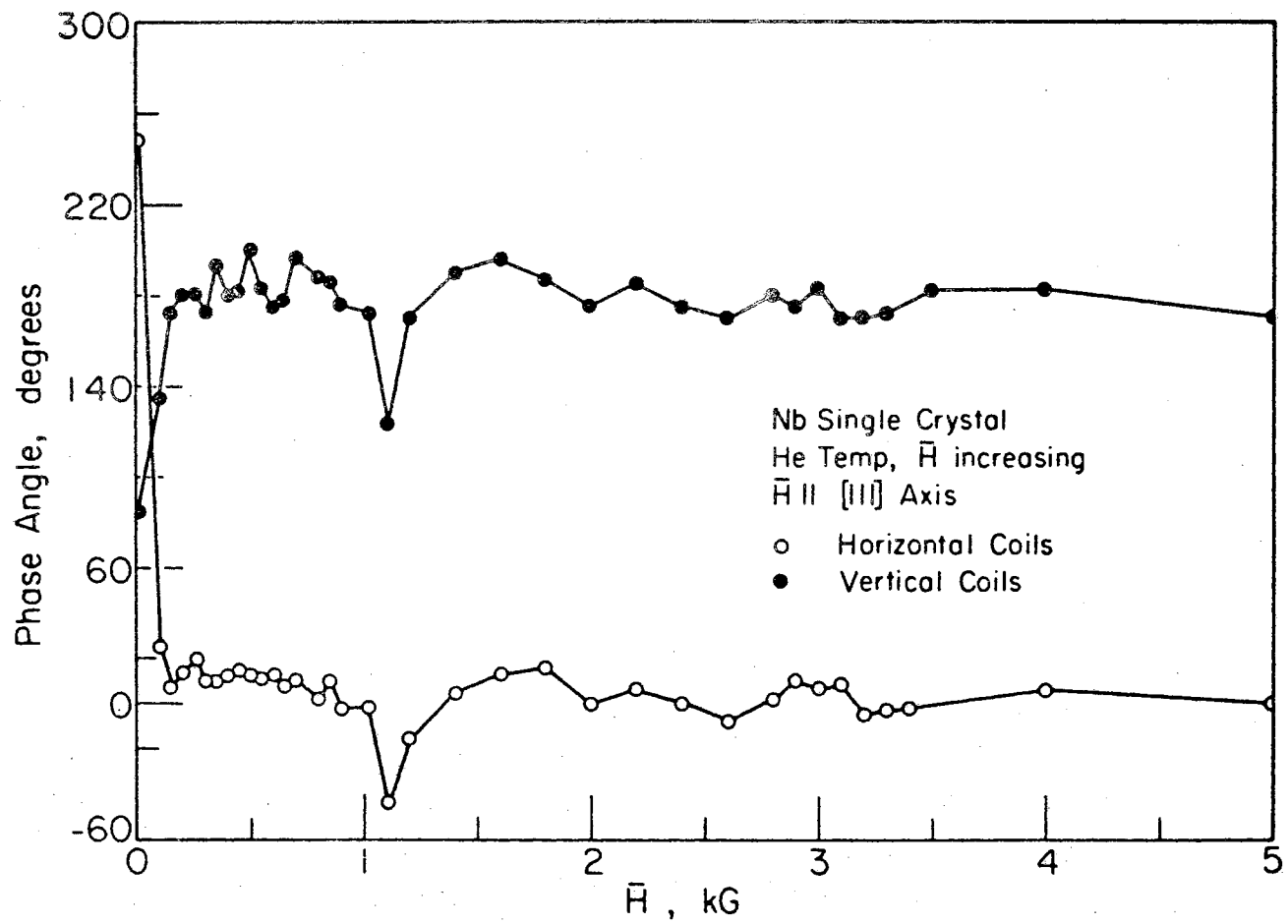


Figure 53. Coils H and V, Phase for Nb V, H Increasing

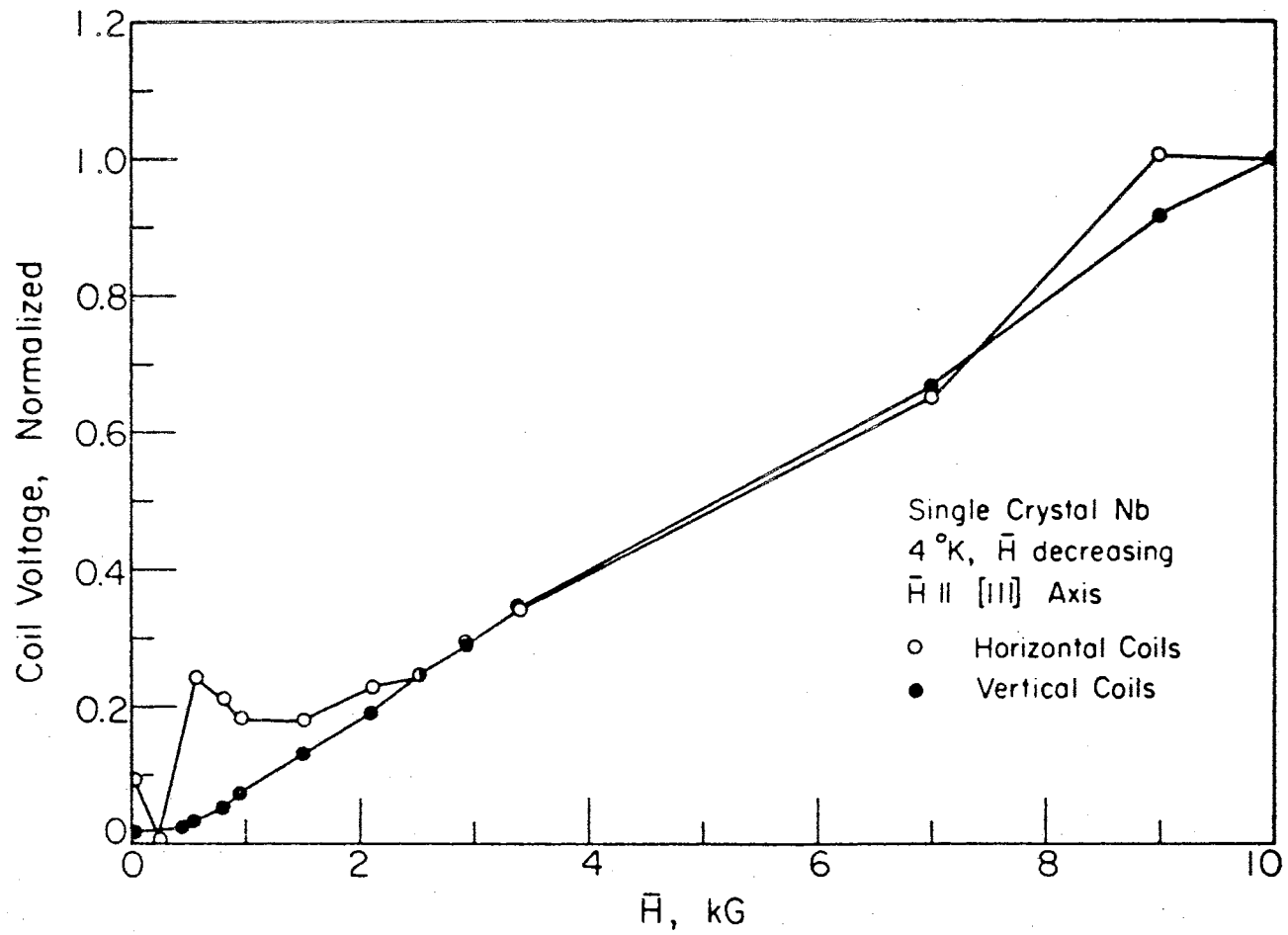


Figure 54. Coils H and V, Amplitude for Nb V, H Decreasing

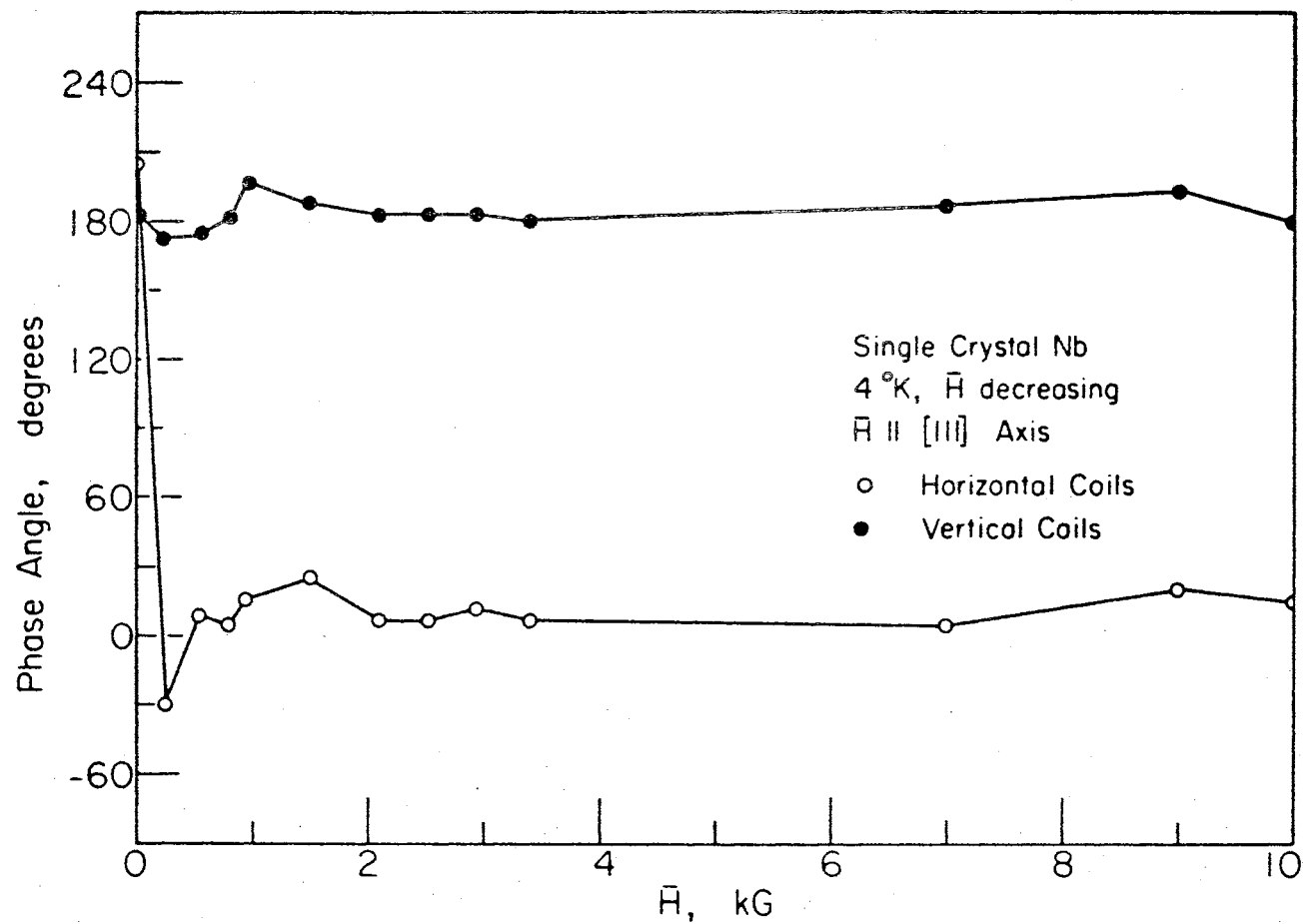


Figure 55. Coils H and V, Phase for Nb V, H Decreasing



#### SELECTED BIBLIOGRAPHY

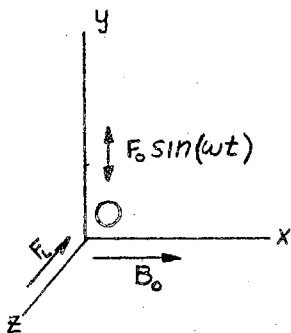
1. Blatt, J. M. Theory of Superconductivity. Academic Press, New York, 1964
2. Brout, R. H. Phase Transitions. W. P. Benjamin, New York, 1965
3. De Sorbo, Warren. Effect of Dissolved Gases on Some Superconducting Properties of Niobium. Physical Review, 132, 107 (1963)
4. Fiori, A. T. and Serin, B. Resistivity and Hall Effect in Superconducting Niobium. Physical Review Letters, Vol. 21, No. 6, p. 359.
5. Hake, R. R. Mixed-State Hall Effect in an Extreme Type II Superconductor. Physical Review 168, 442 (1968)
6. Javid, Mansour and Brown, Philip M. Field Analysis and Electromagnetics. McGraw-Hill, Inc., New York, 1964
7. Kittel, C. Introduction to Solid State Physics. Wiley, New York, 1967
8. Kolsky, Herbert. Stress Waves in Solids. Dover Publishing Co., New York, 1963
9. Kurrelmeyer, Bernhard and Mais, W. H. Electricity and Magnetism. D. Van Nostrand Co., Princeton, New Jersey, 1967
10. Landau. Electrodynamics of Continuous Media
11. Lynton, E. A. Superconductivity. Wiley, New York, 1964
12. Mason, W. P. Physical Acoustics. Vols. I, IIIB, IV. Academic Press, New York, 1964
13. Panofsky, W. K. H. and Phillips Melba. Classical Electricity and Magnetism. Addison-Wesley Publishing Co., Cambridge, Mass., 1955
14. Rickayzen, G. Theory of Superconductivity. Interscience Publishers, New York, 1965
15. Schrieffer, Jr. Theory of Superconductivity. W. A. Benjamin, New York, 1965

16. Ziman, Jim. Principles of the Theory of Solids. Cambridge University Press, 1964

## APPENDIX A

### ANALYSIS OF THE AC HALL EFFECT (LORENTZ EFFECT)

We are interested in obtaining an expression for the magnetic field of a collection of free electrons under the combined influence of a uniform magnetic field, and a sinusoidal forcing function perpendicular to the applied field. We shall assume that the forcing function overshadows such effects as collisions and thermal vibrations. At low temperatures above the superconducting point this assumption is probably valid. We shall adopt an independent-particle model. We are thus interested in the motion of a single electron through the lattice. If the frequency of the forcing function is low, so that the electron wanders over many lattice distances before the force is reversed, one might expect that it sees some averaged, viscous-like effect as the net effect of the lattice. We shall assume that such is the case, and that this viscous retarding force is proportional to the first power of the velocity.



The classical equation of motion then becomes

$$\sum_i \vec{F}_i = F_0 \sin wt \hat{j} - R\vec{v} - e\vec{v} \times \vec{B}_0 = m \frac{d\vec{v}}{dt}$$

where  $R$  is the "coefficient of viscosity,"  $e$  is the charge on the electron (absolute value), and  $F_0$  is a constant.

The field is uniform,

$$\vec{B} = B_0 \hat{i}$$

so that

$$\vec{v} \times \vec{B} = 0 \hat{i} - B_0 v_y \hat{k} + B_0 v_z \hat{j}$$

We separate the equation of motion into its three components to get

$$(1) \quad m \frac{dv_x}{dt} = -Rv_x; \quad v_x = v_{x0} e^{-\frac{R}{m}t}$$

$$\text{or } v_x = v_{x0} e^{-\frac{t}{\tau}} \quad \tau = \frac{m}{R}$$

$$(2) \quad m \frac{dv_y}{dt} = -eB_0 v_z - Rv_y + F_0 \sin \omega t$$

$$(3) \quad m \frac{dv_z}{dt} = -eB_0 v_y - Rv_z$$

Equation (1) is solved immediately to obtain the relaxation time  $\tau$ .

Equations (2) and (3) are mutually coupled in the two unknowns  $v_y$  and  $v_z$ . They can nevertheless be solved exactly as follows.

First, obtain an expression for  $v_y$  from Equation (3):

$$v_y = \frac{1}{eB_0} \left[ m \frac{dv_z}{dt} + Rv_z \right]$$

hence

$$\frac{dv_y}{dt} = \frac{1}{eB_0} \left[ m \frac{d^2v_z}{dt^2} + R \frac{dv_z}{dt} \right]$$

Now substitute these last two expressions into Equation (2), and collect terms to obtain

$$(4) \quad \frac{d^2v_z}{dt^2} + \frac{2R}{m} \frac{dv_z}{dt} + \left( \frac{eB_0}{m} \right)^2 v_z = F_0 \frac{eB_0}{m^2} \sin(\omega t)$$

This is a linear, second-order inhomogeneous differential equation with constant coefficients. To solve such an equation, one first solves the corresponding homogeneous equation (set r.h.s. = 0), and then seeks any particular solution of the inhomogeneous form. The sum of these two

solutions is the general solution. It is apparent, however, that the homogeneous part of the solution must decay with time, since it represents the situation where there is no forcing function to sustain the oscillations. In general, the steady-state solutions come out of the particular solution to the inhomogeneous equation. We are in effect assuming that all transients have died out and only the steady-state part remains. A particular solution which satisfies (4) is

$$V_2(t) = A_1 \sin(\omega t) + A_2 \cos(\omega t)$$

with  $A_1$  and  $A_2$  to be determined. Then

$$\frac{dv_2}{dt} = A_1 \omega \cos(\omega t) - A_2 \omega \sin(\omega t)$$

$$\frac{d^2 v_2}{dt^2} = -A_1 \omega^2 \sin(\omega t) - A_2 \omega^2 \cos(\omega t)$$

If one substitutes into (4) and imposes the condition that the resulting equation be satisfied identically in  $\sin \omega t$  and  $\cos \omega t$ , one obtains

$$A_1 \left[ -\omega^2 + \left( \frac{eB_0}{m} \right)^2 \right] + A_2 \left[ \frac{-2R\omega}{m} \right] = \frac{F_0 e B_0}{m^2}$$

and

$$A_1 \left[ \frac{2R\omega}{m} \right] + A_2 \left[ -\omega^2 + \left( \frac{eB_0}{m} \right)^2 \right] = 0$$

This gives

$$A_1 = \frac{1}{\Delta} \frac{F_0 e B_0}{m^2} \left[ -\omega^2 + \left( \frac{eB_0}{m} \right)^2 \right]$$

$$A_2 = \frac{1}{\Delta} \frac{F_0 e B_0}{m^2} \left[ \frac{2R\omega}{m} \right]$$

where

$$\Delta = \omega^4 - 2\omega^2 \left( \frac{eB_0}{m} \right)^2 + \left( \frac{eB_0}{m} \right)^4 + \left( \frac{2R}{m} \omega \right)^2$$

Let us consider the ratio  $A_2/A_1$ :

$$\frac{A_2}{A_1} = \frac{\frac{2R\omega}{m}}{-\omega^2 + \left( \frac{eB_0}{m} \right)^2}$$

Now even for very small fields, the approximation  $\left(\frac{eB_0}{m}\right)^2 \gg \omega^2$  is very good. For example let  $B = 2.0$  gauss. Then

$$\frac{eB_0}{m} = 3.52 \times 10^7 \text{ (sec}^{-1}\text{)}$$

while

$$\omega = 2\pi(4 \times 10^4 \text{ Hz}) = 25.2 \times 10^4 \text{ SEC}^{-1}$$

We can ignore the term  $\omega^2$  in the denominator except for very low fields.

Thus

$$\frac{A_2}{A_1} = \frac{2 \frac{R}{m} \omega}{\left(\frac{eB_0}{m}\right)^2}$$

The term  $R/m$  has the dimensions of  $(\text{time})^{-1}$ . It is also associated with the influence of the lattice on the free electrons. We shall therefore identify it with the relaxation time  $\tau$  according to

$$\tau = \frac{m}{R} = \rho \epsilon_0$$

where  $\rho$  is the resistivity. This is also suggested by the solution to Equation (1) above.

This gives

$$\frac{A_2}{A_1} = \frac{2\omega}{\tau \left(\frac{eB_0}{m}\right)^2}$$

We shall show that the ratio  $A_2/A_1$  is quite generally much greater than 1, so that only the  $A_2$  term is important in the solution for  $U_z$ . The following table gives the resistivities in  $\mu\text{ohm-cm}$  for lead and niobium at two different temperatures:

$T_1$ °K	Nb	Pb
80	2.6	4.97
295	14.5	21.0

Thus for Pb:

$$\begin{aligned} \tau_{295} &= 21.0 \times 10^{-8} \frac{\text{Volt-meter}}{\text{amp}} \times 8.85 \times 10^{-12} \frac{\text{Coul}^2}{\text{New-meter}^2} \\ &= 1.81 \times 10^{-18} \text{ sec.} \end{aligned}$$

$$\tau_{80} = 4.40 \times 10^{-19} \text{ sec.}$$

For Nb

$$\tau_{295} = 1.28 \times 10^{-18} \text{ sec.}$$

$$\tau_{80} = 2.30 \times 10^{-19} \text{ sec.}$$

The table below gives the ratio  $A_2/A_1$  for Nb and Pb at the two temperatures and two extreme fields B:

Spec.	Temp, °K	B, gauss	$A_2/A_1$
Pb	80	1.0	$3.7 \times 10^9$
Pb	80	$10^4$	37
Pb	295	1.0	$9.0 \times 10^8$
Pb	295	$10^4$	9.0
Nb	80	1.0	$7.1 \times 10^9$
Nb	80	$10^4$	71
Nb	295	1.0	$1.27 \times 10^9$
Nb	295	$10^4$	12.7

TABLE IV

We conclude that, except for high fields at high temperatures, the  $A_1$  term can be ignored. The solution for  $v_z$  is then

$$v_z = A_2 \cos(\omega t)$$

where  $A_2$  is given above. We make one final approximation, that  $\Delta = \left(\frac{2e\hbar}{m} \omega\right)^2$ . This is very good for fields below 10 KG. The term

$\left(\frac{2R}{m}\omega\right)^2$  outweighs all the others by factors of 200 or greater. We are left with

$$A_2 = \frac{F_2 e}{m^2 \omega} \cdot \frac{1}{2\tau} \cdot B_0 = C_1 \frac{B_0}{\omega \tau}$$

To a good approximation, then, the amplitude of the velocity is proportional to B. At high fields the theory predicts a  $B^3$  dependence, due to the  $A_1$  term. One would expect the  $v_z$  term to be the major velocity term involved in the Hall Effects since the forcing function tends to drive the particles in a vertical direction. If this is so, then the Hall current will be determined by  $v_z$  and will be given by

$$\bar{J}_y = -nev_z \hat{R} = -C_1 \frac{ne}{\omega \tau} B_0 \cos(\omega t) \hat{R}$$

where n is the electron concentration

$B_0$  is the applied Field

(identical to  $H_0$ )

The above expression gives the source current density for the a.c. Hall Effect. The actual voltage induced in the coil is determined by an integration over the source region (specimen) and a second integration over the coil system. Since  $B_0$  is independent of any of these variables of integration, the coil voltage is proportional to the field B, as one might expect.

The above theory should not be taken too literally, since it involves rough assumptions. However, the assumptions are not unreasonable, and the conclusions should be at least qualitatively correct. The experimental data presented here definitely confirms the proportionality between V (coil voltage) and  $B_0$ . It is emphasized that the existence of the a.c. Hall Effect is due to the fact that the field is applied perpendicularly to the forcing function, giving rise to the velocity component  $v_z$ .



APPENDIX B

QUASISTATIC APPROXIMATION

From Maxwell's Equations

$$\nabla \times \mathbf{H} = \mathbf{J}_c + \frac{\partial \mathbf{D}}{\partial t}$$

we shall show that  $\frac{\partial \mathbf{D}}{\partial t}$  can be neglected for  $\omega = 2\pi \times 40,000$  cps.

$$\mathbf{J}_c = \sigma \mathbf{E}$$

and  $\mathbf{D} = \epsilon_0 \mathbf{E} + \mathbf{P} = \epsilon_0 \mathbf{E}$  (assumes that the polarization for a metal is negligible)

Also, for a sinusoidal source,

$$\mathbf{J}_c = \mathbf{J}_0 \sin(\omega t)$$

$$\frac{\partial \mathbf{J}_c}{\partial t} = \mathbf{J}_0 \omega \cos(\omega t)$$

or  $\frac{\partial \mathbf{D}}{\partial t} = \frac{\epsilon_0}{\sigma} \mathbf{J}_0 \omega \cos(\omega t) \ll \mathbf{J} = \mathbf{J}_0 \sin(\omega t)$

We must have  $\frac{\epsilon_0}{\sigma} \omega \cos(\omega t) \ll \sin(\omega t)$

This is true for arbitrary time  $t$  if

$$\frac{\epsilon_0}{\sigma} \omega \ll 1$$

but  $\frac{\epsilon_0}{\sigma}$  is the relaxation time  $\tau$ .

We thus conclude that the quasi-static approximation is valid if

$$\omega \tau \ll 1$$

for niobium at room temperature

$$\tau = \rho \epsilon_0 = 1.28 \times 10^{-18} \text{ SEC.}$$

$$W\tau \doteq 3.24 \times 10^{-13}$$

a similar situation holds for lead:

$$\tau = 1.9 \times 10^{-18} \text{ SEC.}$$

$$W\tau \doteq 4.7 \times 10^{-13}$$

The approximation is clearly very good.

## APPENDIX C

### UNITS AND DIMENSIONS

There are three systems of units commonly used in electromagnetic theory, the CGS-EMU (electro-magnetic units), the CGS-ESI (electro-static units), and the MKSA (meter-kilogram-second-ampere) system. The two CGS systems can be expressed in terms of the MKSA system of units, which is here to be regarded as the "more fundamental" system.

In using Table IV, each line of the table should be read as an equality. For example,

$$\begin{aligned} \frac{1}{300} \text{ Statvolts} &= 10^8 \text{ abvolts} = 1.0 \text{ volt} \\ &= 1.0 (\text{kgm})'(\text{meter})^2(\text{sec})^{-2}(\text{coul})^{-1} \end{aligned}$$

The deletions in the table are a consequence of the historical development of the theory of electromagnetism. The ESI system was defined to deal only with electrostatic systems, while the EMU system was defined only for dynamic systems. Thus, there are no units for B in the ESU system since B arises from the dynamical properties of charges. Only after Maxwell's work did it become apparent that the two systems of units were directly related. It was then realized that one system of units should suffice for all electromagnetic phenomena, hence the MKSA system was developed. For a more complete table and explanation of dimensions and units see references 2 and 3 of the Bibliography.

Quantity	Symbol	Unit, ESU	Unit, EMU	Unit, MKSA	Dimensions - MKSA			
					M	L	T	Q
					Kgm	Meter	Sec	Coul
Current	I	$3.0 \times 10^9$ statamp	$10^{-1}$ abamp	1.0 ampere	0	0	-1	1
Potential Diff.	V, E	1/300 statvolts	$10^8$ abvolts	1.0 volt	1	2	-2	-1
Field Intensity	$\bar{H}$	-----	$4\pi \times 10^{-3}$ Oersteds	1.0 amp/meter	0	-1	-1	1
Flux Density	$\bar{B}$	-----	$10^4$ Gauss	1.0 Weber/meter <sup>2</sup>	1	0	-1	-1
Flux	$\phi$	-----	$10^8$ Maxwells	1.0 Weber	1	2	-1	-1
Electrical Displ.	$\bar{D}$	$12\pi \times 10^5 \frac{\text{statcoul}}{\text{cm}^2}$	-----	1.0 coul/meter <sup>2</sup>	0	-2	0	1
Electrical Field	$\bar{e}, \bar{E}$	$1/3 \times 10^{-4} \frac{\text{statvolt}}{\text{cm}}$	-----	1.0 volt/meter	1	1	-2	-1

TABLE V  
UNITS AND DIMENSIONS

VITA 2

Gordon L. Nelson, Jr.

Candidate for the Degree of

Master of Science

Thesis: MAGNETIZATION AND A.C. HALL EFFECTS IN TWO SUPERCONDUCTORS

Major Field: Physics

Biographical:

Personal Data: Born in Flushing, New York, June 29, 1943, the son of Mr. and Mrs. Gordon L. Nelson.

Education: Graduated from Stillwater, Oklahoma High School in 1961; received the B.S. degree in Physics in 1966 from Oklahoma State University, and has recently completed the requirements for the M.S. degree in Physics at Oklahoma State University.

Memberships: Is a member of Sigma Pi Sigma, national honorary society for physics students.